Air Force Institute of Technology
AFIT Scholar

Theses and Dissertations | Student Graduate Works

9-18-2014

Measurements of DNA Damage and Repair in Bacillus anthracis Sterne Spores by UV Radiation

Chelsea C. Marcum

Follow this and additional works at: https://scholar.afit.edu/etd

Recommended Citation
Marcum, Chelsea C., "Measurements of DNA Damage and Repair in Bacillus anthracis Sterne Spores by UV Radiation" (2014). *Theses and Dissertations*. 566.
https://scholar.afit.edu/etd/566

This Thesis is brought to you for free and open access by the Student Graduate Works at AFIT Scholar. It has been accepted for inclusion in Theses and Dissertations by an authorized administrator of AFIT Scholar. For more information, please contact richard.mansfield@afit.edu.

MEASUREMENTS OF DNA DAMAGE AND REPAIR IN *BACILLUS ANTHRACIS* STERNE SPORES BY UV RADIATION

THESIS

Chelsea C. Marcum

AFIT-ENP-T-14-S-01

DEPARTMENT OF THE AIR FORCE
AIR UNIVERSITY

AIR FORCE INSTITUTE OF TECHNOLOGY

Wright-Patterson Air Force Base, Ohio

DISTRIBUTION STATEMENT A.
APPROVED FOR PUBLIC RELEASE; DISTRIBUTION UNLIMITED.

The views expressed in this thesis are those of the author and do not reflect the official policy or position of the United States Air Force, Department of Defense, or the United States Government. This material is declared a work of the U.S. Government and is not subject to copyright protection in the United States.

AFIT-ENP-T-14-S-01

MEASUREMENTS OF DNA DAMAGE AND REPAIR IN *BACILLUS ANTHRACIS* STERNE SPORES BY UV RADIATION

THESIS

Presented to the Faculty

Department of Engineering Physics

Graduate School of Engineering and Management

Air Force Institute of Technology

Air University

Air Education and Training Command

In Partial Fulfillment of the Requirements for the

Degree of Master of Science in Material Science

Chelsea C. Marcum, BS

September 2014

DISTRIBUTION STATEMENT A.
APPROVED FOR PUBLIC RELEASE; DISTRIBUTION UNLIMITED.

AFIT-ENP-T-14-S-01

MEASUREMENTS OF DNA DAMAGE AND REPAIR IN *BACILLUS ANTHRACIS* STERNE SPORES BY UV RADIATION

Chelsea C. Marcum, BS

Approved:

_____//Signed//_____	_____08-25-2014___
Larry W. Burggraf, PhD (Chairman)	Date
_____//Signed//_____	_____08-25-2014___
Douglas R. Lewis, LTC, USA, PhD (Member)	Date
_____//Signed//_____	____08-25-2014____
Yun Xing, PhD (Member)	Date
_____//Signed//_____	_____08-25-2014___
LeeAnn Racz, Lt Col, USAF, PhD (Member)	Date

AFIT-ENP-T-14-S-01

Abstract

Spores of *Bacillus anthracis* (Ba) Sterne were irradiated with 267nm UV light using small light emitting diodes (LEDs). The pRB373 plasmid with a red fluorescent protein was transformed into Ba Sterne cells prior. Following irradiation, germination media was added and the spores were incubated for various times, to allow for DNA repair. The pRB373 plasmid was isolated and analyzed using real-time PCR. Primers were designed across the RFP in the plasmid yielding two amplicons, 245bp and 547bp long. PCR amplification was not achieved for germinated samples. Spore samples isolated using bead beating methods were amplified. Results indicate a quicker amplification (lower Ct) for irradiated samples than for un-irradiated. Lack of PCR amplification in germinated samples is attributed to extremely harsh extraction methods for Ba cells. This observation was not expected. Ba survival curves were also developed using the quadratic fit, $y = \alpha x + \beta x^2$. Averaging results form 3 experiments, α is reported as -0.0144 ± 0.008 and β as -0.00001 ± 0.0002. Fit parameters are reported to a 90% confidence interval. Actinometry experiments corrected for the efficiency of the LEDs in all experimentation. Fluorescence measurements monitored germination and outgrowth; they indicated a delay in germination of irradiated spores. AFM images showed morphological changes in irradiated spores. Spore coats and/or the exosporium appear detached from the spore following irradiation. Irradiated spores also show vegetative growth in much smaller clusters than non-irradiated spores.

Acknowledgments

I owe a large debt of gratitude to my thesis advisor, Dr. Burggraf, and my committee members, LTC Douglas Lewis, Dr. Yun Xing, and LTC LeeAnn Racz. I greatly appreciate your support. I also received an immense amount of guidance from Dr. Thomas Lamkin and his research group members at USAF-SAM: Dr. Roland Saldanha, Heather Fullenkamp and Heather Pangburn. Thank you all for your countless hours of assistance. I would like to extend a special thank you to Tony Kelly for his assistance with statistical analysis of my data. Thank you as well to Michael Spencer for his help with the electronics equipment.

Thank you to all of my Fellow AFIT students for their support and encouragement. I admire your strength and diligence. I would like to especially acknowledge Miss Kandace Bailey, a SOCHE intern. Thank you so very much for all of your assistance in the lab. The intense plating and preparation required for this project would not have been possible without you.

Finally, I'd like to recognize the absolute support system received from my family, friends, and Heavenly Father. To my husband, thank you for the countless reminders of my ability and strength. You are my rock. To my sister, I am thankful to call you my best friend. You are my constant reminder of what it means to be a strong, faithful follower of the Lord. And to my Heavenly Father, I am so humbled by Your greatness. All my praise and glory belongs to You.

To all those I know and love, thank you for walking along side me in this journey we call life.

Chelsea C. Marcum

To my number one fan, my husband. Love conquers all.

"Beyond all these things put on love, which is the perfect bond of unity."

Colossians 3:14

Table of Contents

Page

Abstract iv
Acknowledgments v
Table of Contents vii
List of Figures ix
List of Tables xv
I. Introduction 1
Research Statement 1
Problem Statement 1
Motivation 2
Research Focus 3
Relevant Research 5
Methodology 5
Document Structure 6
II. Background & Theory 7
Chapter Overview 7
DNA 7
Photochemistry 9
Bacillus anthracis 13
DNA Damage 19
DNA Repair 21
Actinometry 24
PCR 26
Gel Electrophoresis 27
Atomic Force Microscopy 27
III. Methodology 29
Chapter Overview 29
Microbial Technique 29
LED UV Irradiator 34
Actinometry 38
Bacillus anthracis Spore Survival Curve 39
DNA Damage & Repair Experimentation 40
PCR 41
IV. Analysis and Results 49
Chapter Overview 49
Actinometry 49
Bacillus anthracis Survival Curve 53
DNA Damage & Repair Experimentation 64
Summary 82
V. Conclusions and Recommendations 84
Chapter Overview 84
Conclusions of Research 84

Future Recommendations 85
Summary 86
Appendix 88
Microbial Technique & Preparation 88
Experimental Information 94
Raw Data 99
Bibliography 115

List of Figures

Page

Figure 1. Structure of DNA. Cytosine and Guanine form the stronger of the two bonds across the sugar backbones. Thymine and Adenine form the weaker of the two bonds. The strength of the bond across the two DNA strands directly correlates to the hydrogen bonds. Figure reprinted with Permission from [11]. 8

Figure 2. Emission Power of AlGaN LEDs over time. LED emission power decreased 40% over 100 hours of operating time. LED Emission power decrease also caused an increase in series resistance of about 1 Ω. Figure reprinted with permission from [9]. Copyright 2011 Elsevier 12

Figure 3. Microscopic image of both Ba cells and spores [17]. During sporulation and germination, cells and spores are often found occurring together as not all individual organisms sporulate/germinate simultaneously. Spores are shown as light orange and ovular. Cells are rod-shaped and form long chains. Figure reprinted with permission from [17]. Copyright 2002 John Wiley & Sons. 14

Figure 4. Layer structure of the spore. The inner core of the spore contains the well protected and tightly stored DNA. The layers in this figure are not to scale. Figure reprinted with permission from [21]. Copyright 2006 John Wiley & Sons. 15

Figure 5. The spore germination process. Germination occurs in 2 main stages. The initiation/activation step involves the enrichment of nutrients. Stage 1 involves release of DPA and hydration of the spore core. Stage 2 involves further hydration and swelling of the spore. During outgrowth, the cell eventually emerges from the spore as metabolic and enzymatic activity reinitializes. Figure Reprinted with Permission from [20]. Copyright 2003 Elsevier. 17

Figure 6. Absorption spectra of DPA. The absorption was measure using optical density of the samples. The unfilled-circles represent DPA prior UV light. The closed-circles represent DPA absorption following UV light exposure ($100 J/cm^2$) by a 450W ozone-free xenon arc lamp. The dashed line represents CaDPA prior to UV light and the solid line represents CaDPA absorption following UV light exposure under the same conditions as the DPA. A small shift in wavelength is observed following exposure to UV light. Figure reprinted with permission from [27]. Copyright 2005 OSA. 18

Figure 7. Thymine cyclobutane dimer formation [29]. The dimer formed is a [2+2] cycloaddition that occurs at 5th and 6th carbon positions (across the double bond) between two adjacent pyrimidines. While thymine-thymine CPDs are most common, other combinations of pyrimidine bases can undergo the same cycloaddition. Figure reprinted with permission from [29]. Copyright 2001 Elsevier 20

Figure 8. Pyrimidine (6-4) Pyrimidone photoproduct. This dimer is created from a [2+2] cycloaddition as well. Figure reprinted and adapted with permission from [29]. Copyright 2001 Elsevier. 20

Figure 9. Spore Photoproduct. UV radiation causes thymine residues to form the spore photoproduct (SP). The spore photoproduct lyase is an enzyme that reverses this thymine damage. Figure Obtained from [13], open access article. 21

Figure 10. Spore photoproduct (SP) repair by Spore Photoproduct Lyase. A free electron originates from a 4Fe-4S cluster and is provided to the SAM enzyme molecule. Reductive cleavage of the C5'-S bond creates a reactive radical 5'-dA. The radical abstracts a hydrogen atom from the spore photoproduct, initiating the repair process [13]. Figure Obtained from [13], open access article. 22

Figure 11. The linear temperature dependence of the KI/KIO_3 actinometer. The temperature dependence of the KI/KIO_s actinometer shows the need for temperature measure and control in the lab apparatus. This linear regression was created using multiple temperatures, each point representing 1 to 5 replicates. Figure reprinted with permission from [36]. Copyright 2007 John Wiley and Sons. 25

Figure 12. AFM images of *Bacillus anthracis* spores before (a) and after (b) heat treatment with a heated AFM tip. Nanoscale blister-like structures were observed on the surface of the spores following heat treatment. Figure reprinted with permission from [38]. Copyright 2013 American Chemical Society. 28

Figure 13. UV reactor designed by Michael Spencer, AFIT [45]. The reactor has 7 LEDs that irradiate from the bottom. Composed of Stainless steel, the reactor allows for a high reflectance. LEDs are sealed with silicon to the bottom of the reactor. The entire reactor sits on a shaker, helping to prevent spore clumping. 35

Figure 14. UV reactor circuitry board and DASY Lab interface. The seven LEDs plug into the circuit board in the locations in series with 20 ohm resistors. The power

supply from DASY Lab is connected into the center of the board, where it then flows to the op-amp on the back of the board before coming back to the input of the LEDs. 36

Figure 15. Gel electrophoresis of PCR controls. Wells 1 and 2 (from the left) show two different ladders. Well 3 is isolated RFP DNA, where only one intense band is shown. This indicates a clean sample, free of contamination. Wells 4 through 8 are the dilution serious 10^1-10^5 of RFP DNA with the first reverse primer (This should be the shorter amplicon, 245 base pairs in length). Well 9 is the DNA ladder again. Wells 10-14 are the dilution serious 10^1-10^5 of RFP DNA with the second reverse primer (This should be the longer amplicon, 547 base pairs in length. And finally, well 15 is another DNA ladder. Wells 4-8 very clearly display an amplicon about half the length of the amplicon in wells 10-14. This gel confirms proper amplification of the designed amplicons. 45

Figure 16. Apparent Quantum Yield. Values used in this graph are reported in Table 8. The first three data points were omitted during quantum yield calculations because the absorbance values at 352nm were too close to the absorbance blank measurements. The quantum yield should remain constant with changing fluence. . 53

Figure 17. Survival Curve 3 surviving fraction of Ba Sterne spores as fluence is varied between 0 and 1000 J/m^2. Fluence carries the units J/m^2. Fluence values displayed in this figure are the corrected values from actinometry results. 55

Figure 18. Survival fraction for Survival Curve 3. The dotted blue line represents the cut-off point for data to be fit. The magnitude of the errors towards the higher fluence values is as large as the spread of the data. The last 6 data points are omitted from the fitting functions seen in the following figures. 56

Figure 19. Log_{10} (N/N_o) as a function of fluence for Survival Curve 3. The blue line indicates the breaking point in the data where errors become too large to trust the data points. The last data point (at $966J/m^2$) is omitted from the plot because the plate counts were zero, making the Survival fraction 0. The log_{10} (0) is undefined..... 57

Figure 20. Log-linear with fit of Survival Curve 3. Fitting only the data up to $240J/m^2$, the Root coding program yields an R^2 value of 0.992. Fitting parameters for this fit are found in Table 9 above. 59

Figure 21. Pearson product-moment correlation plot for Survival Curve 3. The two fit parameters α and β are negatively correlated. The blue area indicates 1 standard deviation from the mean, where 68% of the data lies. The green area indicates 2 standard deviations from the mean, where 95% of the data lies. The red area indicates 3 standard deviations from the mean, where 99.7% of the data lies. 60

Figure 22. Survival Curve for all 3 data sets. Surviving fraction of *Bacillus anthracis* Sterne spores as fluence is varied between 0 and 1000J/m^2. Fluence carries the units J/m^2..... 61

Figure 23. Ba Sterne survival curve showing all 3 experimental data sets. Data from the 3 different experiments varies greatest when fluence is less than 100J/m^2. This plot displays the large increase in error as fluence increases and colony counts are greatly diminished. 62

Figure 24. Log-linear with fit of the Combined Survival Curve. Fitting only the data up to 240J/m^2, the Root coding program yields an R^2 value of 0.876. Fitting parameters for this fit are found in Table 10 above. 63

Figure 25. Pearson product-moment correlation plot for the Combined Survival Curve. The two fit parameters α and β are negatively correlated. The blue area indicates 1 standard deviation from the mean, where 68% of the data lies. The green area indicates 2 standard deviations from the mean, where 95% of the data lies. The red area indicates 3 standard deviations from the mean, where 99.7% of the data lies. .. 64

Figure 26. Fluorescence data collected on irradiated and un-irradiated (control) Ba Sterne spores. This data was collected to monitor the germination and outgrowth stages of the spore. For this experiment, the germination salts were only at half strength. This most likely slowed the germination process for both the control and irradiated spores. An increase in fluorescence intensity indicates an increase in germination as the fluorescence dye will not penetrate the spore. Three measurements were collected at each data point and averaged. The control spores show germination beginning at 200 minutes and the irradiated spores begin to germinate at 350 minutes, a lag time of about 2½ hours. 67

Figure 27. Un-irradiated Spores at Time Zero. Non-irradiated spores immediately following addition of germination salts (half strength). The size, shape, and clustering is typical of Ba spores. Images are courtesy of Dr. Yun Xing [53]. 68

Figure 28. AFM images of un-irradiated control spores: 90 min culture in germination media. Note the presence of normal looking veg cells, pit-like structures and also fibers. Normal spores are approximately 2-5 microns in length, where the vegetative cells are slightly longer. Images are courtesy of Dr. Yun Xing [53]. 69

Figure 29. AFM images of un-irradiated spores control: 150 min culture in germination media. At this point, nearly all germination has taken place. The size, shape, and clustering is typical of Ba vegetative cells in this MOPS AGFK germination media. Images are courtesy of Dr. Yun Xing [53]. 70

Figure 30. Radiated (log kill 1) Spores. This sample is 0 minutes incubation in germination media. The white box indicates the spot at which the bottom two images are focused. In the top image and image on the left, a haze is seen around each spore. It appears (shown in bottom right image) the spores have lost their exosporium and perhaps their spore coats. Images are courtesy of Dr. Yun Xing [53]. 71

Figure 31. Irradiated spores incubated in germination media for 90 minutes. These spores are beginning to germinate. The fibers seen in un-irradiated germinating spores are also seen here. But, the germination is occurring in much smaller clusters then the un-irradiated spores. Images are courtesy of Dr. Yun Xing [53]. 72

Figure 32. Irradiated spores incubated in germination media for 150 minutes. The spores are almost entirely germinated cells. This is also confirmed by the fluorescence measurements. These cells are clustered in 1-3 cell clusters. The un-irradiated cells were clustering in much larger groups of 20-50 cells. Images are courtesy of Dr. Yun Xing [53]. 73

Figure 33. Surviving fraction of DNA damage and repair experiments with varying incubation time. Each data point is representative of 3 plate counts. Plates were counted after 18 hours. The control experiment received no irradiation while the experiments received a dose of 100 J/m^2. 74

Figure 34. Un-germinated spores pre and post-irradiation. Samples for all 3 experiments are displayed. Error bars are included and individual Ct results displayed on the bars. Total DNA concentrations are also shown in a white box at the bottom of each bar. Data in this figure corresponds to the short amplicon, 245bps long. Irradiation of 1-log kill. 76

Figure 35. Un-germinated spores pre and post-irradiation. Samples for all 3 experiments are displayed. Error bars are included and individual Ct results displayed on the bars. Total DNA concentrations are also shown in a white box at the bottom of each bar. Data in this figure corresponds to the long amplicon, 547bps long. Irradiation of 1-log kill. 77

Figure 36. Ct PCR data from experiment 2, where germination samples OR and 1R properly amplified. Germinated samples are viewed on the left, un-germinated on the right. Irradiation of 1-log kill. 78

Figure 37. Ct PCR data from experiment 2, where germination samples OR and 1R properly amplified. Germinated samples are viewed on the left, un-germinated on the right. Irradiation of 1-log kill. 79

Figure 38. Un-germinated Ba spores pre and post-irradiation. Samples for all 3 experiments are displayed. Error bars are included and individual Ct results displayed on the bars. These Ct results have been corrected by total DNA concentration. Data in this figure corresponds to the short amplicon, 245bps long. Irradiation of 1-log kill. 80

Figure 39. Un-germinated spores pre and post-irradiation. Samples for all 3 experiments are displayed. Error bars are included and individual Ct results displayed on the bars. These Ct results have been corrected by total DNA concentration. Data in this figure corresponds to the long amplicon, 547bps long. Irradiation of 1-log kill. 80

Figure 40. Experiment 2, Germinated vs Un-germinated spores. The bars in blue reflect un-irradiated spores and the bars in red reflect irradiated spores. Data in this figure corresponds to the short amplicon, 245bps long .Irradiation of 1-log kill. 81

Figure 41. Experiment 2, Germinated vs Un-germinated spores. The bars in blue reflect un-irradiated spores and the bars in red reflect irradiated spores. Data in this figure corresponds to the long amplicon, 547bps long. Irradiation of 1-log kill. 82

List of Tables

Page

Table 1. LED Characterization and UV reactor measurements. The power output for each LED was measured using an integrating sphere. The Ultraviolet Transmittance (UVT) is the value of UVT in deionized water [9]. 37

Table 2. Fluence/UV Dose Calculations. Irradiance is calculated from the average power divided by the cross-sectional area of the reactor. Fluence is calculated as the product of irradiance, UVT, number of LEDS, and exposure time. The following 11 data points were used to develop survival curves for Ba spores. Fluences were later adjusted by actinometry results. 38

Table 3. Primer and Probe sequences. The two amplicons created with these primers are 245 and 547 base pairs in length. The primers and probe synthesis across the RFP inserted in the pRB373 plasmid. As printed on the screen, the left side of the Probe sequence encodes for the fluorescence. The far right side of the probe encodes for the quencher. 43

Table 4. PCR control DNA concentrations. The control samples were prepared using isolated RFP DNA, purchased from GeneScrip, and provided by Dr. Lamkin's research group at USAF-SAM [37]. The concentration reflects the DNA concentration when the samples were added to the PCR wells. For example, the DNA concentration for the first sample (10^{-1}) was 13ng/µL. 10µL was added to the PCR well for a total concentration of 130ng. 46

Table 5. DNA damage and repair experimentation. Samples 0R and 0NR are spore samples with no irradiation. Samples 1R and 1NR represent the spores after irradiation. 0R represents the most DNA expected to be seen for the spores that outgrew to 450 minutes. 0NR represents the undamaged spores. Sample 1R is representative of spores that were irradiated and allowed to repair; this is the most repair expected from the damaged spores that were incubated for 450 minutes. Sample 1NR represents the most damage to be observed. These first 4 samples are used to develop the calibration curve with which to compare the other samples. Samples 2-12 are spores that were incubated for the designated time. 47

Table 6. PCR temperature protocol. PCR primers and probes are temperature dependent. If the temperature protocol is not correct, amplification will not occur. This protocol worked best with the primers in this project. Phase 1 brings the primers up to proper

temperature. Phase 2 causes DNA to separate into its two strands. Primers attach at Phase 2. Primer extension (amplification) occurs in Phase 3. 48

Table 7. Quantum yield measurements reported by NIST [35]. Quantum yield is apparently linearly dependent upon wavelength. Therefore, the expected quantum yield for the UV LED reactor was determined to be 0.68 at 267nm, once temperature adjusted (the temperature that experiments were conducted at differed from 23.5°C as much as 2 degrees. The LEDs in the UV reactor are approximately 89% efficient. 51

Table 8. Apparent quantum yield and corrected fluence values. 5/23/2014 data was collected prior to all experimentation. 7/21/2014 data was collected after all other experimentation had been conducted. The average quantum yield omits the first three data points, as their absorbance measurements were too similar to the blank measurements to be included. 52

Table 9. Fitting Parameters and statistics for Survival Curve 3. The R^2 is the best for Survival Curve 3 (Of all three curves), at 0.992. Note the magnitude of β is very small, indicating that the fit has a very small quadratic-term. That is to say, the data is mostly linear. 58

Table 10. Fitting Parameters and statistics for the combined survival curve data. Error bars are reported with a confidence interval of 90%. 63

Table 11. Fluorescence data collected on irradiated and un-irradiated (control) Ba Sterne spores. This data was collected to monitor the germination and outgrowth stages of the spore. For this experiment, the germination salts were only at half strength. This most likely slowed the germination process for both the control and irradiated spores. An increase in fluorescence intensity indicates an increase in germination as the fluorescence dye will not penetrate the spore. Three measurements were collected at each data point and averaged. 65

MEASUREMENTS OF DNA DAMAGE AND REPAIR IN *BACILLUS ANTHRACIS* STERNE SPORES BY UV RADIATION

I. Introduction

Research Statement

The primary objective of this research project was to develop *Bacillus anthracis* Sterne spore survival curves for UV C irradiation and to use PCR to model DNA repair following UV irradiation.

Problem Statement

The purpose of this research is to investigate DNA damage and repair of *Bacillus anthracis* spores following UV irradiation. Investigation in this field is driven by both practical and fundamental motivations. There is a need to disinfect drinking water for military personnel in remote locations to limit expensive bottled water usage. Disinfection of water by UV radiation without use of harmful chemicals is also applied in water treatment facilities for waste water and in drinking water disinfection. Disease-causing microorganisms that are very difficult to kill, such as bacterial spores, represent a bounding challenge for water disinfection. In these and other applications there is benefit in understanding fundamental relationships between spore inactivation with DNA damage and repair. Correlation of DNA damage and repair with spore inactivation conditions allows for a better understanding of what UV irradiation doses can render *Bacillus anthracis* spore harmless to the human population. Inactivation of *Bacillus anthracis* spores is of particular interest to the US military in attempts to prevent and counteract terrorist attacks involving *Bacillus anthracis* bio-weapons.

This project aimed to study the relationship between DNA damage and inactivation of *Bacillus anthracis* spores. DNA damage is known to have significance in the inactivation of bacteria, as does enzyme activity. This research analyzed UV irradiation and its direct impact on DNA damage, as it leads to spore inactivation. The spore's ability to repair damaged DNA through use of enzyme activity was also studied.

Motivation

Bacillus anthracis (Ba) is a spore-forming gram-positive bacterium, known for its use as a biological weapon. Ba causes the disease anthrax in humans which can be lethal without treatment or prevention. Anthrax occurs in three forms depending on the exposure path: cutaneous, gastrointestinal, and pulmonary (inhalational) [1]. Of greatest interest to the military is inhalational exposure which causes the most lethal disease. Typically pulmonary disease requires inhalation of approximately 1000 separate spores into the lungs of a healthy person. So dissemination of respirable, dry spores by aerosol methods is most effective in spreading the bacteria to cause disease.

In 1979, anthrax was accidentally released from a research facility in Russia, resulting in 97 cases of human infection [2]. In 2001, the United States was threatened by biological warfare when Ba spores were concealed in letters and mailed to members of the press and members of Congress. According to the Center for Disease Control (CDC), 22 people contracted anthrax disease from these attacks, 11 inhalational and 11 cutaneous. Of the 11 with inhalational anthrax, five individuals perished [2]. The attack in 2001 encouraged the United States to better prepare for biological warfare, especially pertaining to anthrax and other aerosol-mediated weapons. In recent years, the United

States' combat against biological warfare has been defensive in nature. While no concrete evidence has been provided, other countries could continue to produce anthrax for offensive use. Following the first Gulf War, Iraq had a bio-weapons program capable of weaponizing anthrax [3].

Research Focus

At AFIT, previous studies of Ba spores have focused on thermal inactivation to prevent colony formation. Complete inactivation is defined as outgrowth that yields no viable colonies. Models have been created for inactivation at different temperatures and exposure times to create a complete profile of thermal inactivation [4] [5].

When Ba spores are exposed to heat, bound water molecules become mobile in the spore [4]. Water molecules then react with DNA undergoing hydrolysis reactions [5]. Enzymes and the DNA encapsulated inside the spore are both degraded. If the spore is to survive, it must repair its damaged DNA. The repair process relies heavily on enzymes that can retain catalytic activity after thermal exposure [4]. A graduate student at AFIT, Alexis Hurst, modeled survivability rates after thermal exposure based upon criteria including: water mobility, hydrolysis reactions, and repair enzymes. Another graduate student at AFIT, Emily Knight, studied similar phenomenon. In an attempt to mimic effects equivalent to detonation of a conventional weapon, Knight studied high temperature exposure of spores for short durations of time, and the differences in thermal inactivation with a wet and dry spore. Knight also modeled the high temperature exposure for short durations of time [5]. She concluded that wet heating allowed for more hydrolysis reactions, causing more protein damage then did dry heat.

The modeling and measurement approach to understanding spore inactivation, particularly DNA degradation and repair in Ba spores, is now being applied to spore inactivation via UV and ionizing radiation. In this field, little is understood about the inactivation effects produced by DNA damage and repair after exposure to ionizing radiation. UV radiation has been studied in greater detail because of its simpler mechanism and the interest generated by its importance in civil health infrastructure such as waste water treatment facilities. UV water disinfection reduces chemical usage in treatment facilities, and has negligible residual affects harmful to humans.

Damage by ionizing radiation and UV radiation are related. Kinetic mechanisms and yields are nearly identical for that portion of ionizing radiation damage in organic molecules that is produced by disintegration of electronically excited states of those molecules. Kinetic mechanisms and yields that proceed from molecular ion excited states and molecular radicals produced by ionizing radiation are different. Particularly for indirect ionization radiation effects, the radical distributions produced in aquatic systems and the efficiency of DNA damage that can be interpreted via known kinetics mechanisms [6]. To better understand and begin to study ionizing radiation, UV radiation was used as a more simplified platform to begin our new research in this field.

To safely perform this research in a BSL 2 laboratory, the Sterne strain of Ba was used. The Sterne strain lacks the pXO1 plasmid which encodes for the virulence/toxicity of Ba. Without this pXO1 plasmid, the organism loses its virulence. Ba Sterne is even used as an effective vaccine for prevention of anthrax [7].

Relevant Research

Inactivation of spores by UV radiation was previously studied at AFIT by Major Tho Tran [8]. Using the same reactor used in this experimentation, he modeled the inactivation of *Bacillus globigii*. Tran's work concluded that pulsed UV light from Light Emitting Diodes (LEDs) was more effective than continuous UV radiation at inactivating spores. Continuous and pulsed LED irradiation both achieved 6-log kill inactivation, but pulsed was 1.8 times more effective than continuous [8]. Wurtele et al also studied UV-LEDs for waste water disinfection. *Bacillus subtilis* was studied in this experiment where inactivation was achieved at 269 and 282nm, concluding 269nm light was more effective at inactivation of *Bacillus subtilis* than was 282nm [9].

Methodology

A commercial plasmid pRB373 (5800 base pairs) [10] was transformed into Bacillus anthracis. DNA damage can be studied more easily with plasmids, as their size is significantly smaller than the Ba genome. The plasmid contains a red florescent protein and upon expression, the cells are a pinkish-red color. The plasmid also contains an antibiotic resistance gene, which gives the cell an advantage when it keeps the plasmid. Studies will be conducted on Ba spores and vegetative cells. Target radiation dose will correlate to approximately 1-log kill. At this dose, it is expected that the surviving spores will have badly damaged DNA and will yield the most useful damage and repair data. Special primers and probes were designed to work in conjunction with real-time PCR (Polymerase Chain Reaction) and were used to amplify the DNA from the extracted plasmids.

Document Structure

This document is separated into 5 chapters. Chapter 1 introduces the subject matter and discusses the motivations behind the research. Chapter 2 provides the reader with background information and theory behind the research covered in this thesis. Topics covered in chapter 2 include: The Spore, UV photochemistry, and DNA damage and repair. Chapter 3 describes the detailed methods and procedures followed to conduct the research. Chapter 4 presents the data collected by methods following in chapter 3, as well as the data analysis results. Chapter 5 concludes the document and discusses the significance of the research. Chapter 5 also addresses recommendations for future research in this area. Following the fifth chapter, the appendix provides additional information not pertinent to the content of the thesis, but necessary for reproducibility of results. The appendix also provides the raw data for all experiments conducted. The bibliography follows the appendix and annotates all sources and documents used in research and creation of this project.

II. Background & Theory

Chapter Overview

The purpose of this chapter is to provide relevant background information regarding *Bacillus anthracis* and UV radiation. Topics discussed in this section include DNA, photochemistry, DNA damage and repair, and spore structure. This section also previews the experimentation including the irradiation system used, configured with small, light-emitting diodes (LEDs).

DNA

Deoxyribonucleic acid (DNA) is a molecule that contains the individual genetic code used to create new cells and life. Nucleic acids, lipids, proteins and carbohydrates are all necessary molecules for life. DNA double strand structure is composed of two anti-parallel strands containing the same genetic code. It has a double helical structure where the backbone is comprised of phosphorous ribose sugar molecules. DNA is a linear polymer with its repeating units having different component bases. Four bases make up the code in DNA: cytosine, guanine, thymine, and adenine. Adenine and guanine are purines and have double ring structures. Thymine and cytosine are pyrimidines and have a single ring structure. Because of geometry and hydrogen bonding between the bases, adenine exclusively pairs with thymine and cytosine exclusively pairs with guanine. Figure 1 below shows the hydrogen bonding of pyrimidines and purines [11]. Adenine and thymine linkages are held together by two hydrogen bonds. Cytosine and guanine linkages are held together by 3 hydrogen bonds. Therefore, CG bonds are stronger than AT bonds.

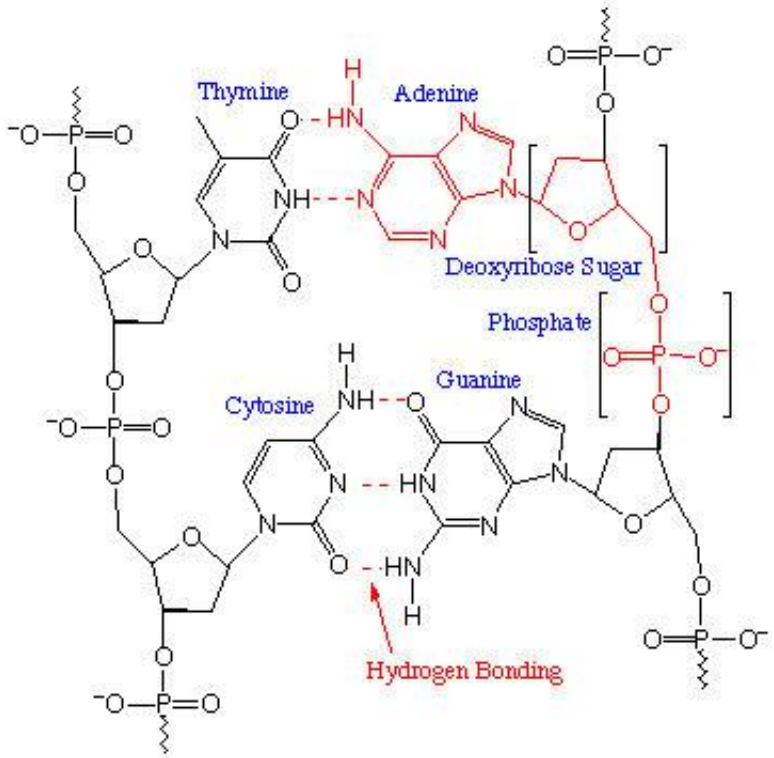

Figure 1. Structure of DNA. Cytosine and Guanine form the stronger of the two bonds across the sugar backbones. Thymine and Adenine form the weaker of the two bonds. The strength of the bond across the two DNA strands directly correlates to the hydrogen bonds. Figure reprinted with Permission from [11].

When DNA is not actively being used to synthesize new DNA, it is wound tightly into chromosomal structure, which serves to protect the DNA. The DNA is coiled several times and wrapped tightly around proteins. The wrapping helps the DNA keep its chromatin structure. When DNA is to be replicated, enzymes unwind the chromosomal DNA. Therefore, DNA is not specifically used for any function other than a storage library for the genetic code. Therefore, the cell protects and preserves the DNA as much as possible. If damage occurs and is not repaired or repaired improperly, mutations may occur in descendant generation cells.

DNA can take on several different conformational forms. B conformation of DNA (B-DNA) is the most common form under aqueous, low salt conditions. When Watson and Crick first discovered the structure of DNA, they were primarily studying B-DNA with X-ray diffraction [12]. In most typical cells, the B conformation is predominant [13]. While Watson and Crick were aware of a second DNA confirmation, A-DNA, it has just recently been studied in detail. A-DNA is most prevalent in low-water content and high salt environments [12]. A-DNA is more compact than B-DNA, which helps protect the DNA. The difference between A-DNA and B-DNA is discussed later regarding its importance in this project. DNA inside the spore adopts A-DNA conformation, leading to unique DNA damage called the spore photoproduct. Other confirmation forms of DNA exist including Z-, C-, D-, and E-DNA, but are not relevant to this project.

Ba encapsulates its DNA deep within the spore. However, the DNA is still susceptible to damage via heat, chemicals, and radiation. UV radiation, or photochemistry, causes conformational changes of the DNA within spores, which help to better protect the DNA.

Photochemistry

Photochemistry involves chemistry following the absorption of one or more photons; for this project, photons in the ultraviolet energy range. Absorption of a photon by a molecule causes an electronic excitation to quantized excited states described by quantum mechanics. The collection of additional energy in the form of UV light causes molecules to undergo vibrational-electronic (vibronic) excitation that can produce conformation changes and chemical changes. For DNA, the chemical changes can alter

the genetic code producing mutations that can ultimately lead to cell death or the inability of a cell to replicate. [1]

Calvert and Pitts consider photochemistry as a bimolecular reaction in which the two reactants are light and a molecule [14]. The light and molecule interact and undergo chemical and/or physical changes. Therefore, it is important to discuss light when discussing photochemistry. Because light can cause a heating effect much like the sun does, and because energy is defined as heat or anything transferable to heat, light is considered a form of energy [14].

Photochemistry follows a set of laws discovered in the 1800s. The first law of photochemistry discovered by Grotthus (1817) and Draper (1843) states: Only the light which is absorbed by a molecule can be effective in producing photochemical change in the molecule. The second law of photochemistry, also termed the photo-equivalence law, states: For each photon of light absorbed by a chemical system, only one molecule is activated for subsequent reaction [14]. The second law was developed in large by Max Planck's discovery of quantum theory. Planck believed that molecules could only absorb fixed quantities or quanta of light energy. Planck related this light energy, E to the frequency of light as seen below:

$$E = h\nu \qquad (1)$$

Where h is Planck's proportionality constant and ν is the frequency of light or radiation. Quantum yield is defined as the number of defined events occurring per photon absorbed by the system [15]. In photochemical reactions, quantum yield Φ is calculated

[1] For the purposes of this research, "cell death" is considered to be the inability to outgrow a viable colony of daughter cells.

for any resulting product. Given the following chemical reaction where B is formed from the decomposition of A and hν signifies light radiation,

$$A + h\nu \rightarrow B \qquad (2)$$

Φ_B=Molecules of B formed per unit volume per unit time/quanta of light absorbed by A per unit volume per unit time [14]. Quantum yields of photochemical reactions are used to determine the rate of photon absorption using chemical actinometers, to be discussed further in later sections.

The ultraviolet spectrum is divided in three sections: UV-A (315-400nm), UV-B (280-315nm), and UV-C light (100-280nm). The UV light used in this project is UV-C light at approximately 267 nm. UV-C light is the most harmful and causes the most DNA damage [16]. UV-A light acts a photo-sensitizer and the damage may be easily reversed. UV-B and UV-C radiation causes more damage and more complex repair mechanisms are required [16].

The sources of UV irradiation used in this project are small, light emitting diodes (LEDs). The LEDs are flat windowed and composed of aluminum gallium nitride (AlGaN) semiconducting material. Research using these AlGaN LEDs is a new exploration, and not without its issues. Experimentation during this project revealed the LEDs burn out if the current exceeds 20mA. These LEDs are of great interest for use in waste water treatment facilities because they contain no mercury and can therefore be disposed of more easily, they require no start-up or warm-up time, and can be powered on and off quickly [9]. Würlte et al. studied the emission power of AlGaN LEDs over time. Their study showed that LEDs lose emission power significantly over 100 hours.

Figure 2 below displays this relationship [9]. After 30 hours of operation, their emission output declines linearly and slowly, but not negligibly, at about 0.2% per hour.

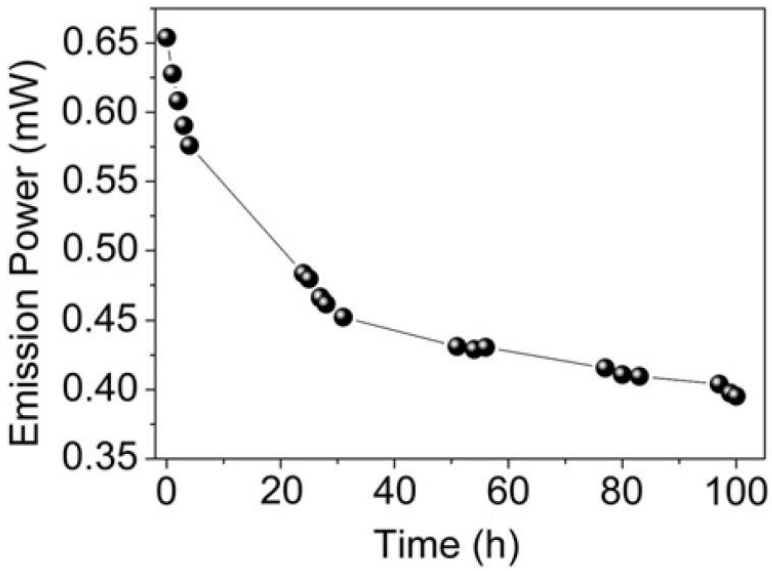

Figure 2. Emission Power of AlGaN LEDs over time. LED emission power decreased 40% over 100 hours of operating time. LED Emission power decrease also caused an increase in series resistance of about 1 Ω. Figure reprinted with permission from [9]. Copyright 2011 Elsevier

The emission power decreased 40% after 100 hours of operation. However, this decrease in emission power did not change the emission wavelength (269 nm) [9]. This change in emission power will alter the efficiency of the LEDs to inactivate Ba spores. To account for this near-linear diminishment in light output, actinometry experiments were conducted. The potassium iodate/iodide chemical actinometer was used to measure fluence before and after irradiation experiments are conducted to monitor changes in the LEDs.

Actinometry measurements will allow for better characterization of the UV irradiation imposed upon the Ba spores. To understand the protection mechanisms the spore offers to its DNA, the next sections describe the Ba spore in detail.

Bacillus anthracis

The organism *Bacillus anthracis* is found naturally in domesticated and wild animals; such as sheep's wool. In unfavorable conditions lacking nutrients, the organisms sporulate. Figure 3 below shows a microscopic image of both Ba cells and spores [17]. Bacillus organisms, including Ba, form long chains of rod like structures stained black in Figure 3. Endospores are seen in Figure 3 as light orange, ovular structures. Cells that have just sporulated are still connected in long chains. Spores that are released from the vegetative cells are isolated or conglomerated with other spores in clumps. It is common to see cells and spores together as neither germination nor sporulation are simultaneous for all cells. One study by Pandey showed the start of germination occurring on average around 63 minutes after LB-MOPRs germination media with AGFK germination salts was added. However, the germination process had a standard deviation of 56 minutes, showing that not all spores within the same preparation batch germinate at the same time [18].

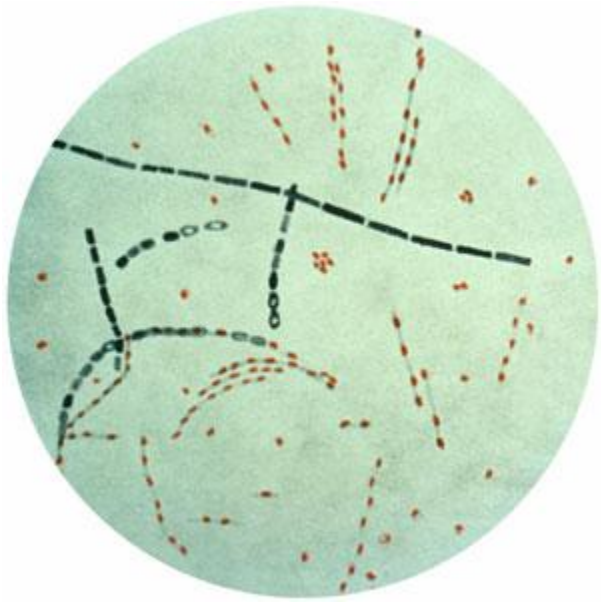

Figure 3. Microscopic image of both Ba cells and spores [17]. During sporulation and germination, cells and spores are often found occurring together as not all individual organisms sporulate/germinate simultaneously. Spores are shown as light orange and ovular. Cells are rod-shaped and form long chains. Figure reprinted with permission from [17]. Copyright 2002 John Wiley & Sons.

When forming a spore, the cell dehydrates, binding its DNA securely with small, acid-soluble proteins (SASPs). The DNA is ensconced in a matrix of mainly calcium dipicolinate. Metabolic activity ceases and the cell's membrane breaks open, ejecting the spore [19]. Spores of Ba are extremely resistant to the environment and can survive in soil for decades [2]. Since the spore contains few energy compounds such as ATP and limited water, no metabolic activity takes place. The spore also lacks enzymatic activity and therefore cannot repair DNA damage until germination and outgrowth stages [20]. If too much damage occurs while the spore is dormant, the repair systems may become overwhelmed, and germinated spores may not survive to outgrowth or even be able to germinate. The endospore (commonly referred to as a spore) has a well-engineered survival mechanism for many different bacterial species, including *Bacillus anthracis*. The spore is an ovular structure with layers of protection surrounding its core where the

DNA is contained. Figure 4 below depicts the structure of a typical spore. The outermost layer, the exosporium, is not exhibited in all species but is considered an extension of the outermost core layer for some species. The exosporium contains special coat proteins, the function of which is not entirely understood. The spore coat combines several smaller layers and contains at least 50 proteins [21]. The spore coat plays little role in resistance to UV radiation [22]. The next innermost layer, the outer membrane, is not fully understood but isn't thought to play a significant role in resistance to UV radiation [21]. The next layer, the cortex plays an important role in spore formation and outgrowth. During spore germination, the cortex breaks down and allows for expansion of the core and outgrowth [21]. The inner membrane protects the core, where DNA is stored tightly.

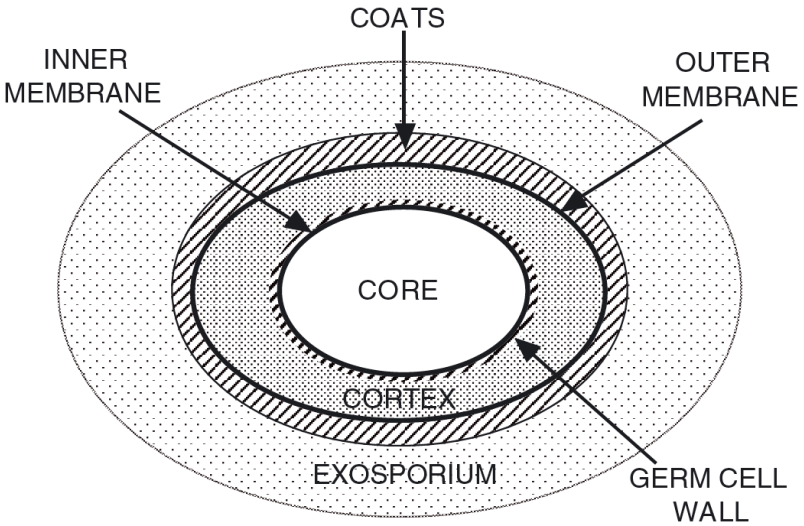

Figure 4. Layer structure of the spore. The inner core of the spore contains the well protected and tightly stored DNA. The layers in this figure are not to scale. Figure reprinted with permission from [21]. Copyright 2006 John Wiley & Sons.

When oxygen and nutrients are conducive for growth, the spore undergoes the process of germination. Figure 5 below shows a flow chart of occurrences during spore germination [20]. The process of germination converts the dormant spore back into a growing cell. The germination process is well described by Peter Setlow [20] and is reiterated below. A special mixture of asparagine, glucose, fructose, and potassium ion (AGFK) initiates spore germination. The initiation (activation) process is yet to be well understood. During Stage 1 of germination, a cation release from the spore coat causes a change in pH. This pH change is essential for enzymatic activity which will occur during germination. Following this pH change, the spore core releases its storage of dipicolinic acid (DPA) and replaces it with water. Replacement of DPA with water suggests that at this point, the spore has a decreased resistance to wet-heat [21]. Stage 2 involves more hydration, first hydrolysis of the spore cortex. The spore core begins to swell as water content increases. After this large increase of water, protein motility begins and enzymatic activity is initiated. The outgrowth period of germination is the only step that contains enzymatic activity. The germination process is of importance to this project because it is well known that DNA repair occurs mainly during the germination process [23].

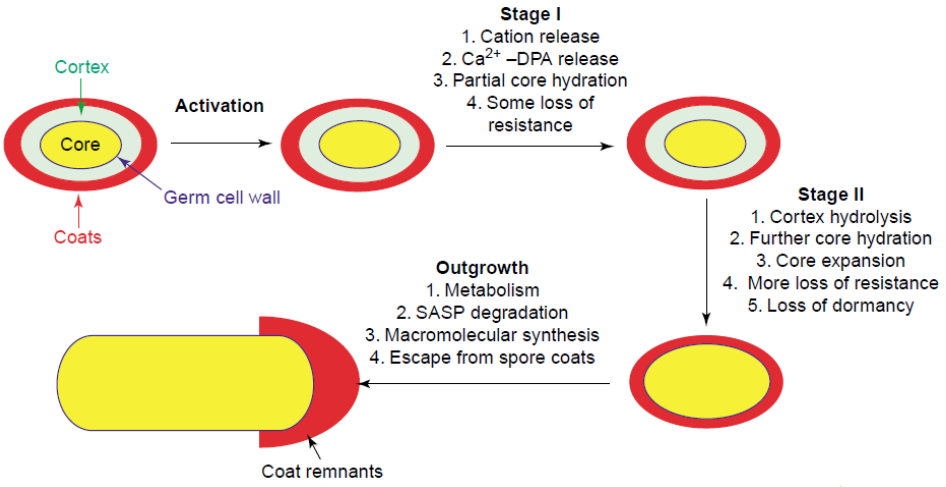

Figure 5. The spore germination process. Germination occurs in 2 main stages. The initiation/activation step involves the enrichment of nutrients. Stage 1 involves release of DPA and hydration of the spore core. Stage 2 involves further hydration and swelling of the spore. During outgrowth, the cell eventually emerges from the spore as metabolic and enzymatic activity reinitializes. Figure Reprinted with Permission from [20]. Copyright 2003 Elsevier.

Spores contain two unique substances which are involved in the relationship between DNA damage and UV irradiation: dipicolinic acid (DPA) and SASPs. Ba spores contain three main SASPs, α, β, and γ [24]. These SASPs are created during sporulation and degrade very quickly during germination. Dr. James Mason studied spores lacking one or more of these SASPs [24]. His studies on α and β type SASPs determined that spores without these SASPs had significantly increased UV radiation sensitivity. Dr. Ralf Moeller et al. also confirmed these findings regarding UV radiation and ionizing radiation [25]. Evidence supports a connection between SASPs and DPA, but the mechanistic connection is not well known. Dr. Barbara Setlow studied this connection. Spores with an intentional deficiency of DPA were studied. These DPA-less spores lacked the γ SASP altogether [26]. Dr. Setlow also found that spores lacking both DPA and SASPs were not viable following heat and irradiation because of extensive DNA

damage [26]. Figure 6 below displays the absorbance spectrum of DPA, with respect to wavelength [27]. The figure displays the changes in optical density of DPA and Calcium DPA (CaDPA) before and after UV light exposure(100J/cm^2) by a 450W ozone-free xenon arc lamp. A small shift in wavelength is observed following exposure to UV light. This shift is not well understood. Research of DPA suggests it acts as both a protectant of DNA and a photosensitizer. One study by Thierry Douki concluded that photoexcitation energy is transferred from DPA to thymine residues (the main form of DNA damage inside spores) [28].

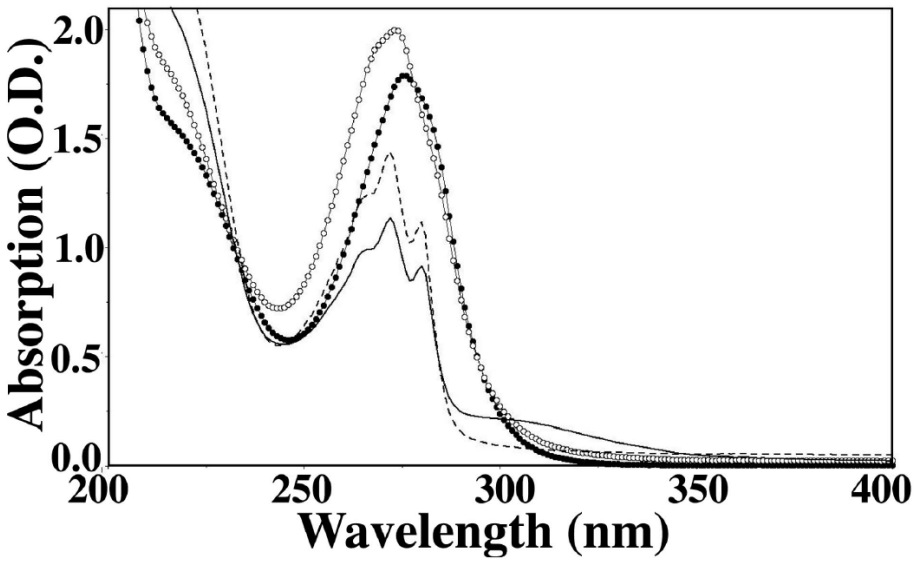

Figure 6. Absorption spectra of DPA. The absorption was measure using optical density of the samples. The unfilled-circles represent DPA prior UV light. The closed-circles represent DPA absorption following UV light exposure (100J/cm^2) by a 450W ozone-free xenon arc lamp. The dashed line represents CaDPA prior to UV light and the solid line represents CaDPA absorption following UV light exposure under the same conditions as the DPA. A small shift in wavelength is observed following exposure to UV light. Figure reprinted with permission from [27]. Copyright 2005 OSA.

DNA Damage

DNA damage caused by UV radiation is well known. Dr. Jean-Luc Ravanat studied the effects of UV radiation on DNA and its components [29]. DNA is a major target of UV radiation as it directly absorbs the photons of excited light. Discussed below are the main photoproducts observed from UV-B radiation. UV-C radiation exhibits the same photoproducts, but to a much more severe extent. The radiation used in this project (267nm) is near the absorption maxima of DPA, in the UV-C range.

Of the four bases in DNA, thymine is most sensitive to UV radiation. In most cells, genomic DNA is of the B-type conformation. This conformation leads to several widely recognized thymine dimers in the presence of UV radiation: the cyclobutane pyrimidine dimer (CPD) and the pyrimidine (6-4) pyrimidone photoproduct (PD) are the main two dimers [13]. Figures 7 and 8 below show the formation of CPDs and (6-4) PD dimers [29]. Figure 7 displays the formation of thymine cyclobutane dimers. These dimers arise from a [2+2] cycloaddition of the C5-C6 carbon bonds [29]. There are six diastereomers that can be generated from these cycloadditions because of cis/tran stereochemistry. The formation of these Pyr<>Pyr dimers can be repaired by UV-C radiation by splitting the cyclobutane ring.

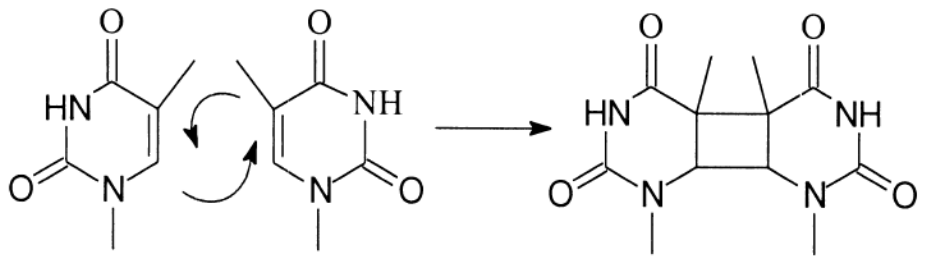

Figure 7. Thymine cyclobutane dimer formation [29]. The dimer formed is a [2+2] cycloaddition that occurs at 5th and 6th carbon positions (across the double bond) between two adjacent pyrimidines. While thymine-thymine CPDs are most common, other combinations of pyrimidine bases can undergo the same cycloaddition. Figure reprinted with permission from [29]. Copyright 2001 Elsevier

Pyrimidine (6-4) pyrimidone photoproducts are another type of DNA damage that cells can incur. It is known and well understood that the cell repairs (6-4) photoproducts at a faster rate than it repairs CPDs [30]. Figure 8 shows the production of the (6-4) photoproduct. UV-C or UV-B light first forms an unstable oxetane. Spontaneous rearrangement leads to the (6-4) photoproduct formation.

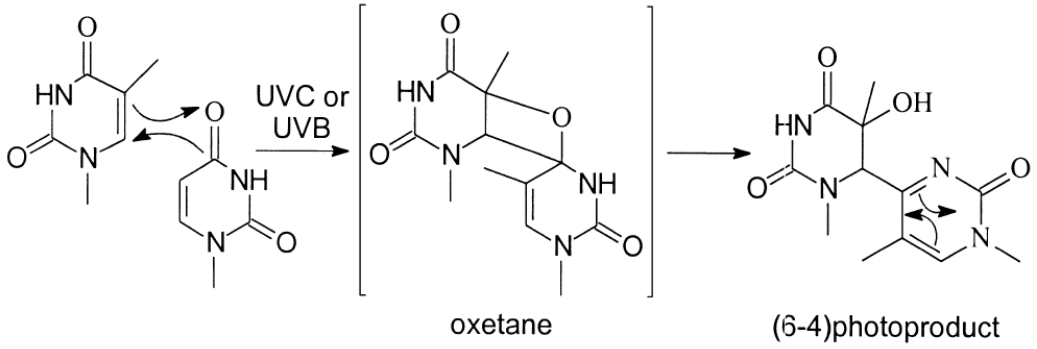

Figure 8. Pyrimidine (6-4) Pyrimidone photoproduct. This dimer is created from a [2+2] cycloaddition as well. Figure reprinted and adapted with permission from [29]. Copyright 2001 Elsevier.

Unlike DNA in a vegetative cell, DNA inside the spore adopts A-DNA conformation. A-DNA only occurs in a low water, high salt environment; the spore exhibits this conformation, making the DNA in the spore's core one of the few known sources of naturally occurring A-DNA. Therefore, unique damage occurs inside the spore termed the spore photoproduct (SP). This project focuses on DNA damage inside the spore. According to a study by Setlow in 2006, SP is generated in Ba spores as frequently as are CPDs and PDs in cells [26]. However, SP is repaired far more rapidly by the spore photoproduct lyase (SPL) in active cells. Figure 9 below displays the spore photoproduct and its repair via SPL. SP is formed from an intermolecular H-atom transfer.

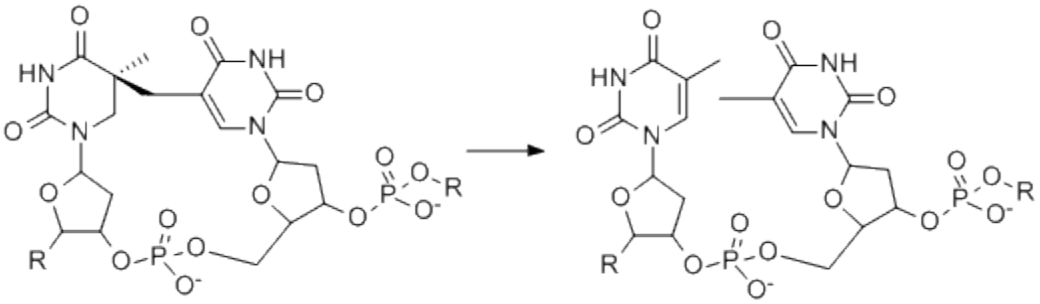

Figure 9. Spore Photoproduct. UV radiation causes thymine residues to form the spore photoproduct (SP). The spore photoproduct lyase is an enzyme that reverses this thymine damage. Figure Obtained from [13], open access article.

DNA Repair

Once DNA in the spore has been damaged, to achieve outgrowth it must be repaired during germination. The spores are at least 10 times more resistant to UV radiation than are Ba vegetative cells [31]. During germination, spores utilize two repair mechanisms: nucleotide excision repair (NER) and SP repair via spore photoproduct lyase (SPL) [13]. Repair of DNA in Ba spores does not begin until germination. Spores

of Ba exposed to UV-C light accumulate a special type of thymine dimer, the spore photoproduct (SP) [32]. The SP totals 95% of the UV-C damage incurred in the Ba spore [13]. The SP is then repaired during germination by two repair mechanisms: SP lyase and NER. The spore photoproduct occurs in place of other pyrimidine dimers because the chemical interactions between DNA and small acid-soluble proteins are unique to spores. Several mechanisms are proposed for the spore photoproduct lyase repair of the SP. The radical enzyme S-adenosyl methionine (SAM) is believed to be responsible for the repair of SP [33]. Figure 10 below depicts the mechanism through which spore photoproduct lyase repairs the spore photoproduct.

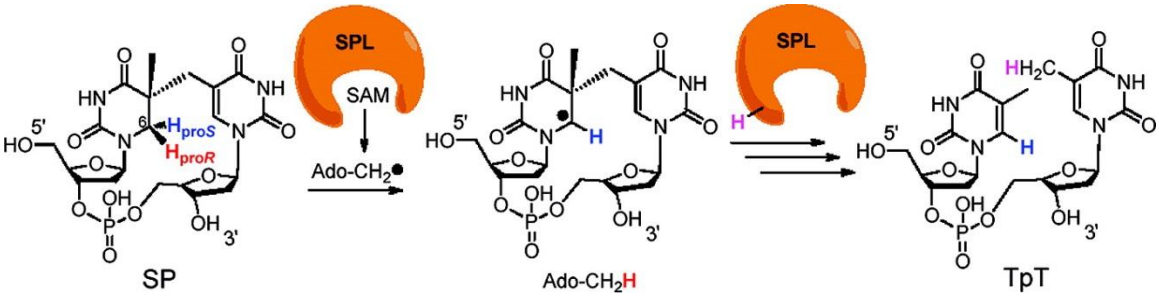

Figure 10. Spore photoproduct (SP) repair by Spore Photoproduct Lyase. A free electron originates from a 4Fe-4S cluster and is provided to the SAM enzyme molecule. Reductive cleavage of the C5'-S bond creates a reactive radical 5'-dA. The radical abstracts a hydrogen atom from the spore photoproduct, initiating the repair process [13]. Figure Obtained from [13], open access article.

The repair process that follows is detailed by Linlin Yang in her article titled "The Enzyme-Mediated Direct Reversal of a Dithymine Photoproduct in Germinating Endospores" [13]. The SAM enzyme uses a tri-cysteine motif to bind to a cluster of iron-sulfide compounds (4Fe-4S). The 4Fe-4S compound provides an electron to the SAM, reductively cleaving the C5'-S bond. This cleavage creates a highly reactive radical, 5'-deoxyadensoyl (5'-dA). The radical created then abstracts a hydrogen atom from the C6

carbon of the SP. This initiates the repair process. The new SP radical fragments to create a thymine methyl radical. The thymine radical accepts hydrogen back and creates the repaired TpT. The hydrogen donor is believed to be a neighboring cysteine [13].

Nucleotide excision repair (NER) is a more common method of DNA repair, not exclusive to spores. In NER, the damaged portion of a single strand of DNA is removed. The undamaged portion of the complementary DNA strand is used as a template to repair the damaged section. UVrA, UVrB, and UVrC endonuclease enzymes also play important roles in repair of the DNA [34]. UVrA recognizes the distortions in the DNA caused by the dimers. UVrB and UVrC form a complex capable of cleaving the template DNA 4 bases down from the damage [34]. DNA helicase II removes the excised fragment of DNA. DNA polymerase synthesizes the new, repaired portion and DNA ligase binds the two single strands back together. A similar repair mechanism, base excision repair, reverses single base pair damage. Double stranded DNA damage can occur when two single strand breaks are in close proximity to each other. Double stranded breaks are most damaging to the cell and hardest to repair. This project will focus not on specific repair mechanisms, but rather the rate at which damaged DNA is repaired inside the spore.

DNA damage and repair play an important role in this research. The AFIT research program aims to understand, and possibly even model the kinetics of DNA repair. However, to accurately measure UV radiation to which the Ba spores are exposed to, actinometry experiments are necessary. The next section introduces actinometry and its importance with radiation measurements.

Actinometry

An actinometer measures the number of photons available in a photochemical system via photochemical reactions where the quantum yield is well known [35]. Actinometers also require a thermally stable reaction. Equation 3 below shows a commonly used iodide-iodate chemical actinometer [35].

$$8I^- + IO_3^- + 3H_2O + hv \rightarrow 3I_3^- + 6OH^- \qquad (3)$$

Upon UV exposure, as the reaction shown in Equation 3 progresses in the forward direction the photoproduct, the tri-iodide compound (I_3^-), is created. The tri-iodide complex has a maximum absorption at 352 nm. This particular actinometer can be used in room light, as it does not react to UV light at wavelengths greater than 320nm [35]. By performing an actinometry experiment, the exact number of photons occurring in the UV reactor for this research can be determined.

For the actinometer to accurately represent this research, it must mimic closely the actual UV radiation experiments. Sample volume and reaction conditions must be kept consistent with the UV experiments. The quantum yield of the actinometer is calculated using the following equation [35]:

$$\Phi = \frac{Moles\ of\ I_3^-}{Einsteins\ of\ UV\ light\ absorbed\ at\ Wavelength\ \lambda} \qquad (4)$$

The KI/KIO_3 actinometer is temperature dependent. RO Rahn, 2003 reported the temperature dependence of the KI/KIO_3 actinometer between 22°C and 42°C [36]. The temperature dependence can be easily accounted for as it has been well studied and is typically linear. Figure 11 below reports the linear regression of data from Rahn's study in 2003 showing the linear dependence on temperature of the KI/KIO_3 actinometer quantum yield.

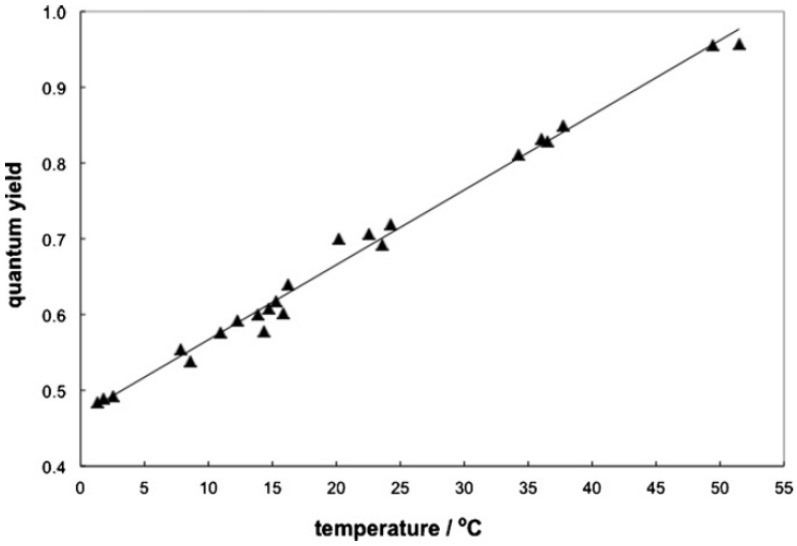

Figure 11. The linear temperature dependence of the KI/KIO_3 actinometer. The temperature dependence of the KI/KIO_s actinometer shows the need for temperature measurement and control in the lab apparatus. This linear regression was created using multiple temperatures, each point representing 1 to 5 replicates. Figure reprinted with permission from [36]. Copyright 2007 John Wiley and Sons.

The temperature dependence of the quantum yield at 253.7nm is seen below where t is temperature in degrees Celsius.

$$\Phi = (0.471 \pm 0.020) + (0.0099 \pm 0.0004)t \qquad (5)$$

Equation 5 will be used to adjust for lab temperatures on various experiment days. A collection of quantum yield values at varying wavelengths was collected by NIST at 23.5°C ±1°C [35]. As quantum yield is also apparently linear with wavelength over a narrow range, the calculated yield at (21°C and 22°C) will be compared to NIST data collected at a higher temperature. To accurately compare the NIST quantum yield data with the yield determined in these experiments, the quantum yield from NIST will be adjusted using equation 5 above to correlate to the temperature of these lab experiments.

PCR

Studying DNA damage and repair is often achieved using polymerase chain reaction, PCR. Studying DNA quantitatively requires PCR, as it exponentially increases the copies of DNA present in sample. In a PCR procedure, DNA is heated and cooled in a cyclical process. PCR was developed by Kary Mullis in 1983 and is only made possible by use of a unique enzyme from the bacterium *Thermus aquaticus*. This enzyme is nicknamed Taq polymerase and is stable under high temperatures, as the bacterium originates from hot spring geysers. In the presence of the appropriate primers (short single-stranded DNA fragments), bases and enzymes, the DNA is heated (to approximately 95°C) and the strands separate. The reaction is then cooled to around 60°C. In principle, the shorter DNA fragments termed primers are statistically more probable to recognize their match in the two single strands than for the two single strands to recognize each other and re-anneal. The primers are the starting point of double stranded DNA for the Taq polymerase to perform synthesis. When the primer attaches it begins to synthesize a specific section of the DNA strand. The process of heating and cooling is typically repeated approximately 40 times, yielding only the sequenced strand designated by the primers. Primers for this research were chosen to operate across the red fluorescent protein (RFP) in the plasmid.

This project utilizes a specific type of PCR, termed real-time PCR. Real-time PCR tracks the DNA amplification in real time and allows for quantification. Real-time PCR can be used in two main ways. The first method employs a fluorescent dye that only intercalates into double-stranded (DS) DNA. SYBR Green is a commonly used DS-DNA intercalated dye. This project utilizes the second method, which employs a probe which

carries a combination quencher/fluorophore pair. Prior to sequence binding, the quencher and fluorophore are in close proximity and fluorescence signal is quenched. When the primer synthesizes and reaches the probe, the quencher and the fluorophore are separated. The quencher and fluorophore are no longer in close proximity, so the fluorophore fluoresces. The real-time PCR reads the fluorescence from the fluorophore. For every amplification, the fluorescence increases. In this way, the probe is used in tandem with real-time PCR to determine amplification based on relative fluorescence intensities.

Gel Electrophoresis

PCR is an effective and useful method to amplify DNA. Gel electrophoresis is often used in tandem with PCR to determine size of amplicons. Even when Real-time PCR is performed, gel electrophoresis is used to confirm the fragments of interest are indeed the DNA being amplified by the primers. Gel electrophoresis applies an electric field, which causes the negatively charged DNA molecules to move through an agarose gel. The length at which the DNA fragments move through the gel is determined by their size. Smaller fragments move fastest through the gel and large fragments move the slowest. The fragments are then compared to a DNA ladder, a series of known fragments resolved on the gel as well. With the help of software, concentration of DNA can even be determined based upon the intensity of bands resolved in the gel.

Atomic Force Microscopy

Atomic force microscopy (AFM) is one type of scanning probe microscopy. AFM uses a sharp tip, termed the probe, to very carefully scan the surface of a sample. The tip is attached to a thin, long arm, called the cantilever, that rasters the tip back and forth

across the sample. The tip never touches the sample; rather the cantilever is deflected with respect to the forces of attraction between the tip and the sample. Deflection of the cantilever is the actual measurement used by the AFM to map out the surface topography of a sample. Cantilever deflection obeys Hooke's law seen below,

$$F = kX \tag{6}$$

Where F is the force applied to extend the cantilever X distance, and k is the spring constant [37]. Force, pertaining to AFM, can be attributed to van der Waals forces, chemical bonding, capillary force, electrostatic force, and more.

AFM has been used to characterize Ba spores, although it is not widely popularized. Dr. Xing and Dr. Li from AFIT utilized AFM to study surface changes in spores following exposure to high temperatures. They observed nanoscale blister-like structures on the surface of the spore using a heated AFM tip [38]. Figure 12 below shows spores: a) prior to heat treatment b) following heat treatment.

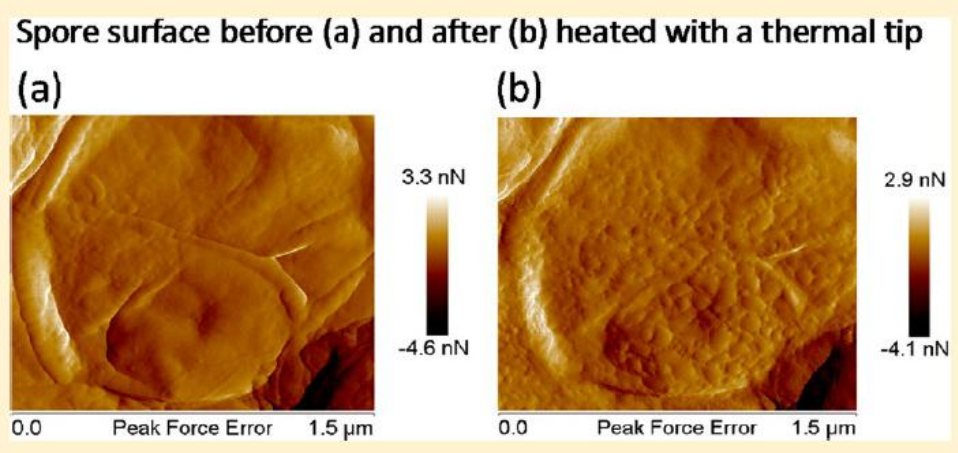

Figure 12. AFM images of *Bacillus anthracis* spores before (a) and after (b) heat treatment with a heated AFM tip. Nanoscale blister-like structures were observed on the surface of the spores following heat treatment. Figure reprinted with permission from [38]. Copyright 2013 American Chemical Society.

III. Methodology

Chapter Overview

This chapter details the methods developed and adapted to characterize DNA damage in *Bacillus anthracis* (Ba) Sterne spores by UV radiation at ~267nm. The pRB373 plasmid with a turbo-red fluorescent protein (RFP) [10] was transformed into Ba cells prior to UV radiation and the cells were allowed to sporulate. Spores were then irradiated at 267nm and allowed to repair for various times including prior to germination, immediately following germination, and during vegetative outgrowth. Following irradiation and repair, the plasmids were isolated and their DNA analyzed using PCR and selectively designed primers. Also detailed in this section is the development of Ba sterne inactivation curves, as well as actinometry experiments that were used to determine the efficiency and quantum yield of the LED reactor.

Microbial Technique

Initial samples of the pRB373 plasmid [10] and Ba Sterne were provided by Dr. Thomas Lamkin and his research group at AFRL USAF-SAM [39]. When the plasmid was successfully transformed into Ba Sterne, the cells/spores were a bright pink hue. The plasmid carries ampicillin resistance (AmpR)[2].

E. coli Transformation

In order to enumerate the plasmid, transformation was first performed into Escherichia coli (E. coli) following the protocol provided with the competent E. coli cells [40]. A pre-measured tube from the manufacturer of DAM-/DCM- cells was thawed until

[2] See Appendix for Plasmid Information sheet.

the ice crystals disappeared. The tube was gently mixed by hand and 50 µL of DAM-/DCM- cells were added to a transformation tube on ice. A transformation tube can simply be a 1 or 2mL micro centrifuge tube. 5µL of plasmid was added to the cell mixture. The concentration of plasmid DNA was 47.3ng/µL. The tube was flicked by hand 4 to 5 times, allowing the cells and DNA to mix[3]. The resulting mixture was placed on ice 30 minutes. The mixture was then heat shocked at exactly 42ºC for 30 seconds. Immediately following heat shock, the mixture was placed on ice for another 5 minutes. Afterwards, 950µL of SOC[4] (a chemical provided in the transformation kit) was added to the transformation tube. The new mixture was then incubated at 37ºC for 1 hour with vigorous shaking (approximately 150-200 rpm). While incubating the sample, selection plates (LB media with 50µg/mL ampicillin) were allowed to warm. Ampicillin selection plates are used because the plasmid contains a marker gene for AmpR. If the E. coli cells were successfully transformed and contain the plasmid, they will have AmpR and will grow on the selective plates. Following incubation, 100µL of the transformation mixture was placed on selective media. A multitude of colonies were observed 12 hours later, indicating transformation had occurred. An isolated colony was inoculated in an overnight culture with 50µg/mL ampicillin to enumerate the plasmid DNA.

Plasmid Isolation

Plasmid isolation was performed using the overnight culture. When isolating the plasmid, the goal was to get a high plasmid yield (100ng) to prepare for transformation

[3] Vortexing can be damaging and should not be used at this step.
[4] SOC: Super Optimal Broth with added Glucose. SOC is a super nutrient rich growth medium.

into Ba. It can be difficult to transform into Ba and a higher plasmid concentration increases the probability of success. Plasmid isolation, properly termed plasmid purification, was performed following the Qiagen EndoFree Plasmid Maxi-Prep Purification Handbook [41]. The bacterial culture enumerated the night before was centrifuged at 6000 RCF (relative centrifugal force) for 15 minutes at 4° C. Following the buffer labels in the maxi-prep lot, the bacteria pellet was suspended in 10mL of buffer P1. 10mL of buffer P2 was then added and mixed thoroughly by tube inversion at least 4 times. The mixture was incubated at room temperature for 5 minutes. Following incubation, 10mL of chilled buffer P3 was added to the mixture tube and inverted and shaken strongly (but not vortexed) 4-6 times. This lysate mixture was placed into the plunger included with the kit and incubated for 10 minutes. The lysate filtered by gravity within about 20 minutes. Following filtration, the filtered lysate was saved. 2.5mL of buffer ER was added to the filtered lysate and incubated on ice for 30 minutes. 10mls of buffer QBT was added following incubation and the column emptied via gravity flow again within 20 minutes. The column was washed twice with 30mLs of buffer QC each time. The DNA was then eluted with 15mL of buffer QN. The eluted DNA can be precipitated if necessary but was left in solution for future purposes. Using a Nano-Drop 2000c, the final plasmid concentration was determined. Agarose gels and/or UV spectrometry can also be used to measure the final plasmid concentration. The Qiagen protocol details these measurement techniques [41].

Transformation/Electroporation into Ba

In order to transform the pRB373 plasmid into Ba, electroporation was utilized. Electroporation applies an external electrical field to a sample mixture of plasmid and cells. The increase in electrical conductivity causes the permeability of the cell membrane to change, and eventually incorporate a plasmid into the cell. This process is termed transformation. Electroporation transformation protocol was taken from Koehler et al. [42] using a Bio-Rad Gene Pulser Xcell Total System. An overnight culture of Ba cells was prepared. One milliliter of the culture was added to 100mL of Blood Heart Infused (BHI) media with 0.5% glycerol. The sample was incubated with vigorous shaking at 200rpm. When the optical density (A_{600}) reached 0.6, the cells were harvested by centrifugation. Cells were washed four times with 25mL of ice-cold electroporation buffer, suspending the cells and centrifuging after each wash. The electroporation buffer was made prior to experimentation (1mM HEPES, 10% glycerol, pH 7.0). Following washes, the cells were re-suspended in electroporation buffer to 5mL. Approximately 3µg of plasmid DNA was added to 0.4mL of the cell suspension on ice in a pre-chilled 0.4cm-gap electroporation cuvette made by Bio-Rad [43]. Ba cells were exposed to one electrical pulse at 2.5kV, 25µF and 400Ω. Immediately following the pulse, the cells were transferred to a solution of 1mL BHI with 10% glycerol, 0.4% glucose, and 10mM $MgCl_2$. The solution was incubated for 1 hour so expression of the antibiotic resistance could occur prior to plating on selective plates (50µg/mL of ampicillin) [42]. Observable pink colonies on selective plating indicated successful transformation.

Spore Preparation

Scale-up Cultures

Following successful transformation, the Ba cells were used to prepare spores to be used for experimentation. The procedure for sporulation was adapted from Leighton and Doi [44]. Using ampicillin selective TSA plates, a culture of Ba was streaked and incubated at 37°C overnight. From a well isolated colony on the overnight plate, a 2X nutrient broth was inoculated. Nutrient broth is used at a volume 1/10th the intended volume for the subsequent spore culture. 20mL of nutrient broth was used for this project. The new culture was incubated at 37°C and 130rpm overnight.

Inoculation of Spore Culture

200mL of Leighton-Doi Spore Media[5] and 20mL of the previous overnight culture was added to a 1L flask (5 times larger than the volume of culture) which allowed for air exchange. This culture was incubated at 37°C and 130rpm overnight. Sporulation was tested by removing about 10µL of culture to a microscope slide. The slide was observed under phase contrast at 1000X. Culture ready for harvest exhibits mostly phase bright spores.

Harvesting spores

Spores were centrifuged at 8000rpm for 20 minutes at 4°C. Supernatant was removed and spores re-suspended in ice cold water via repetitive pipetting. Spores were pelleted by centrifugation under the same previous conditions. Three more additional

[5] See Appendix for Leighton-Doi Media recipe

washes were repeated. Spores were re-suspended in 3mL of phosphate buffered saline with 0.05% Tween (PBST) [45]. PBST acts as a detergent and prevents spores from clumping and aggregating. Spores were stored in suspension at 4°C.

LED UV Irradiator

This section explains the reactor used to perform UV irradiation experiments. Figure 13 below displays the UV reactor. 7 light emitting diodes (LEDs) surround the bottom of the reactor. The LEDs were purchased from Sensor Electronic Technology Incorporated (SETi), part number UVTOP260TO39 [46]. The LEDs peak at the wavelength 267nm. Before adhering of the LEDs to the reactor cell with silicon putty, they were first characterized using an integrating sphere [47]. The integrating sphere accurately measures the power output of the LEDs. Measurements were made in duplicate for each LED on the integrating sphere. The average power of all 6 LEDs used, determined by the integrating sphere, was 1.4mW. The same 6 LEDs were used for the entire experimentation period. Peak wavelength was measured for each LED and averaged to be 267nm. LEDs for purchase from SETi range in wavelength.

The wavelength of LEDs chosen mimics the UV-C range used in another similar study of UV irradiation on *Bacillus subtilis* [9]. A separate study validated *Bacillus subtilis* as a surrogate organism for Ba, as their UV inactivation curves are very similar [48]. The reactor radius measures 3.64cm and is composed of highly reflective stainless steel. The lid swivels on and off for easy sample collection but stays tightly shut during experimentation. LED configuration in direct contact with the radiation solution allows for a critical angle of UV output of 41.6 degrees. This higher critical angle increases the

optical efficiency by approximately 46% [8]. The entire reactor sits on a Thermo Scientific Max-Q 2000 shaker [49].

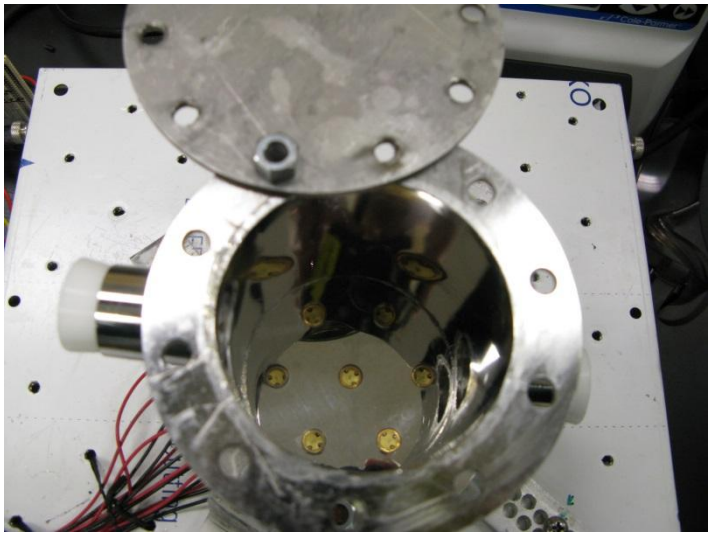

Figure 13. UV reactor designed by Michael Spencer, AFIT [47]. The reactor has 7 LEDs that irradiate from the bottom. Composed of stainless steel, the reactor allows for a high reflectance. LEDs are sealed with silicon to the bottom of the reactor. The entire reactor sits on a shaker, helping to prevent spore clumping.

During irradiation, the reactor shakes at approximately 120rpm. Shaking helps prevent the spores from aggregating on the sides of the reactor. The LEDs are extremely sensitive and burn-out instantaneously if current exceeds 20mA. Therefore, current flowing through the LEDs is maintained at 20mA using 25Ω variable resistors (also termed potentiometers). During experimentation, a voltmeter was used to monitor voltage and ensure proper usage/operation of the electronics. The UV reactor is connected to a power board and power supply, both of which are operated by DASYLab software [50]. Figure 14 below displays the circuitry configured for powering the LEDs. Once characterized, the LEDs were glued to the bottom of the reactor in Figure 13 using silicon putty. Then, the leads for each LED were soldered to wires on the bottom of the reactor.

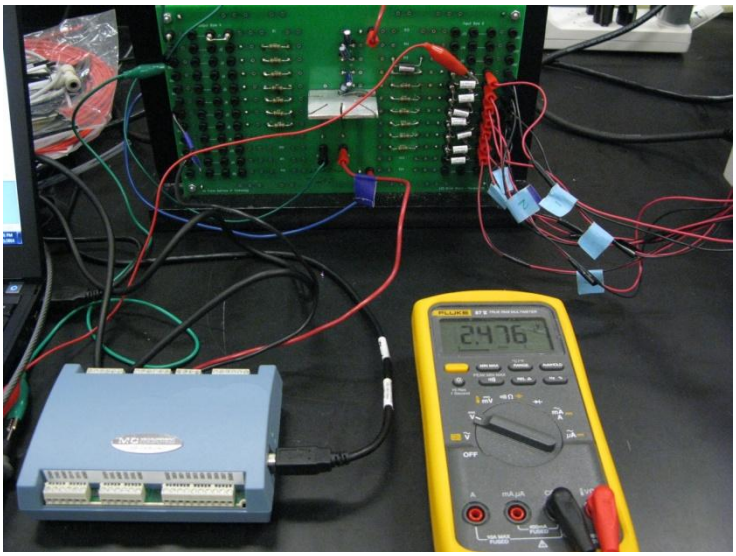

Figure 14. UV reactor circuitry board and DASY Lab interface. The seven LEDs plug into the circuit board in the locations in series with 20 ohm resistors. The power supply from DASY Lab is connected into the center of the board, where it then flows to the op-amp on the back of the board before coming back to the input of the LEDs.

Once characterized and glued to the reactor cell, the LEDs were ready to operate. Table 1 below displays the power measurements taken for the 6 LEDs used during experimentation[6]. More LEDs were purchased, but several burned out during the preliminary stages of testing. The ultraviolet transmittance (UVT) was taken as the value of UVT for deionized water, 0.975. The physical measurements for the reactor cell are also given in Table 1 below.

[6] 10 LEDs were purchased in total. Six to seven were used for the experimentation reactor (the reactor was operated with up to 1 LED burned out).

Table 1. LED Characterization and UV reactor measurements. The power output for each LED was measured using an integrating sphere. The Ultraviolet Transmittance (UVT) is the value of UVT in deionized water [9].

Radius (cm)	3.64
Cross-Sectional Area (cm^2)	41.74
Ultraviolet Transmittance	0.975
Number of LEDs	6
Peak Wavelength	267nm
Measured P (mW)	Average P (mW)
1.298	1.40
1.297	
1.46	
1.52	
1.466	
1.37	

Using the important information from Table 1 above, the UV fluence was then calculated as it related to dose time (in seconds). Table 2 below contains this information. Irradiance was calculated from the average power determined by the integrating sphere divided by the cross-sectional area of the reactor. Calculated fluence is a product of irradiance, UVT, number of LEDs and exposure time. These eleven data points were used as a starting point for experimentation. More collection time points were added to the survival curves as the important time regions became more apparent.

Table 2. Fluence/UV Dose Calculations. Irradiance is calculated from the average power divided by the cross-sectional area of the reactor. Fluence is calculated as the product of irradiance, UVT, number of LEDS, and exposure time. The following 11 data points were used to develop survival curves for Ba spores. Fluences were later adjusted by actinometry results.

Irradiance = Avg* P/Cross-Sectional Area		
Fluence = (Irradiance*UVT*Numbers of LEDs*Exposure Time)		
Exposure Time (sec)	Fluence (mJ/cm²)	Fluence (J/m²)
0	0	0
26	5.1	51
51	10.0	100
77	15.1	151
102	20.0	200
127	25.0	250
178	35.0	350
229	45.0	450
331	65.0	650
433	85.1	851
560	110.0	1100

Prior to irradiation with LEDs, actinometry experiments were first conducted. Fluence doses were later adjusted based on the apparent quantum yield determined by actinometry. The actinometer used for this project is a potassium iodide/iodate actinometer.

Actinometry

Actinometry measurements were taken before and after UV irradiation experiments to measure fluence by determining the number of photons per unit time. Chemical actinometers have been specially designed with a well-defined quantum yield. A potassium iodide-iodate actinometer was used for this project. The actinometer solution was prepared as follows: 9.96grams KI, 2.14grams KIO_3, and 0.381grams of sodium tetraborate ($Na_2B_4O_7$• $10H_2O$) to 100mL of deionized water. 60mL of water was

added to a 100mL volumetric flask, and then the chemicals were added. The solution was well mixed, and then diluted to volume[7]. The solution was added to the UV reactor. 3mL blank measurements were taken at 352nm, on a UV-Vis spectrometer for 10 minutes (one measurement reading every 30 seconds), the longest UV experiment time. The whole solution was then irradiated at time samples corresponding to those used for DNA damage and repair experiments. After each time point, a 3mL sample was collected in a UV cuvette and read on the UV spectrometer from 200-700nm. The room temperature was recorded throughout the experimentation, as the iodide-iodate actinometer varies with temperature. Actinometry experiments were performed before and after irradiation experiments and anytime reaction conditions changed (the most common changing reaction condition was LEDs being replaced and/or burning out). Whenever the number of LEDs in the reactor changed, new actinometry experiments were conducted.

Bacillus anthracis **Spore Survival Curve**

Survival Curves were developed to correlate UV dosage with surviving fraction of Ba spores. Ba spores of final concentration 1.0×10^7spores/mL were diluted from a stock concentration of spores in distilled, sterile water. The spore solution was placed in the UV reactor and a non-irradiated sample was taken and termed N_o. N_o represents the initial spore concentration, 1.0×10^7spores/mL. The UV reactor was then prepared and the shaker was turned on (~120rpm). The spores were irradiated for various times corresponding to specific doses of UV light. At each time point, the LEDs were turned off and a 100µL sample was collected. A serial dilution was performed for each

[7] The solution should be used within 4 hours and was kept in the dark.

collection point. Each dilution point was plated in triplicate and incubated at 37°C. The colonies were counted 18 hours later. Table 2 above shows the data collection points used for both actinometry and Ba survival curve experiments. The results of the survival curve determined proper UV dosage for DNA damage and repair experimentation. It was important to dose at a level that would create a large amount of DNA damage, but not so much as to completely inactivate all spores.

DNA Damage & Repair Experimentation

Determined by the survival curves, a 1-log kill was chosen for DNA damage and repair experiments. 1-log kill corresponded to approximately 100J/m^2. For the LED configuration in place, 100J/m^2 dose corresponded to 51 seconds with the LEDs on. Following actinometry corrections, 51 seconds actually corresponded to a fluence of approximately 88J/m^2. A spore concentration of 1.0x10^{7}spores/mL was prepared from a stock solution in distilled, sterile water. The spore solution was placed in the UV reactor. The LED reactor was then prepared as detailed in the LED reactor section and the shaker was turned on (~120rpm). The spore solution was dosed for 51 seconds (88J/m^2). Immediately following the radiation, 100mL of double strength germination media was added following protocol from research performed by Dr. Pandey [18]. This research tracked individual spores' progress through the germination and outgrowth stages using a newly developed technique which they termed the SporeTracker [18]. The germination media was LB-MOPS media with special germination "boosters" added [18]. These germination salts/sugars are termed "AGFK" which stands for the ingredients used: 10mM L-asparagine, 10mM glucose, 1mM fructose, and 1mM potassium chloride. The

LB-MOPs media needed to be double strength because it was added to the 100mL of spore solution, making it “single strength”. For this reason, the AGFK salts/sugars also needed to be doubled in concentration in the LB-MOPS media. Once media was added, the entire reactor and shaker were placed in the incubator. Samples were collected at various times to track the spores’ progress through germination, repair, and outgrowth. Atomic force microscopy (AFM) images were taken to help track spore progress through the germination and outgrowth processes. At each time point, triplicate 1mL samples were collected and stored for later PCR analysis at -20°C. These samples were washed several times by a centrifugation/re-suspension cycle. Following sample washes and collection, they were stored in the freezer at -4°C until PCR analysis. At each time point, a 100µL was also collected for serial dilution plating. Each time sample was plated in triplicate for each serial dilution point. Collection times were: Control (prior to irradiation), T=0 (immediately following irradiation), 30min incubation, 60, 90, 120, 150, 180, 210, 270, 330, 390, and 450min incubation. In addition to these samples collected, a second set of samples were collected. A 1mL sample of T=0 and the control sample were also incubated for the full incubation time (450 minutes). The second set of samples was collected to use as controls for the real-time PCR experimentation.

PCR

Sample Preparation

Following irradiation of Ba Sterne spores, the samples needed to be prepared for PCR analysis. The first step in sample preparation was to remove the DNA from inside the spore. DNA isolation was achieved using the bead beating method. Qiagen bead

beating kit ASAY-ASY-0503 was used [51]. The DNA isolation in a water sample protocol was used. A small amount of antifoam powder was added to each bead beating tube. Then, 800µL of sample (in water) was added to the tube. The tubes were placed in a disruptor Genie. The samples were bead beat on high for 5 minutes. Following bead beating, 60µL of proteinase K solution was added to a separate small receiver tube. If available, 10 µL of carrier RNA is also added. To the small receiver tube, 600µL of buffer AL was added. Finally, 600µL of the bead beaten sample was added to the small receiver tube. This mixture was vortexed quickly and then incubated in dry heat at 60° C for 1 hour. These initial steps cause physical lysing. Following incubation, new spin column tubes were labeled with sample names. Next, 600µL of ethanol (200 proof, molecular biology grade) was added to the heated sample and mixed by repeated pipetting. 600µL of the heated mixture was transferred to the pre-labeled spin columns. The columns were centrifuged for 1.5 minutes at 6000g. The centrifugation was repeated two more times using the same column, but with new collection tubes. Using a new collection tube, 500µL of AW1 buffer was then added to column and centrifuged for 1.5 minutes at 6000g. Using again a new collection tube, 500µL of AW2 buffer was added to the column and centrifuged under the same conditions. Following washes with the buffers, one final centrifugation cycle at 12000g for 3 minutes was performed using a new collection tube. The last portion of the sample preparation requires elution of the DNA off the spin column and into the final collection tube. To the spin column and a new small receiver tube, 230 µL of buffer AE (preheated to 68° C) was added. The column and elution buffer was incubated for 5 minutes at 68-72° C in a heat block or vacuum-drying oven. Following incubation, the column was centrifuged at 6000 g for 1.5

minutes. The spin column is discarded and the final solution contains the genomic and plasmid DNA. The DNA was stored at -20° C until analysis.

In order for PCR to function properly, primers are designed to amplify across certain portions of DNA. Table 3 below displays the primer sequences and probe sequence used in PCR reactions for this project. The primers and probe were all constructed using Primer3Plus, a program designed by Bioinformatics [52]. The primers and probe in Table 3 were designed across the RFP sequence. Also displayed in Table 3 are the primers' starting positions. During the PCR reactions, these primers yield two fragments (amplicons) of DNA; the forward primer and first reverse primer (RP1) yield a 245 base pair amplicon, and the forward primer and second reverse primer (RP2) yield a 547 base pair amplicon.

Table 3. Primer and Probe sequences. The two amplicons created with these primers are 245 and 547 base pairs in length. The primers and probe synthesize across the RFP inserted in the pRB373 plasmid. If DNA damage is too severe across the plasmid DNA, the primers may not attach and properly synthesize. As seen in the table, the left side of the Probe sequence encodes for the fluorescence. The far right side of the probe encodes for the quencher.

Name	Primer Sequence 5' to 3'	Position
Short Forward	CGTTACCATTCGCTTTCGAT	183
Short Reverse	CCGGACCATTACTTGGAAAA	428
Long Forward	CGTTACCATTCGCTTTCGAT	183
Long Reverse	TTAACGGTGCCCTAATTTGC	730
TaqMan Probe	6FAM-TCCCACGTAAATCCTTCAGG-MGBNFQ	306

During initial PCR experimentation, the FAM probe yielded no fluorescence. Temperature protocols were adjusted several times with no success. To continue on with sample analysis, SYBR Green was used in place of the probe[8]. Where the FAM probe

[8] See Appendix for SYBR Green Master Mix Recipe

binds specifically to the primer yielded fragments, SYBR Green intercalates into any double stranded DNA after the PCR extension step. SBYR Green is less specific, but works sufficiently for samples that are not contaminated and contain only the DNA of interest. No contamination presented itself during this project. Microscope images proved the evidence of clean samples during experimentation. Gel electrophoresis was also performed to confirm appropriate fragmentation. Figure 15 below shows the gel. Wells 1 and 2 (from the left) show two different ladders. Well 3 is isolated RFP DNA, where only one intense band is shown. This indicates a clean sample, free of contamination. Wells 4 through 8 are the dilution serious 10^1-10^5 of RFP DNA with the first reverse primer (This should be the shorter amplicon, 245 base pairs in length). Well 9 is the DNA ladder again. Wells 10-14 are the dilution serious 10^1-10^5 of RFP DNA with the second reverse primer (This should be the longer amplicon, 547 base pairs in length). And finally, well 15 is another DNA ladder. Wells 4-8 very clearly display an amplicon about half the length of the amplicon in wells 10-14. This gel confirms proper amplification of the designed amplicons in Table 3.

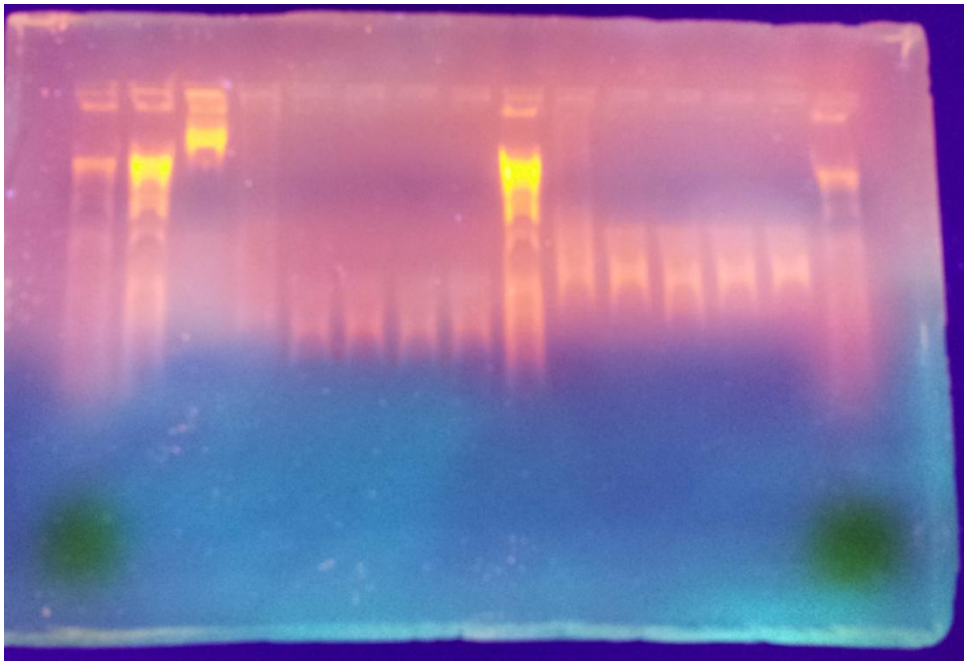

Figure15. Gel electrophoresis of PCR controls. Wells 1 and 2 (from the left) show two different ladders. Well 3 is isolated RFP DNA, where only one intense band is shown. This indicates a clean sample, free of contamination. Wells 4 through 8 are the dilution serious 10^1-10^5 of RFP DNA with the first reverse primer (This should be the shorter amplicon, 245 base pairs in length). Well 9 is the DNA ladder again. Wells 10-14 are the dilution serious 10^1-10^5 of RFP DNA with the second reverse primer (This should be the longer amplicon, 547 base pairs in length. And finally, well 15 is another DNA ladder. Wells 4-8 very clearly display an amplicon about half the length of the amplicon in wells 10-14. This gel confirms proper amplification of the designed amplicons.

PCR Experimentation

PCR experiments were performed using a Bio-Rad CFX Connect [53]. PCR controls were designed using isolated RFP DNA in serial dilution (10^1-10^5). The initial dilution contained DNA at a concentration of 130ng. This concentration is indicative of the concentration in the PCR well. The controls were analyzed in the same spot for every experiment. PCR reactions were performed using 25µL of SYBR Green Master Mix and 10µL of sample (10µL of control as well). Adding 10µL of each control sample, Table 4 below shows the control DNA concentrations. Samples 0R, 0NR, 1R, and 1NR taken

during the UV experimentation are all used to develop a calibration curve. The calibration curve is relative only to the experimental samples. Comparing the calibration curve to the serial dilution of control samples (with a known DNA concentration) allows for the determination of DNA concentrations in experimental samples. The serial dilution of RFP is of known DNA concentration; the experimental samples are of unknown DNA concentration. The calibration curve using the initial experimental samples bridges this gap.

Table 4. PCR control DNA concentrations. The control samples were prepared using isolated RFP DNA, purchased from GeneScrip, and provided by Dr. Lamkin's research group at USAF-SAM [39]. The concentration reflects the DNA concentration when the samples were added to the PCR wells. For example, the DNA concentration for the first sample (10^{-1}) was 13ng/µL. 10µL was added to the PCR well for a total concentration of 130ng.

Dilution Factor	DNA Concentration (ng)
10^{-1}	130
10^{-2}	13
10^{-3}	1.3
10^{-4}	0.13
10^{-5}	0.013
10^{-6}	0.0013
10^{-7}	0.00013
10^{-8}	0.000013
10^{-9}	0.0000013
10^{-10}	0.00000013

The dilution controls were run in duplicate for every experiment. Each full experiment was divided into two PCR runs. To better understand necessity for a calibration curve, samples 0R, 0NR, 1R, and 1NR need more explanation. Table 5 below displays sample collection times for the DNA damage and repair experiments. Samples 0R and 0NR are spore samples with no irradiation. Samples 1R and 1NR represent the

spores after irradiation. 0R represents the un-irradiated spores that have been cultured in germination media for 450 minutes and are expected to have the highest yield of DNA. Sample 0NR represents the undamaged spores and un-germinated spores. Sample 1R is representative of spores that were irradiated and allowed to repair; this is the most DNA repair expected from the damaged spores that were incubated for 450 minutes. Sample 1NR represents the un-germinated irradiated spores in which the most damage is expected. These first 4 samples are used to develop the calibration curve with which to compare the other samples. Samples 2-12 are spores that were incubated for the designated time.

Table 5. DNA damage and repair experimentation. Samples 0R and 0NR are spore samples with no irradiation. Samples 1R and 1NR represent the spores after irradiation. 0R represents the most DNA expected to be seen for the spores that outgrew to 450 minutes. 0NR represents the undamaged spores. Sample 1R is representative of spores that were irradiated and allowed to repair; this is the most repair expected from the damaged spores that were incubated for 450 minutes. Sample 1NR represents the most damage to be observed. These first 4 samples are used to develop the calibration curve with which to compare the other samples. Samples 2-12 are spores that were incubated for the designated time.

Sample Name	**Incubation Time (Minutes)**	**Sample Description**
0R	Control	Prior to irradiation; incubated for 450 minutes
0NR	Control	Prior to irradiation; no incubation
1R	0	Immediately following irradiation; incubated for 450 minutes
1NR	0	Immediately following irradiation; incubated for 450 minutes
2	30	Incubated for 30 minutes
3	60	Incubated for 60 minutes
4	90	Incubated for 90 minutes
5	120	Incubated for 120 minutes
6	150	Incubated for 150 minutes
7	180	Incubated for 180 minutes
8	210	Incubated for 210 minutes
9	270	Incubated for 270 minutes
10	330	Incubated for 330 minutes
11	390	Incubated for 390 minutes
12	450	Incubated for 450 minutes

While several PCR temperature protocols were tested, the protocol in Table 6 worked best. Phase 1 of the protocol is meant to bring the sample up to primer operation temperature. Phases 2 and 3 are the steps where primer sequencing and amplification occurs. Phases 2 and 3 were repeated 40 times (40 cycles). DNA that has been properly amplified doubles each cycle.

Table 6. PCR temperature protocol. PCR primers and probes are temperature dependent. If the temperature protocol is not correct, amplification will not occur. This protocol worked best with the primers in this project. Phase 1 brings the primers up to proper temperature. Phase 2 causes DNA to separate into its two strands. Primers attach at Phase 2. Primer extension (amplification) occurs in Phase 3.

Phase	**Temperature & Time**
1	95°C for 30 seconds
2	95°C for 10 seconds
3	55°C for 45 seconds

IV. Analysis and Results

Chapter Overview

This chapter presents the data collected during the research portion of the project. Data sets presented include Ba survival curves, actinometry measurements to account for changes in efficiency of the LEDs, and real time-PCR results of the DNA damage and repair experiments. Other additional analyses were performed to determine efficiency and success of main experiments. Additional analysis included fluorescence experiments to monitor germination times of Ba and atomic force microscopy images to observe morphological changes of Ba before and after irradiation.

Actinometry

Actinometry experiments were performed using the potassium iodate/iodide actinometer. The actinometry experiment conducted on 5/23/2014 was representative of the LEDs operation prior to all experimentations. Actinometry conducted on 7/21/2014 represents the LED operation conditions following all experimentation. By comparing these two actinometry experiments, the reduction in LED power output could be determined based on quantum yield calculations of the actinometer. The following calculations were obtained from James Bolton and his quantum yield calculations of the potassium iodate/iodide actinometer [35]. Quantum yield was calculated by first calculating the concentration of I_3^- following equation 7 below [35]:

$$[I_3^-] = \frac{[Abs_{352} - Abs_{Blank}]}{27.636}\ (M) \qquad (7)$$

Where Abs_{352} is the absorbance of the sample at 352nm and Abs_{blank} is the absorbance of the blank at 352nm. The blank sample is non-irradiated potassium

iodate/iodide solution. 27.636 is the molar absorbance coefficient of I_3^- as tabulated. Next, using the calculation of $[I_3^-]$, the moles of $[I_3^-]$ generated in the reactor were calculated using the following equation [35],

$$moles\ of\ I_3^-\ generated = \frac{[I_3^-]*V}{1000} \qquad (8)$$

Where V is the volume in the reactor, 100mL. Next, the number of Einstein's of UV absorbed at 267nm (the peak wavelength of the LEDs) were calculated using equation 9 below [35],

$$einsteins\ of\ UV\ absorbed\ at\ 267nm = \frac{P(1-R)t(1-10^{-Abs\lambda})}{U_\lambda} \qquad (9)$$

Where P is the average power of the UV LEDs (Watts), R is the reflection coefficient of reflected UV light (0.975) for DI water, t is the exposure time in seconds, Abs_λ is the absorbance of the actinometer solution at the exposure wavelength, 267nm, and U_λ is the energy per Einstein at 267nm, given to be 447938.1277 J/Einstein. Using equation 4[9], the quantum yields were calculated[10].

Because the potassium iodate/iodide solution is temperature dependent and because the temperature differed on the two collection days, the quantum yield was adjusted based on equation 5. The temperature dependence is linear. Once the quantum yield was adjusted for temperature differences, it was compared to the quantum yield determined by the National Institute of Standards and Technology (NIST) at 23.5°C ± 1°C [35]. Table 7 below lists the data points collected in this study. Quantum yield is approximately linearly dependent on wavelength. Using this data, the quantum yield expected to see for these LEDs at 267nm was 0.5315 (using an approximate least squares

[9] See Chapter 2, Actinometry
[10] See Appendix for Calculations of Quantum Yield

fit). 0.5315 was representative of the yield at 23.5°C ± 1°C. Adjusting for temperature using equation 5 in chapter 2, the expected quantum yield is calculated to be 0.68. The quantum yield of the UV LED reactor was calculated to be 0.60. Based on this quantum yield, the fluence values for both collected actinometry experiments were adjusted to reflect the ratio of the experimentally determined yield to the yield reported by NIST. The LEDs in the UV reactor are calculated to be approximately 89% efficient.

Table 7. Quantum yield measurements reported by NIST [35]. Quantum yield is apparently linearly dependent upon wavelength. Therefore, the expected quantum yield for the UV LED reactor was determined to be 0.68 at 267nm, once temperature adjusted (the temperature that experiments were conducted at differed from 23.5°C as much as 2 degrees. The LEDs in the UV reactor are approximately 89% efficient.

NIST Data @ 23.5°C ± 1°C	
Wavelength (nm), λ	**Quantum Yield**
240.7	0.82
253	0.68
255.3	0.73
289	0.26
302	0.15

Table 8 below shows the adjusted quantum yield values as they relate to the temperature corrected fluence values. Figure 16 below displays this relationship. To determine the average quantum yield values, the first three data points were omitted because their absorbance measurements were too close to the absorbance blank values, thereby introducing an unnecessary uncertainty[11]. It is postulated the deviation in quantum yield from the average around the first few collection times is because of this closeness in absorbance values to the blank correction values.

[11] See Appendix for absorbance values

Table 8. Apparent quantum yield and corrected fluence values. 5/23/2014 data was collected prior to all experimentation. 7/21/2014 data was collected after all other experimentation had been conducted. The average quantum yield omits the first three data points, as their absorbance measurements were too similar to the blank measurements to be included.

Corrected Fluence (J/M^2)	5/23/2014 Apparent Quantum Yield	7/21/2014 Apparent Quantum Yield
51.85	0.87	0.98
103.70	0.80	0.82
155.55	0.69	0.78
207.40	0.58	0.68
259.25	0.56	0.68
311.10	0.58	0.63
362.94	0.60	0.63
414.79	0.57	0.62
466.64	0.57	0.61
517.61	0.59	0.63
569.46	0.59	0.61
621.31	0.58	0.61
673.16	0.58	0.60
725.01	0.58	0.62
741.71	0.58	0.60
828.71	0.60	0.61
880.56	0.60	0.60
932.41	0.58	0.59
984.26	0.59	0.61
1036.11	0.58	0.60
Average:	**0.58**	**0.62**

Figure 15 below displays the apparent quantum yield as fluence changes. The functionality seen at the beginning of the plot is not typical of actinometry experiments. The absorbance values are measured at 352nm, the absorbance wavelength of the actinometer solution. The blank values at this wavelength were very close in value to the absorbance of the actinometer solution near the beginning of the experiment (the first few data points). This is attributed to the uncertainty introduced in having the blank values so close to the experimentally collected data.

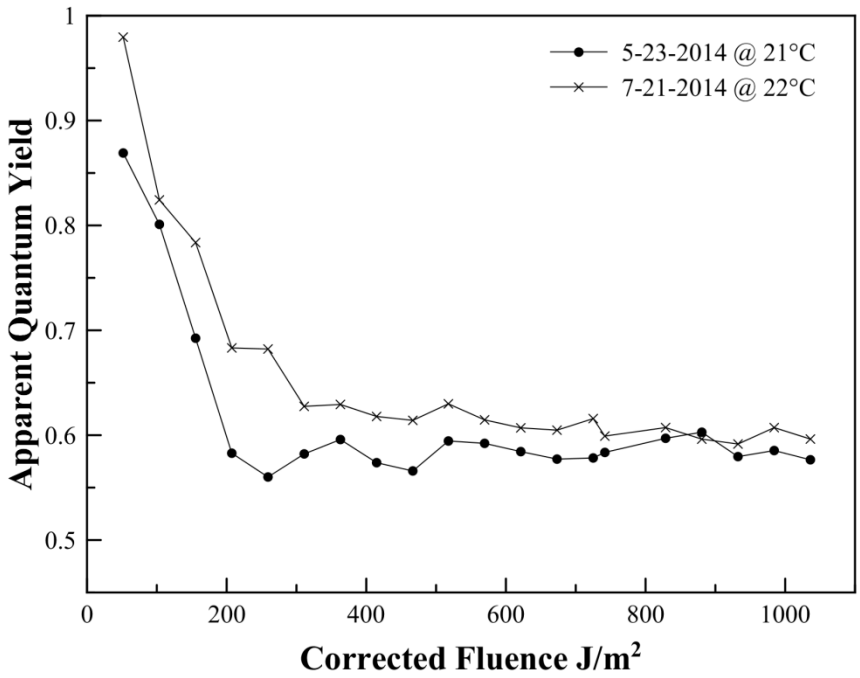

Figure16. Apparent Quantum Yield. Values used in this graph are reported in Table 8. The first three data points were omitted during quantum yield calculations because the absorbance values at 352nm were too close to the absorbance blank measurements. The quantum yield should remain constant with changing fluence.

The ultimate goal in conducting actinometry experiments was to determine the proper fluence values to be used for the rest of the research. The corrected fluence values reported in Table 5 were used for the remainder of the project.

Bacillus anthracis Survival Curve

The first set of experiments conducted led to the creation of the Ba survival curves. Fluence values were adjusted based on the actinometry results in the above section. Ba spores ($1x10^7$ spores/mL) were irradiated for a total of approximately 10 minutes (approximately $1000J/m^2$) while 100µL samples (in triplicate) were taken

frequently throughout. Samples were plated in triplicate[12]. The surviving fraction was calculated at each point for each plate. The following figures display data for Survival Curve 3 (corresponding to Experiment #3) because the triplicate plate counts were the tightest groups of all 3 experiments[13] and had the smallest standard deviations. Then, the data for all three experiments was averaged and presented below as well. Figure 17 below displays the surviving fraction of Survival Curve 3. Data was collected in all three experiments up to approximately 1000J/m^2. N and N_o are representative of physical plate counts, an average of three plates counted in triplicate per data point. The survival fraction changes dramatically in the first three data points and exhibits a tailing effect for the duration of the experiments. Other studies have supported evidence of both a shoulder and tailing effect [48]. More data points are needed at lower fluences to determine if there indeed exists a shoulder. The tailing effect is exhibited in Figure 17.

[12] See Appendix for Plate Counts
[13] See Appendix for Survival Curve 1 and 2 figures

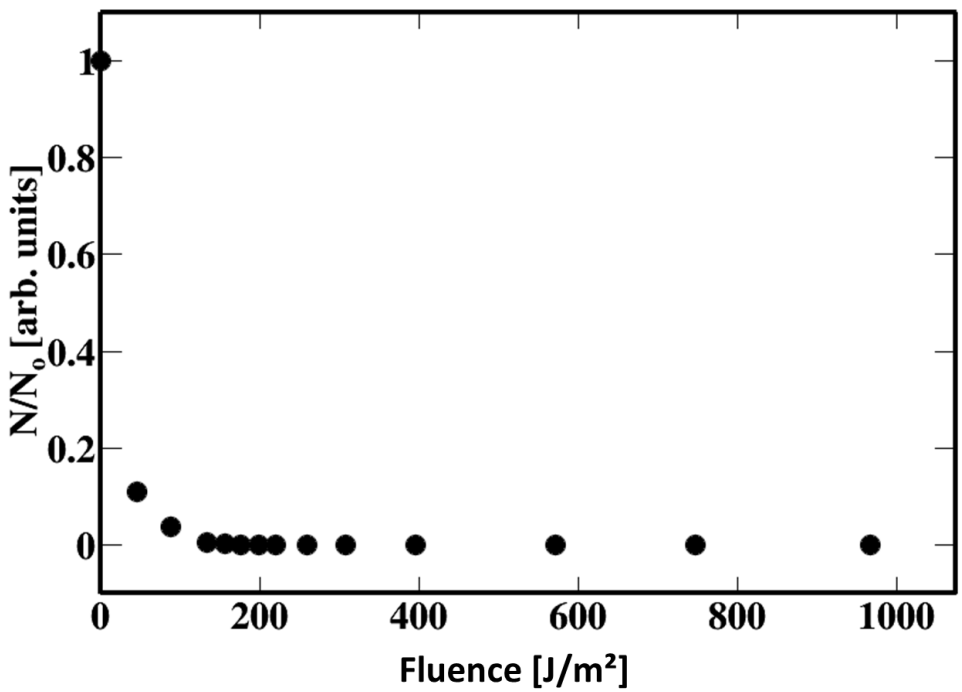

Figure17. Survival Curve 3 surviving fraction of Ba Sterne spores as fluence is varied between 0 and 1000 J/m^2. Fluence carries the units J/m^2. Fluence values displayed in this figure are the corrected values from actinometry results.

To better understand the data observed, error bars were utilized in Figure 18. Error was calculated using counting statistics where several assumptions were made. The counting error statistics assume a normal or Gaussian distribution, where the error in the value n (the counted statistic) goes as the square-root of n. This calculation is most accurate when n is very large. The data towards the end of the survival curve is based on counting one or two colonies per plate out of a starting concentration of spores that was 1x10^{7}spores/mL. This indicates that n is very small and the error statistics are less accurate for the smaller values of n. The error values are ultimately the division of σ_T/C_T, where σ_T is the error associated with the colony count value, C_T. The error

calculation also assumes that x and y are independent variables. The error equation is given by equation 10 below,

$$\frac{\delta z}{z} = \sqrt{(\frac{\delta x}{x})^2 + (\frac{\delta y}{y})^2} \qquad (10)$$

Equation 9 assumes the central limit theorem. The central limit theorem states that "the distribution of the average of a large number of independent, identically distributed variables will be approximately normal, regardless of the underlying distribution" [54] . Because the error becomes extremely large after 240J/m^2, only the first 8 data points were used for fitting purposes. The dotted blue line represents this cut-off point in Figure 18 below.

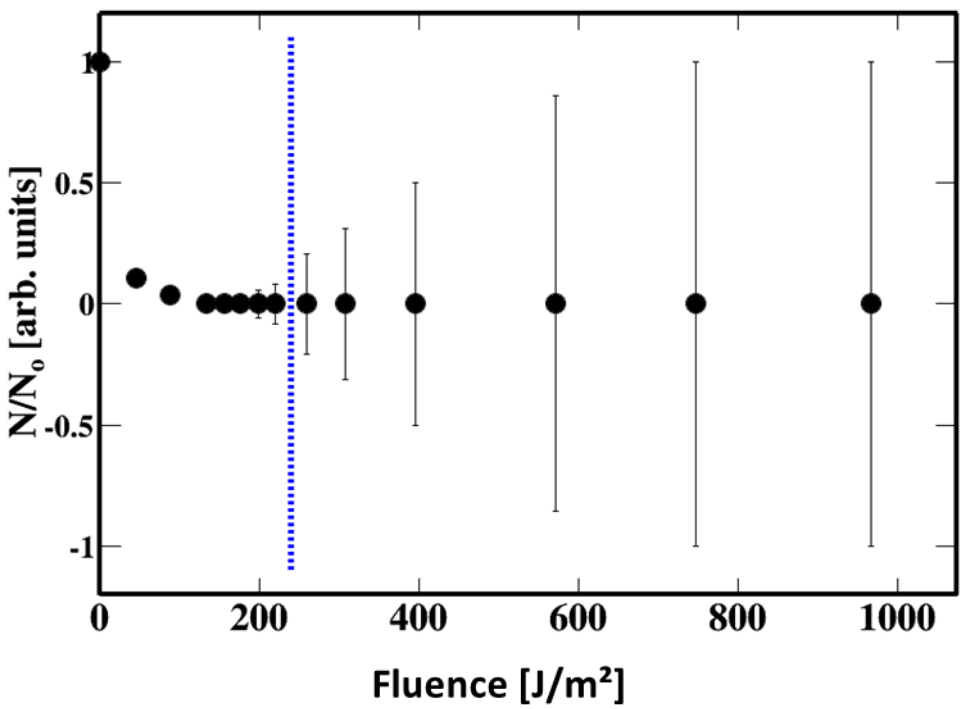

Figure 18. Survival fraction for Survival Curve 3. The dotted blue line represents the cut-off point for data to be fit. The magnitude of the errors towards the higher fluence values is as large as the spread of the data. The last 6 data points are omitted from the fitting functions seen in the following figures.

Figure 19 below displays the log(N/N_o) as a function of fluence. The dotted blue line shows the cut-off point for data to be fitted. This figure represents data taken from the third experiment, Survival Curve 3. The last data point at 966J/m^2 is omitted from the plot because the plate counts were zero, making the Survival fraction 0. The $\log_{10}$ (0) is undefined.

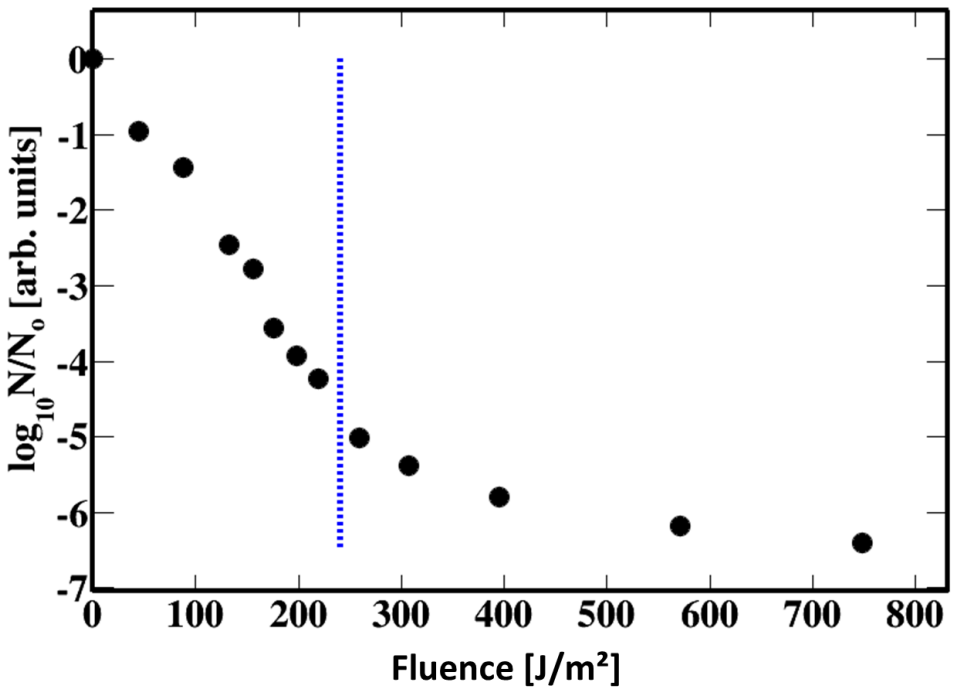

Figure 19. Log_{10} (N/N_o) as a function of fluence for Survival Curve 3. The blue line indicates the breaking point in the data where errors become too large to trust the data points. The last data point (at 966J/m^2) is omitted from the plot because the plate counts were zero, making the Survival fraction 0. The $\log_{10}$ (0) is undefined.

Figure 20 below shows the log-linear fit for Survival Curve 3. The fitting function is as follows,

$$y = [\alpha]x + [\beta]x^2 \qquad (11)$$

Where α and β are the fit parameters to be compared between experiments. The α-term is representative of the linear functionality of the data and β is representative of the

quadratic functionality. All fitting for the survival curves was performed in Root, a large scale data fitting and analysis program. Fitting the data up to 240J/m^2 for Survival Curve 3, the fitting statistics are as follows in Table 9.

Table 9. Fitting Parameters and statistics for Survival Curve 3. The R^2 is the best for Survival Curve 3 (Of all three curves), at 0.992. Note the magnitude of β is very small, indicating that the fit has a very small quadratic-term. That is to say, the data is nearlylinear.

Survival Curve #3	
α	-0.017
β	-0.000013
Reduced X^2	0.022
R^2	0.992

The β-term is very small because the data is mostly linear and only has a slight quadratic tendency. Chi-square, X^2, measures the goodness of a fit to its modeled data. X^2 is described in equation 12 below:

$$X^2 = \frac{(Observed\ Value - Expected\ Value)^2}{Expected\ Value} \qquad (12)$$

Chi-square values around 1 indicate a good fit of the data. Values larger than 1 indicate a bad fit of the data. The X^2 reported in Table 9 above is less than 1, indicative of an overfitting of the data. This is logical, as the quadratic component of the fit is existent, but very small. The reduced chi-square value is the calculated chi-square divided by the degrees of freedom. Figure 20 below shows the fitting of Survival Curve 3. Only data up to 240 J/m^2 was fitted. This included the first 8 data points.

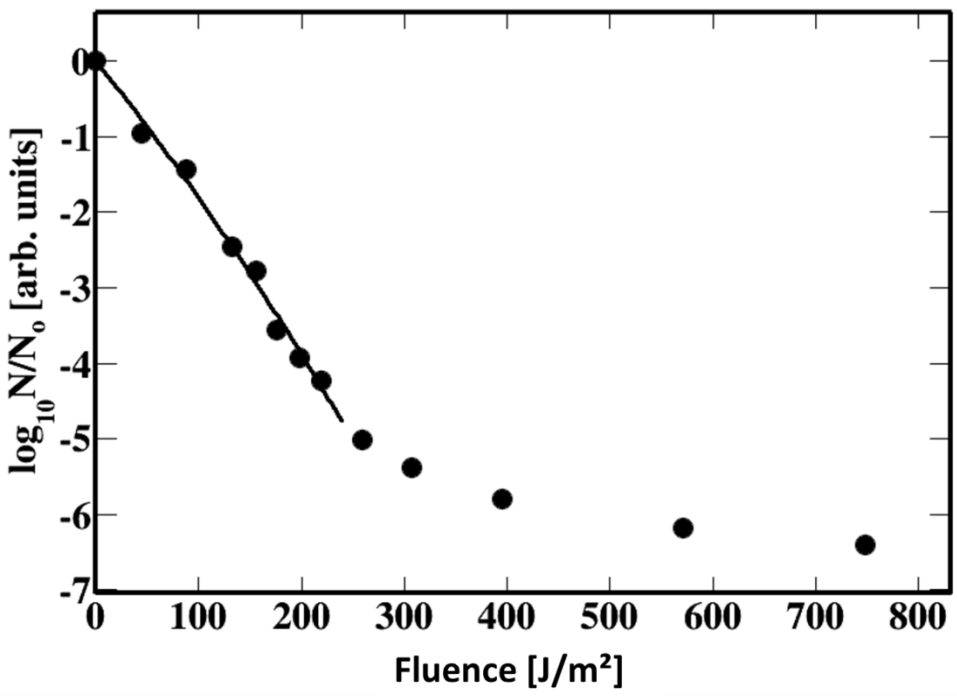

Figure 20. Log-linear with fit of Survival Curve 3. Fitting only the data up to 240J/m^2, the Root coding program yields an R^2 value of 0.992. Fitting parameters for this fit are found in Table 9 above.

Figure 21 below displays the correlation plot for Survival Curve 3. The correlation plot is developed using a Pearson product-moment correlation coefficient, r. Information about the Pearson coefficient was taken from the Laerd Statistics website [55]. The Pearson coefficient, r, is a measure of the relationship between two variables. The Pearson coefficient can take on values between -1 and 1. A Pearson coefficient value of 0 means that the two variables have no association with each other. A value between 0 and +1 indicates positive correlation; as one variable increases in value, so does the other. The closer r is to +1, the more strongly positively correlated the two variables are. A value between 0 and -1 indicates negative correlation; as one variable increases in value, the other variable decreases. The closer r is to -1, the more strongly negatively correlated

the two variables are. Figure 21 below indicates a negative correlation between the two fit parameters of the survival curve data, α and β. The closer r is to +1 or -1, the better the data fits the model chosen. The blue area indicates 1 standard deviation from the mean, where 68% of the data lies. The green area indicates 2 standard deviations from the mean, where 95% of the data lies. The red area indicates 3 standard deviations from the mean, where 99.7% of the data lies.

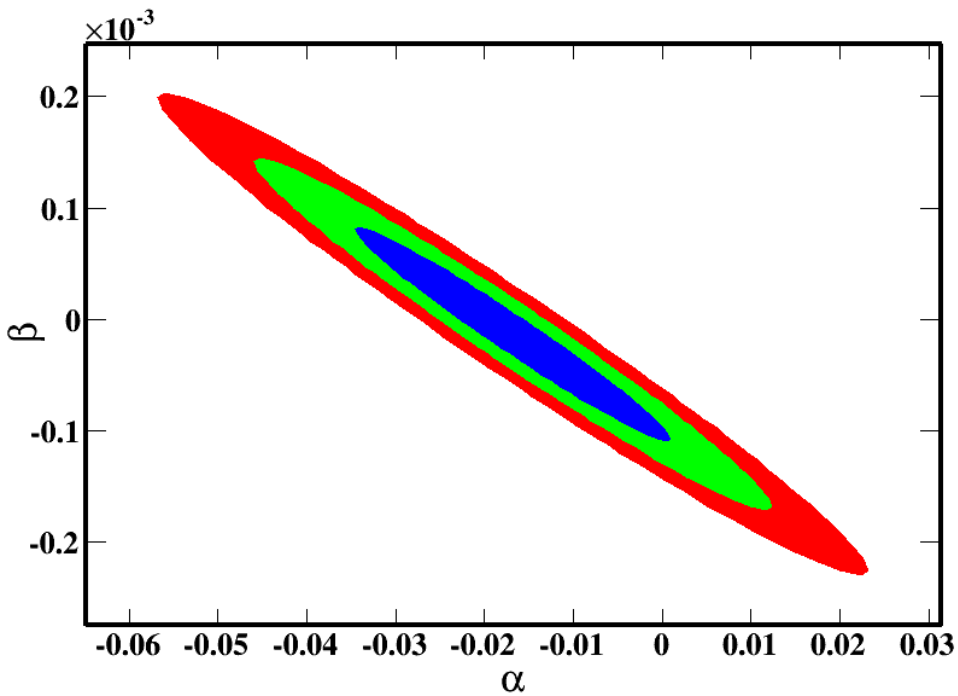

Figure 21. Pearson product-moment correlation plot for Survival Curve 3. The two fit parameters α and β are negatively correlated. The blue area indicates 1 standard deviation from the mean, where 68% of the data lies. The green area indicates 2 standard deviations from the mean, where 95% of the data lies. The red area indicates 3 standard deviations from the mean, where 99.7% of the data lies.

The next set of figures displays data for all three experiments (Survival Curves 1,2 &3) combined on one plot. Figure 22 displays the combined survival curve for N/N_0 as a function of fluence in J/m^2.

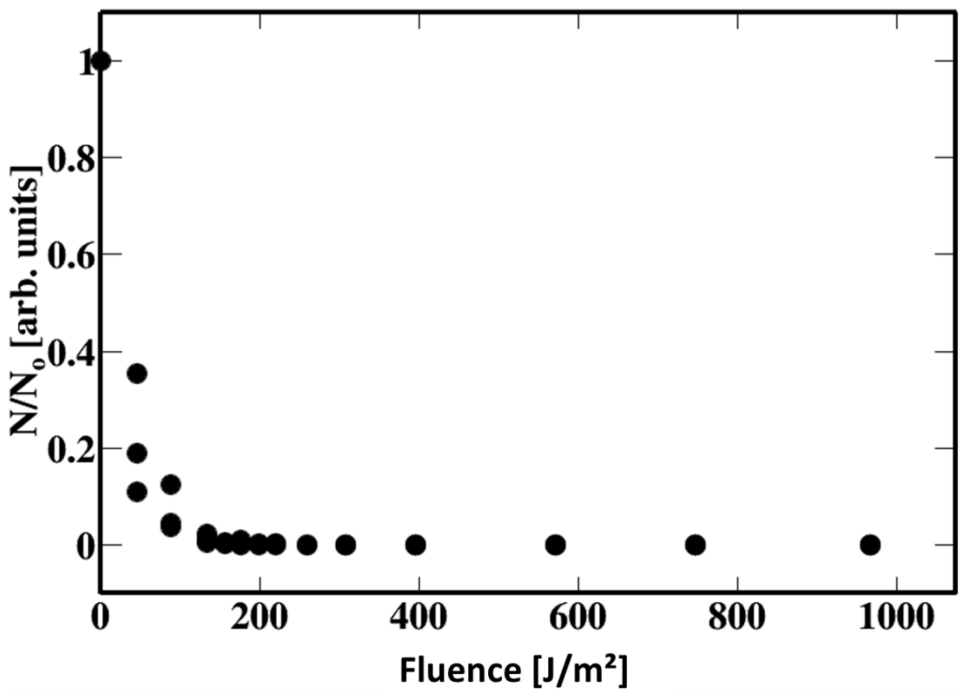

Figure 22. Survival Curve for all 3 data sets. Surviving fraction of *Bacillus anthracis* Sterne spores as fluence is varied between 0 and 1000J/m^2. Fluence carries the units J/m^2.

Figure 23 below shows the large increase in error that occurs in all three survival curves as fluence increases. All fitting of the data was only from 0 to 240J/m^2. Fitting parameters for the combined survival curve are the reported α and β terms for the project. The fit parameters and the fit curve are found in Table 10 and Figure 24 respectively.

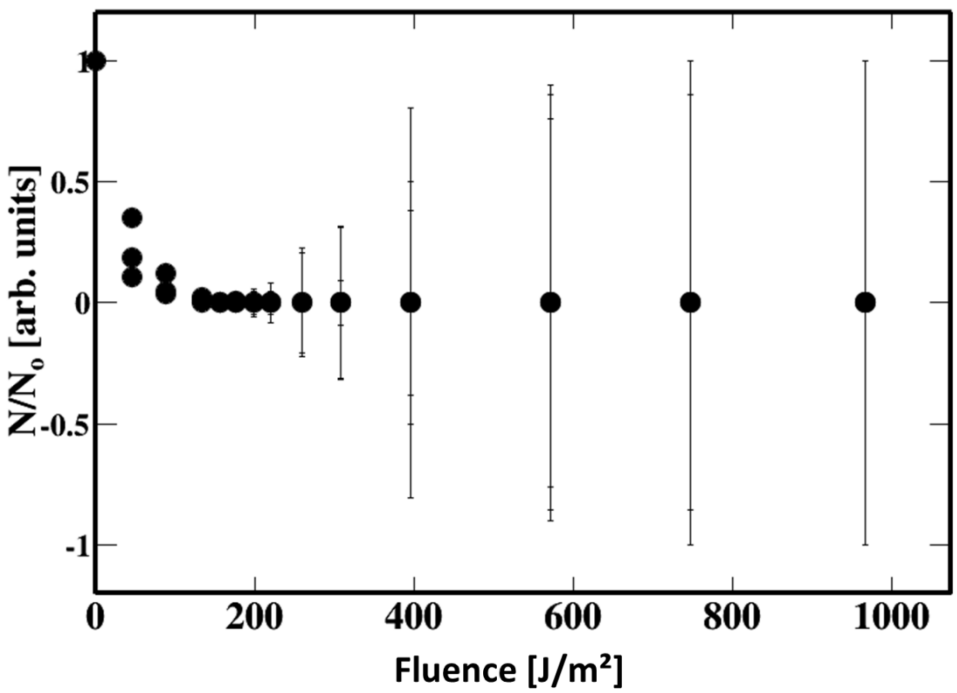

Figure 23. Ba Sterne survival curve showing all 3 experimental data sets. Data from the 3 different experiments varies greatest when fluence is less than 100J/m^2. This plot displays the large increase in error as fluence increases and colony counts are greatly diminished.

Combining the data from all 3 experiments, the fit parameters below are reported with a 90% confidence. This confidence interval was calculated using equation 13 below:

$$\bar{X} = \frac{ts}{\sqrt{N}} \qquad (13)$$

Where $\bar{X}$ is the mean of the data points (the average of the three α or β values from all 3 survival curves), t is a designated constant determined by the confidence level and degrees of freedom, and s/$\sqrt{N}$ is the standard deviation of the data.

Table 10. Fitting Parameters and statistics for the combined survival curve data. Error bars are reported with a confidence interval of 90%.

Combined Survival Curve	
α	-0.0144 ± 0.008
β	-0.00001 ± 0.0002
Reduced X^2	0.192
R^2	0.876

The fit parameters in Table 10 above are derived from the Root software coding program of the fit in Figure 24 below. Figure 24 below shows three data points for each fluence dose. Each data point is the result of three separate plate counts. An R^2 of 0.876 is not considered extremely great. But, this can most likely be attrubuted to the slight quadratic tendancy of the fit.

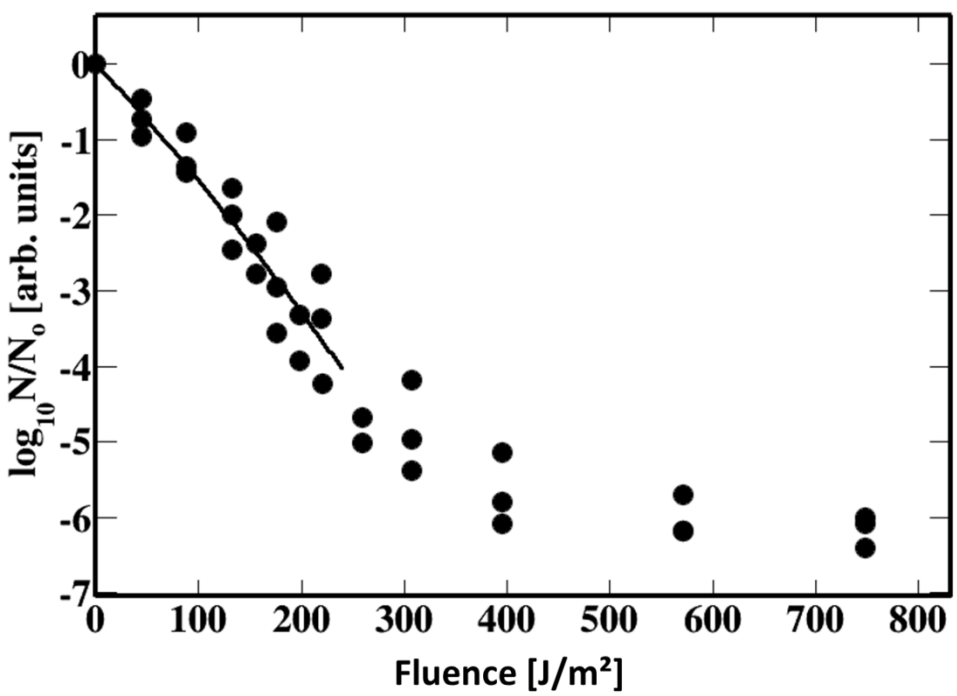

Figure 24. Log-linear with fit of the Combined Survival Curve. Fitting only the data up to 240J/m^2, the Root coding program yields an R^2 value of 0.876. Fitting parameters for this fit are found in Table 10 above.

Figure 25 below displays the Pearson product-moment correlation plot for the Combined Survival Curve. The two fit parameters α and β are again negatively correlated. The blue, green and red areas are again indicative of the confidence intervals for where the data lies 1 (blue), 2 (green) and 3 (red) standard deviations from the mean.

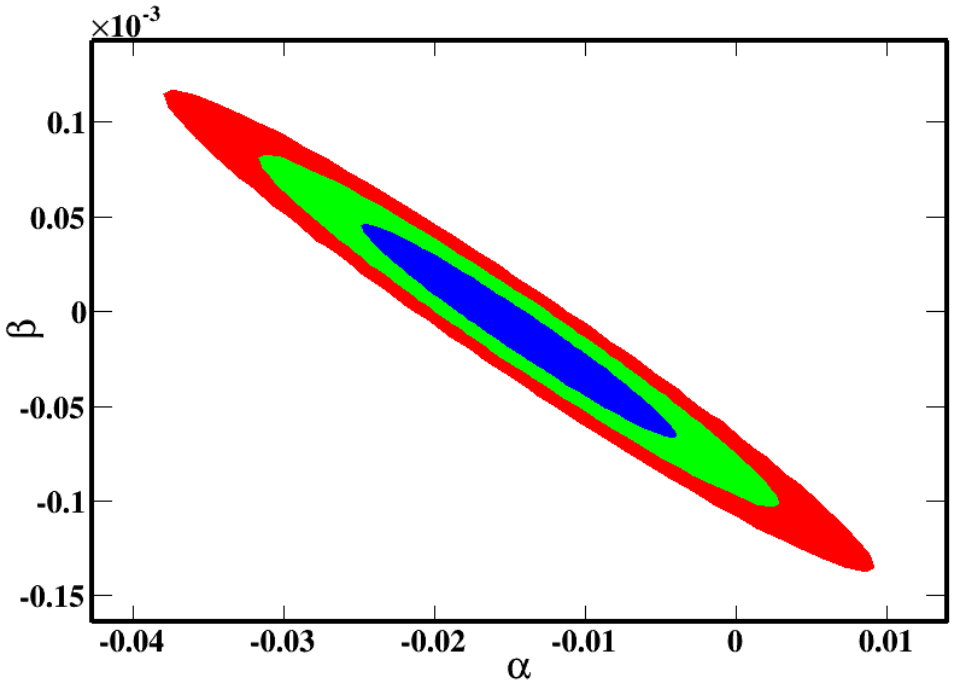

Figure 25. Pearson product-moment correlation plot for the Combined Survival Curve. The two fit parameters α and β are negatively correlated. The blue area indicates 1 standard deviation from the mean, where 68% of the data lies. The green area indicates 2 standard deviations from the mean, where 95% of the data lies. The red area indicates 3 standard deviations from the mean, where 99.7% of the data lies.

DNA Damage & Repair Experimentation

The final experimentation in this project was performed to monitor DNA repair following irradiation. As discussed previously, no repair of DNA occurs in the dormant spore. The repair process occurs during germination and outgrowth. To assure spores were germinating in the time frame of data collection, fluorescence experiments were

conducted. Germination salts were only concentrated at half strength for fluorescence experiments and were adjusted to full strength for the DNA damage and repair experiments analyzed with PCR. A lessened concentration of germination salts most likely slowed the germination process. This was evident when microscopic and AFM images were taken during experimentation where full strength salts were used and germination was seen as early as 90 minutes in the irradiated spores. Table 8 below shows the fluorescence data. Triplicate readings were taken on the spectrometer for each sample point. The three readings were averaged. The standard deviation in the triplicate readings is displayed in Table 11 as the intensity error.

Table 11. Fluorescence data collected on irradiated and un-irradiated (control) Ba Sterne spores. This data was collected to monitor the germination and outgrowth stages of the spore. For this experiment, the germination salts were only at half strength. This most likely slowed the germination process for both the control and irradiated spores. An increase in fluorescence intensity indicates an increase in germination as the fluorescence dye will not penetrate the spore. Three measurements were collected at each data point and averaged.

Incubation Time, Minutes	Average Intensity, RFU		Intensity Error	
	Un-Irradiated	Irradiated	Un-Irradiated	Irradiated
Control	142390	47620	2475.7	242.7
0	119190	102633.3	367.6	2355.6
30	126836.7	140566.7	992.9	1501.1
60	243506.7	85303.3	39283.9	1218.3
90	249456.7	97532.1	124202.5	696.2
120	276527.5	106043.3	4025.5	2081.7
150	172553.3	99250	5812.8	221.7
200	794500	5181430	7326.5	127567.6
250	15836330	212790	2906885.9	10663.2
300	21860346.7	1197630	574442.2	16984.7
350	20660606.7	303903.3	32597.4	3806.0
400	19257616.7	7213123.3	26133.2	112645.4
450	19725483.3	8311860	11818.2	297451.8

Figure 26 below displays the fluorescence data as a function of incubation time (minutes). A sharp intensity increase is seen at 200 minutes for the control data, indicating the beginning of germination. The same increase is not observed in the irradiated spores until approximately 350 minutes. This delay time is attributed to the spore recovering from the UV damage before beginning outgrowth. A sharp increase is seen at 200 minutes for the irradiated sample. This sharp increase intensity could be attributed to the burst time of the spore. The burst time is defined as when the cell emerges from the spore coat [18]. This fluorescence tracking of the germination process was developed from a study performed by Kong et al, where germination was monitored and reported with respect to time [56].

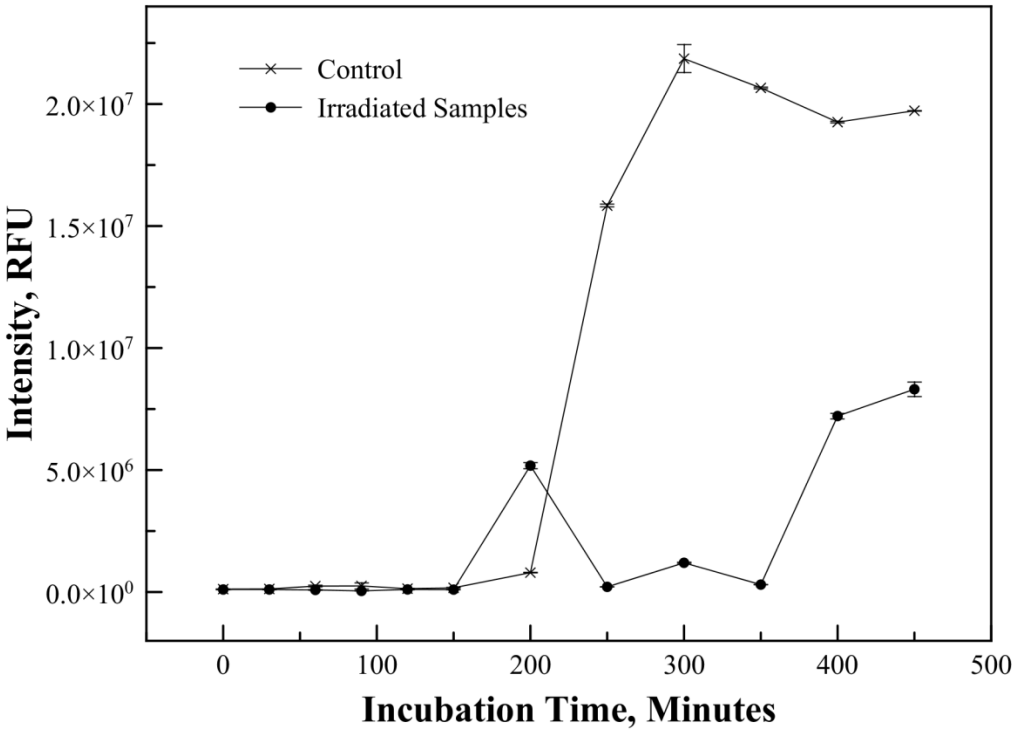

Figure 26. Fluorescence data collected on irradiated and un-irradiated (control) Ba Sterne spores. This data was collected to monitor the germination and outgrowth stages of the spore. For this experiment, the germination salts were only at half strength. This most likely slowed the germination process for both the control and irradiated spores. An increase in fluorescence intensity indicates an increase in germination as the fluorescence dye will not penetrate the spore. Three measurements were collected at each data point and averaged. The control spores show germination beginning at 200 minutes and the irradiated spores begin to germinate at 350 minutes, a lag time of about 2½ hours.

To accompany fluorescence data, Atomic Force Microscopy (AFM) images were collected throughout the incubation time. AFM images were prepared and collected by Dr. Yun Xing, a fellow AFIT researcher [57]. AFM images were taken after incubation media was added at the following incubation times: 0, 90 and 150 minutes. Figures 27-29 show images of un-irradiated spores in germination media. Un-irradiated spores appeared normal, meaning they matched the spores from the reference article where the growth conditions were the same (AGFK in MOPS media) [18]. Figures 30-32 display images of

the irradiated spores in germination media. Note that for the experiments displaying AFM images, as with fluorescence experiments, germination salts (AGFK) were at full strength. The irradiated spores did germinate. However, the clustering of the spores seemed to be in groups of two or three spores; whereas the un-irradiated spores clustered in very large groups.

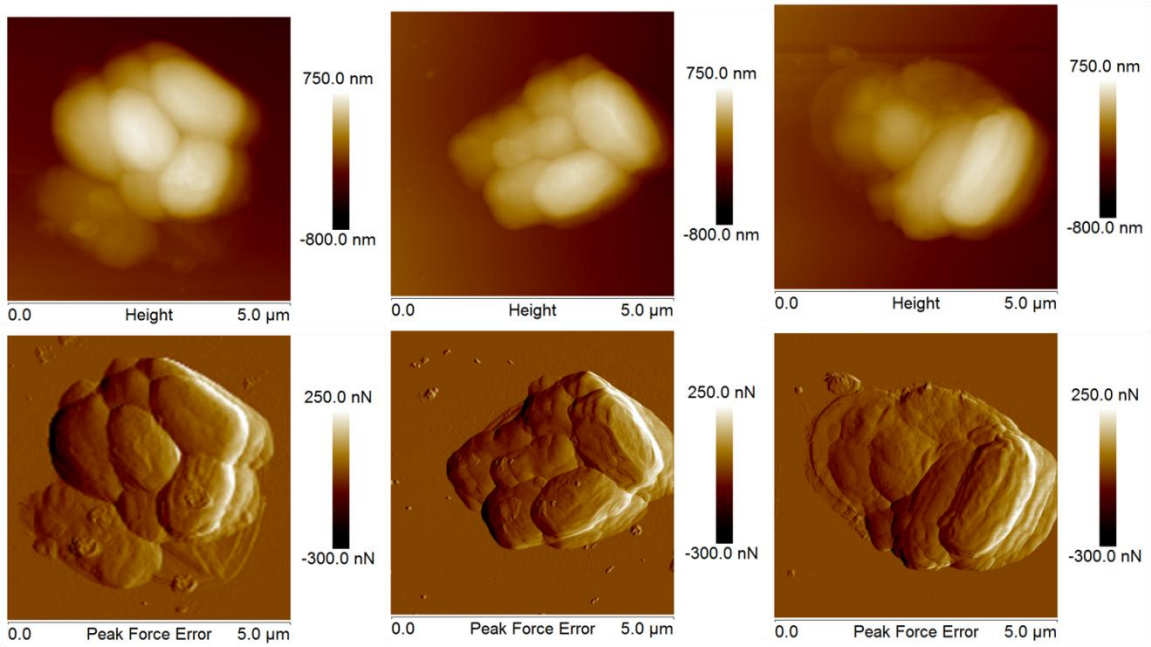

Figure 27. Un-irradiated Spores at Time Zero. Non-irradiated spores immediately following addition of germination salts (half strength). The size, shape, and clustering is typical of Ba spores. Images are courtesy of Dr. Yun Xing [57].

In Figure 27 above, spores look normal. Clustering and size are indicative of Ba spores. The spores have an exosporium layer, evident in the images encasing the spore. Spores in this first figure have not been given the opportunity to germinate. In Figure 28 below, spores have been in germination media (half strength AGFK salts) for 90 minutes. Germination is occurring. The vegetative cells are not forming their normal long-chain structures. However, their growth pattern is indicative to the growth pattern in Pandey,

where similar growth conditions we used [18]. The fibers surrounding the spores are commonly observed as well.

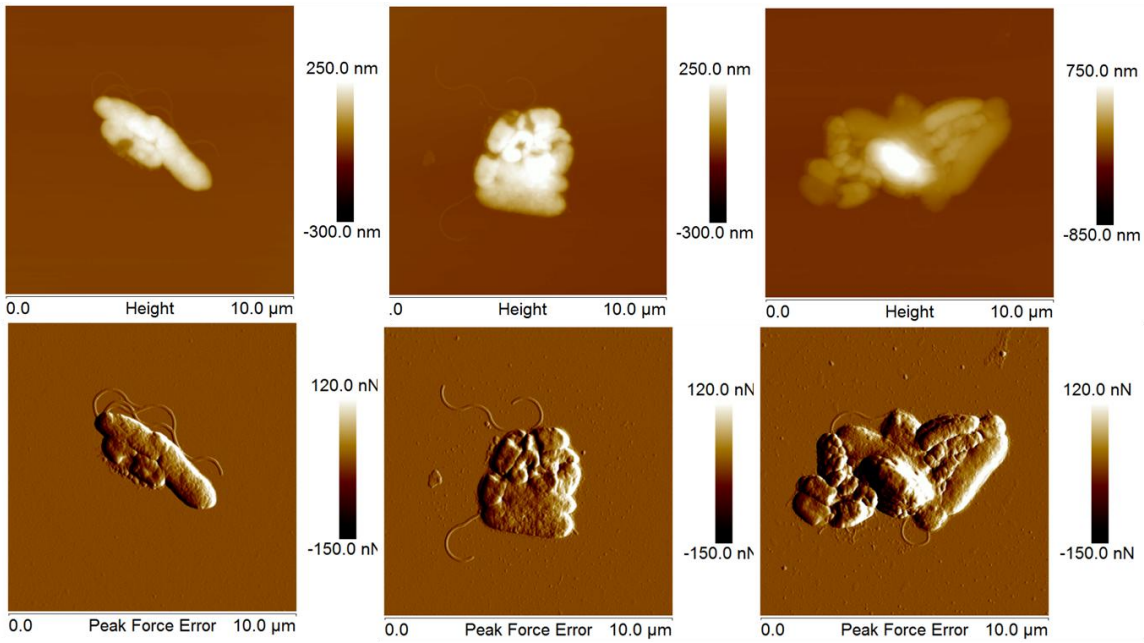

Figure 28. AFM images of un-irradiated control spores: 90 min culture in germination media. Note the presence of normal looking veg cells, pit-like structures and also fibers. Normal spores are approximately 2-5 microns in length, where the vegetative cells are slightly longer. Images are courtesy of Dr. Yun Xing [57].

Figure 29 below demonstrates to a larger degree these clusters of vegetative cells. The cluster of cells is large, but normal in size for this germination media. The germination media is minimal media buffered to a pH of 7.4 with 3-(N-morpholino) propanesulfonic acid (MOPS) [18]. In addition, the media was supplemented with AGFK: 10mM L-asparagine, 10mM glucose, 1mM fructose, and 1mM potassium chloride.

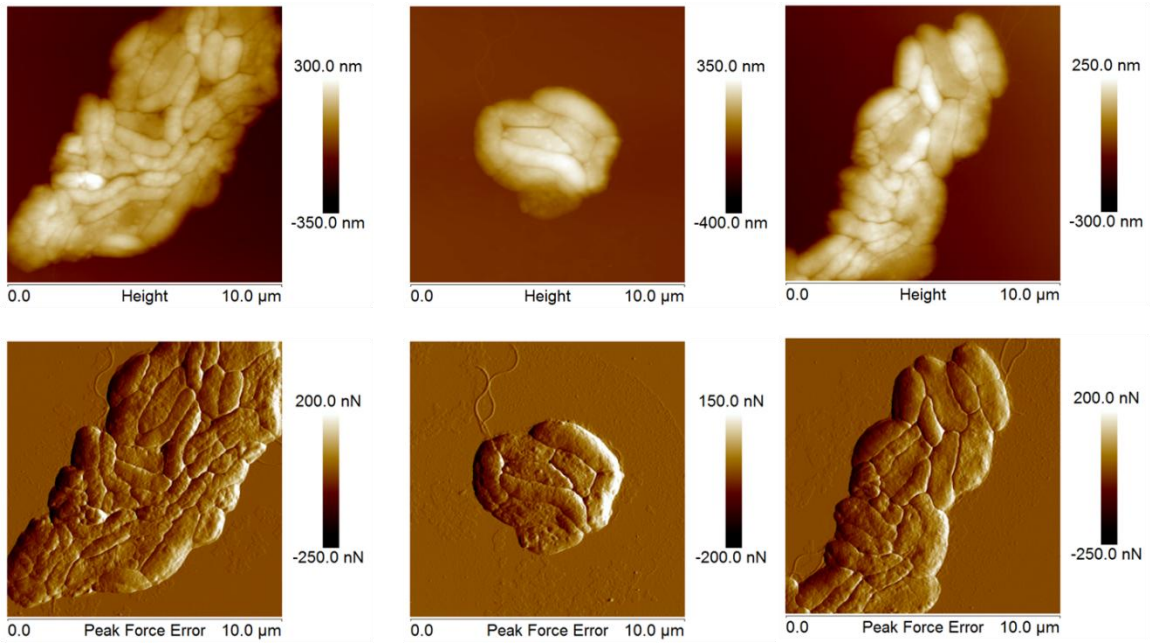

Figure 29. AFM images of un-irradiated spores control: 150 min culture in germination media. At this point, nearly all germination has taken place. The size, shape, and clustering is typical of Ba vegetative cells in this MOPS AGFK germination media. Images are courtesy of Dr. Yun Xing [57].

The following 3 figures display AFM images of spore following irradiation. Overall, the spores have a different morphology then the un-irradiated spores. While this morphology change is not well identified or understood, it is evident in the images below. The spore coat or exosporium appears to be attached from the spore itself in Figure 30 below.

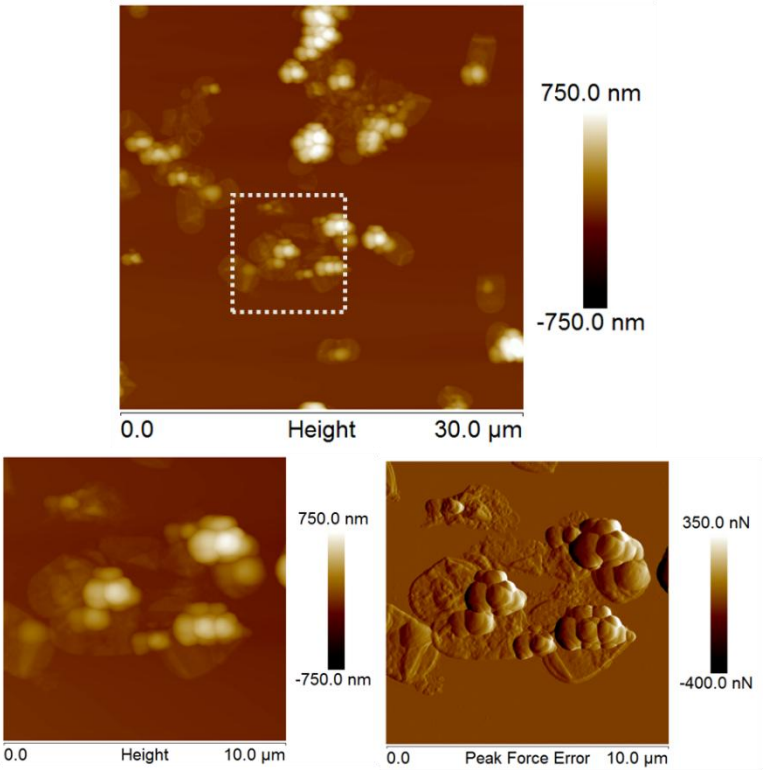

Figure 30. Radiated (log kill 1) Spores. This sample is 0 minutes incubation in germination media. The white box indicates the spot at which the bottom two images are focused. In the top image and image on the left, a haze is seen around each spore. It appears (shown in bottom right image) the spores have lost their exosporium and perhaps their spore coats. Images are courtesy of Dr. Yun Xing [57].

In Figure 31 below, after 90 minutes in germination media the spores are germinating. However, the clusters of germinating spores are much smaller. This figure also displays the debris of what appears to be a spore coat or exosporium as the spore is germinating. The far right image displays this well. Normal looking fibers are also seen in these germinating spores.

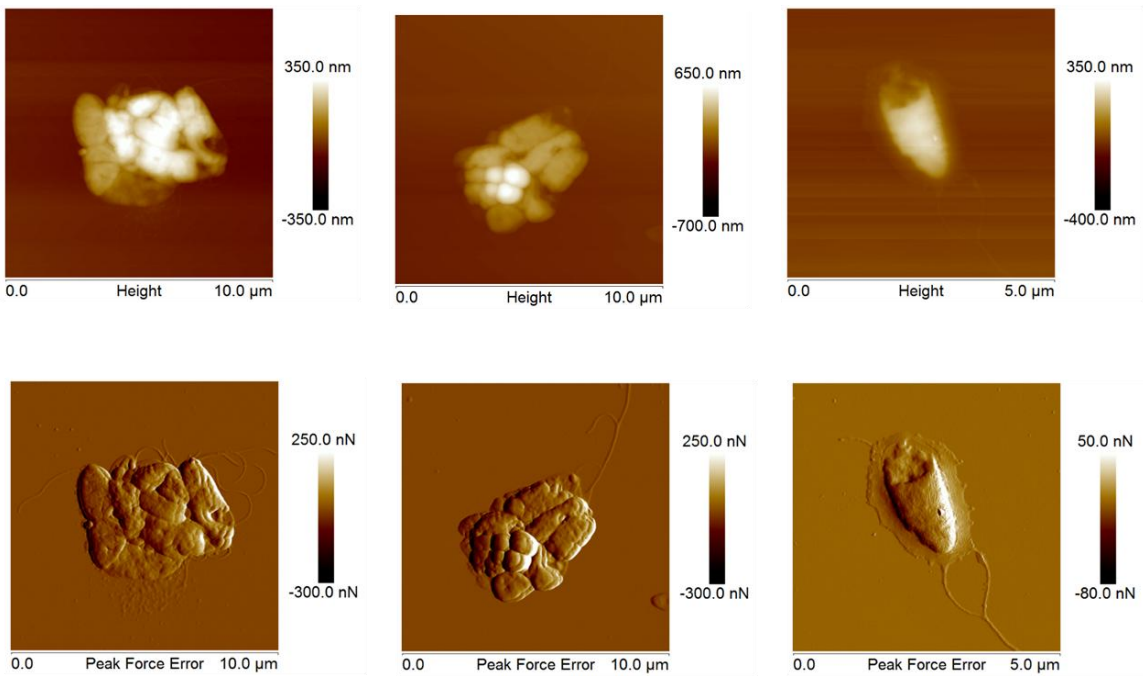

Figure 31. Irradiated spores incubated in germination media for 90 minutes. These spores are beginning to germinate. The fibers seen in un-irradiated germinating spores are also seen here. But, the germination is occurring in much smaller clusters then the un-irradiated spores. Images are courtesy of Dr. Yun Xing [57].

The final AFM image, the irradiated spores are now fully germinated cells. Evidence of complete germination is also supported by the fluorescence data. The cells look normal. Again in Figure 32 below, clusters of cells are much smaller containing 1-3 cells. Clusters of cells in un-irradiated spores contained 20-50 cells. Some morphological difference must be changing this growth habit of the Ba cells. Further imaging is needed to better understand this behavior.

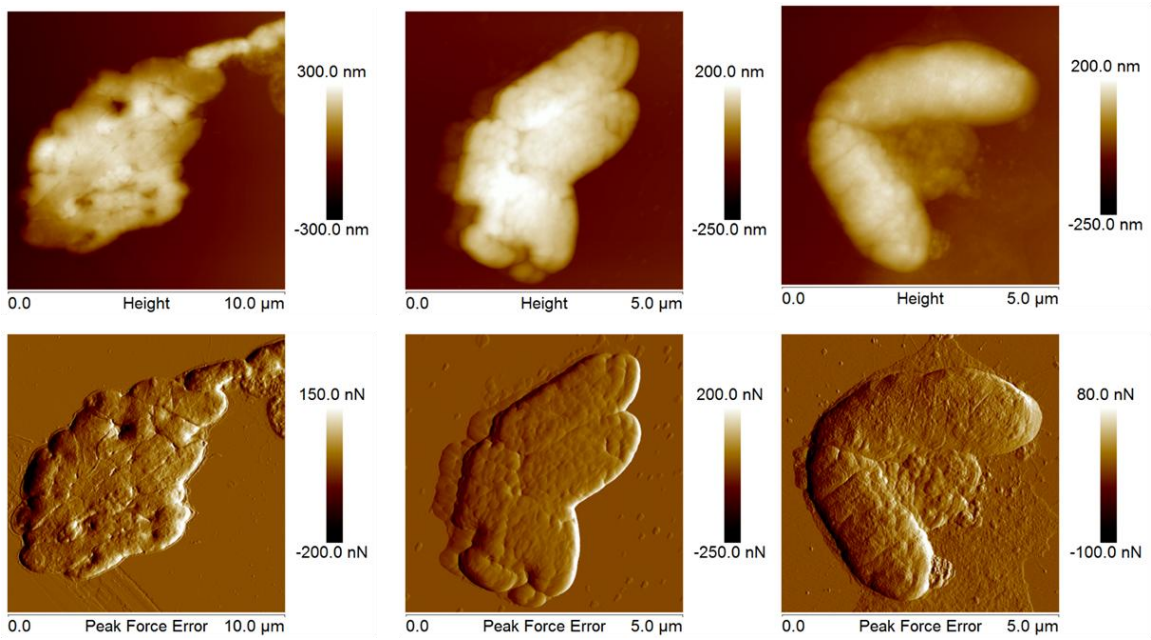

Figure 32. Irradiated spores incubated in germination media for 150 minutes. The spores are almost entirely germinated cells. This is also confirmed by the fluorescence measurements. These cells are clustered in 1-3 cell clusters. The un-irradiated cells were clustering in much larger groups of 20-50 cells. Images are courtesy of Dr. Yun Xing [57].

During irradiation experiments, samples were collected for several different analysis methods including AFM images, fluorescence measurements and PCR. To accompany all of this data, plate counts were also taken in triplicate at each time collection point. Plates were plated in serial dilutions and incubated at 37°C for 18 hours before being counted. Figure 33 below displays these plate counts. A few statements can be made regarding this figure. It is evident that all 3 experiments irradiated spores in a fairly consistent fashion, as their plate growth habits were all very similar. The cell counts of the damaged spores never reached the same level as the un-irradiated spores (control), as expected. The steep decline in surviving fraction towards low incubation times probably can be attributed to the recovery time of the damaged spores before outgrowth.

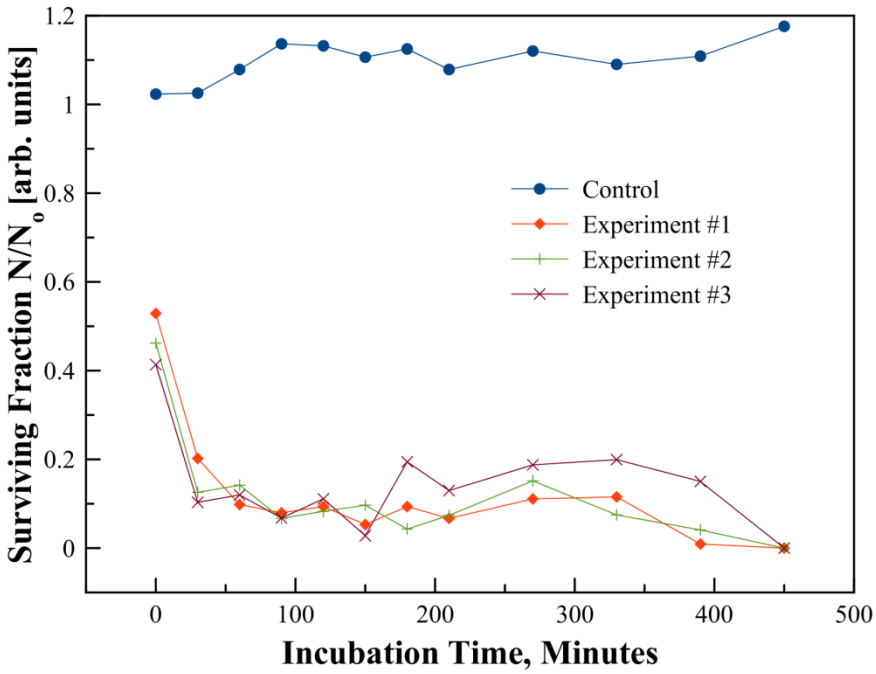

Figure 33. Surviving fraction of DNA damage and repair experiments with varying incubation time. Each data point is representative of 3 plate counts. Plates were counted after 18 hours. The control experiment received no irradiation while the experiments received a dose of 100 J/m^2.

Following AFM images and fluorescence measurements, DNA damage and repair experiments were still analyzed by PCR using SYBR Green. The real-time PCR produces a reading for each sample called Ct. Ct is determined by a threshold fluorescence value that is just above background fluorescence. The number of cycles required to reach this threshold fluorescence is termed Ct. The following figures display the PCR data from all three experiments. The short amplicon figures indicate the samples utilizing the forward primer and the first reverse primer. The long amplicon figures indicate the samples containing the forward primer and the second reverse primer. PR1 yields the shorter amplicon fragment in Table 3 and PR2 yields the longer amplicon fragment.

After conducting all the PCR analysis, samples yielded few results. No amplification was observed for any samples past the incubation/germination stage (samples 2-12). The lack of amplification is most likely attributed to DNA isolation techniques. The same bead beating method of DNA isolation was used for all samples: 0R, 0NR, 1R, 1NR and 2-12. It is hypothesized that this method of isolation was too severe and damaging to the germinated samples 2-12. Ba spores are much harder to lyse open than are Ba cells. The bead beating isolation protocol worked well for spore samples, but may have been too damaging to germinated samples. Too much damage across the plasmid DNA would result in PCR failure. The primers wouldn't be able to identify the complementary strand of the template DNA and would fail to attach. The taq polymerase would then fail to synthesize. The PCR primers were tested against a separate isolated sample of RFP DNA and were successful, so improperly functioning primers could be ruled out.

Figures 34 and 35 below display the only data points collected in all three experiments, samples 0NR and 1NR. Figure 34 shows data for the short amplicon and Figure 35 shows data for the long amplicon. NR samples were not allowed to incubate at all. Sample 0NR was taken immediately following the spore solution preparation and sample 1NR was taken immediately following irradiation. These two samples should show the healthiest spores (0NR) and the most damaged spores (1NR).

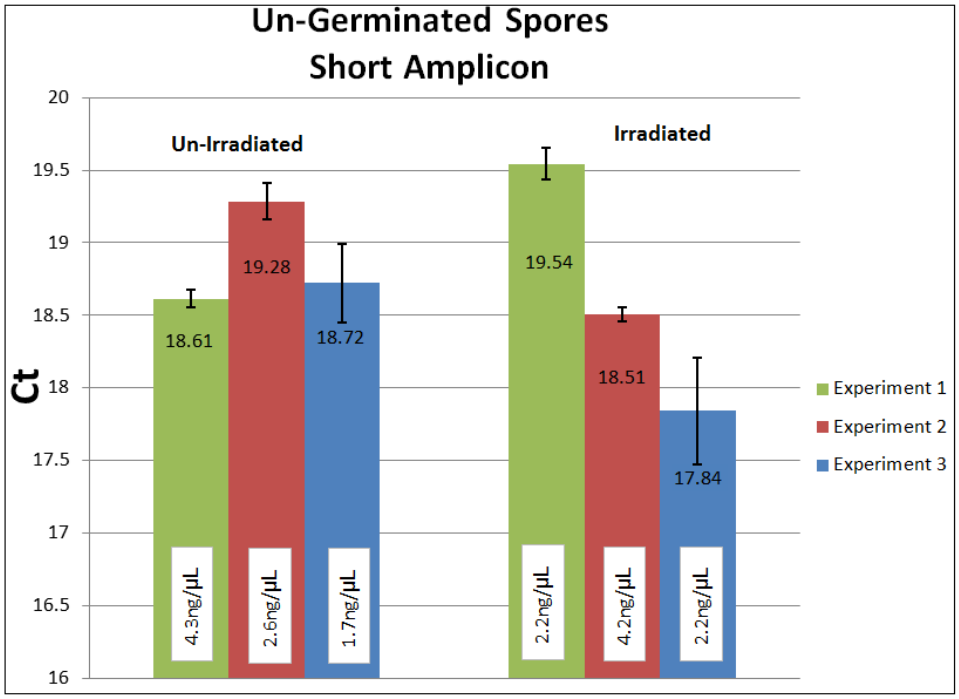

Figure 34. Un-germinated spores pre and post-irradiation. Samples for all 3 experiments are displayed. Error bars are included and individual Ct results displayed on the bars. Total DNA concentrations are also shown in a white box at the bottom of each bar. Data in this figure corresponds to the short amplicon, 245bps long. Irradiation of 1-log kill.

In Figure 34 above, two different trends are observed. In Experiment 1, PCR amplification occurs faster in the un-irradiated spores than in irradiated as expected. When the DNA is damaged, it's expected to take longer (higher Ct) to amplify in the PCR (less complete, undamaged copies of template DNA are available). However, in experiments 2 and 3, the opposite trends are observed. It should be noted that these spores have not germinated. No repair has occurred. Samples in Figure 34 should be directly reflective of the damage incurred by the DNA during log kill1 irradiation. Figure 35 below displays the same samples as Figure 34, with the longer amplicon primers.

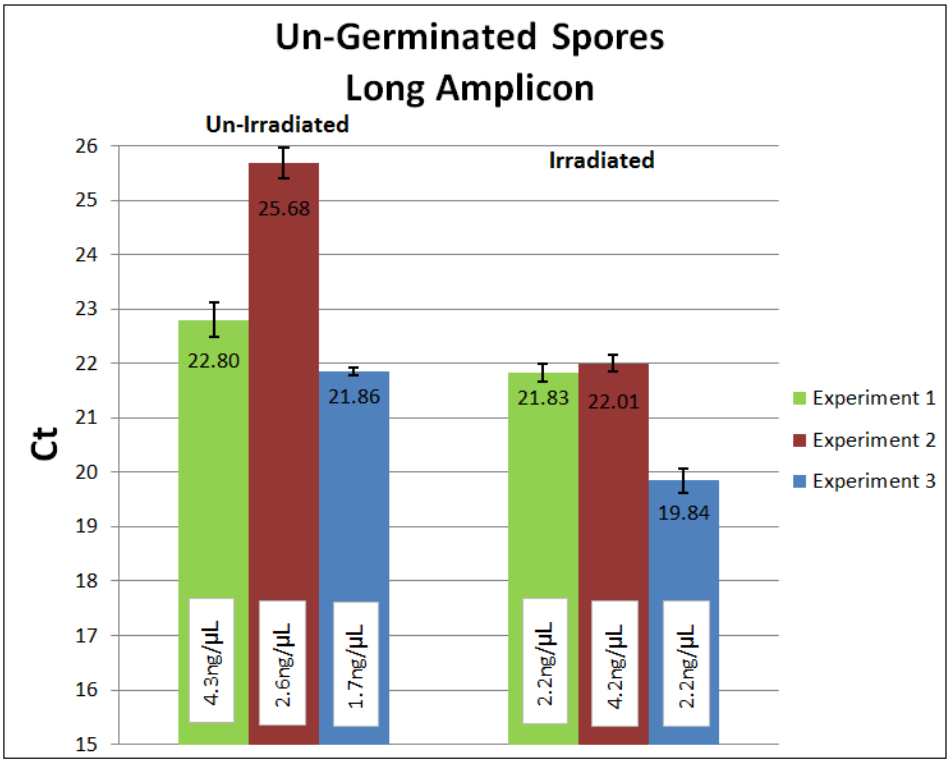

Figure 35. Un-germinated spores pre and post-irradiation. Samples for all 3 experiments are displayed. Error bars are included and individual Ct results displayed on the bars. Total DNA concentrations are also shown in a white box at the bottom of each bar. Data in this figure corresponds to the long amplicon, 547bps long. Irradiation of 1-log kill.

In all 3 experiments displayed in Figure 35, the irradiated DNA is more efficiently amplified then is the un-irradiated DNA. To better interpret this data, Figures 38 and 39 display the same data, but it has been corrected by DNA concentrations. As displayed in Figure 34-37, total DNA concentrations (displayed in white boxes at the bottom of each bar) varied from sample to sample. This variance is most likely attributed to inconsistent isolation efficiency. It should be noted that total DNA concentration accounts for both genomic DNA and plasmid DNA. Had the PCR properly amplified all samples, Ct values would have been calibrated based on only plasmid DNA.

Figures 36 and 37 below display data from experiment 2, where 2 germination samples OR and 1R properly amplified. Figure 36 shows data for the short amplicon and Figure 37 for the Long amplicon. Notice the errors for germinated samples in Figure 36 are very large. On average, the data in Figures 36 and 37 again show a faster efficiency of amplification after irradiation. This was not the expected trending. Making conclusions from this data would not tell the full story. Conclusions should instead be drawn from concentration corrected data in Figures 38-41.

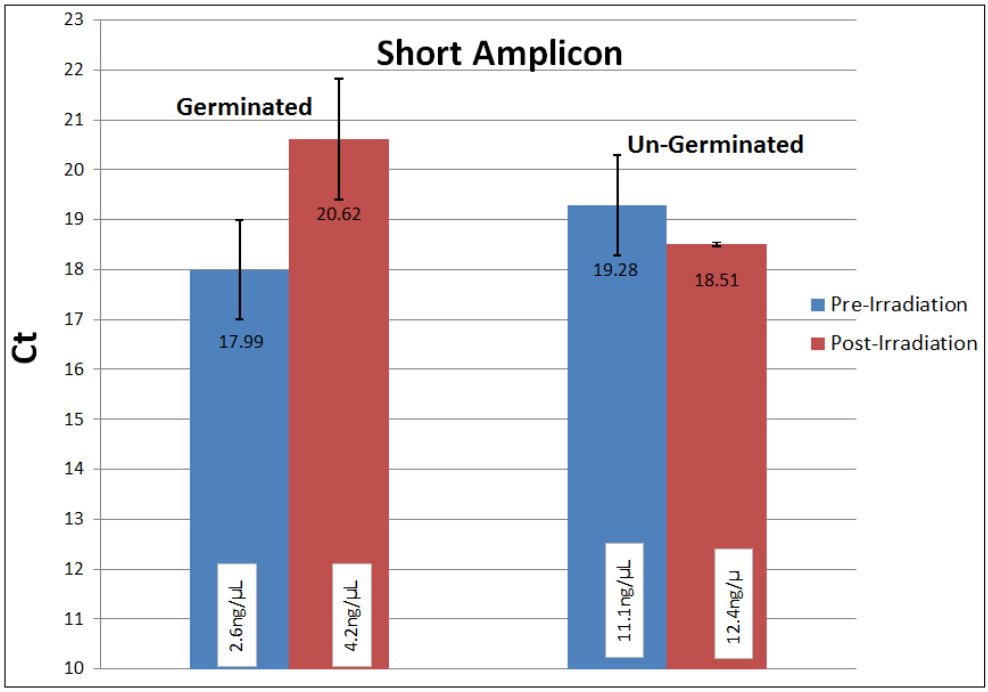

Figure 36. Ct PCR data from experiment 2, where germination samples OR and 1R properly amplified. Germinated samples are viewed on the left, un-germinated on the right. Irradiation of 1-log kill.

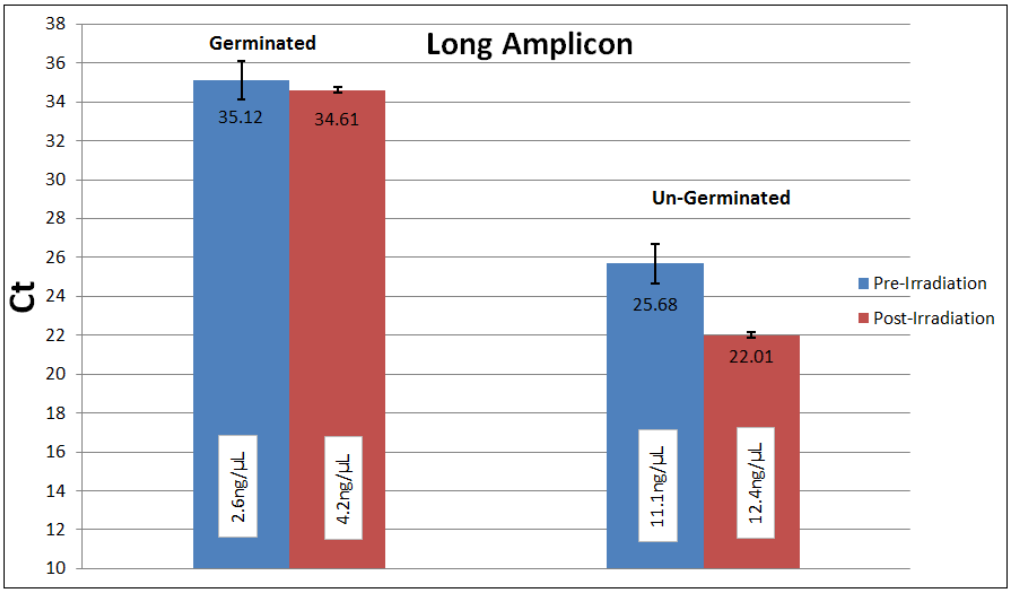

Figure 37. Ct PCR data from experiment 2, where germination samples OR and 1R properly amplified. Germinated samples are viewed on the left, un-germinated on the right. Irradiation of 1-log kill.

The following 4 figures display the same data observed in the above 4 figures. However, the data has been corrected by DNA concentration. Experiments 2 and 3 seem to be in agreement with each other, where as experiment 3 exhibits opposite trending. For the two experiments in agreement, in Figures 38 and 39, irradiated samples are more efficient at amplification than are un-irradiated. This is not the expecting trending. Figure 38 displays data for the short amplicon and Figure 39 for the long amplicon. Ct values for the next four plots are corrected by multiplying the Ct value by the total DNA concentration (ng/µL).

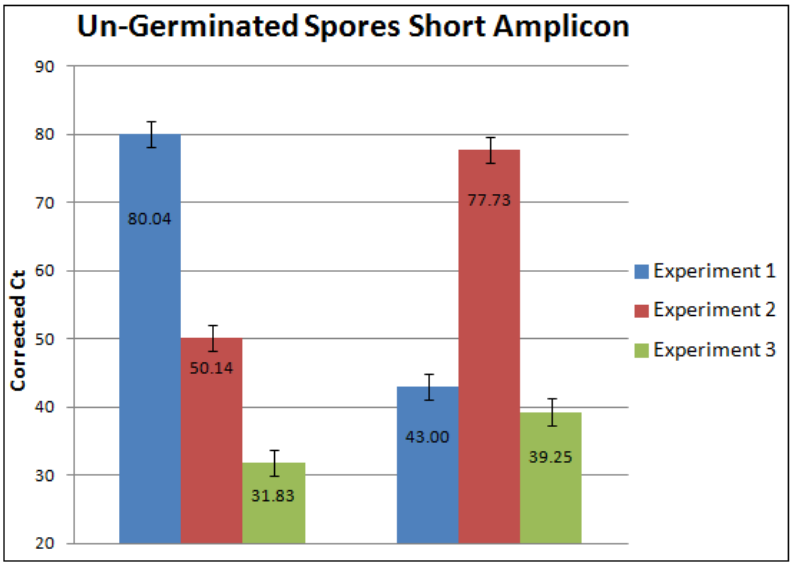

Figure 38. Un-germinated Ba spores pre and post-irradiation. Samples for all 3 experiments are displayed. Error bars are included and individual Ct results displayed on the bars. These Ct results have been corrected by total DNA concentration. Data in this figure corresponds to the short amplicon, 245bps long. Irradiation of 1-log kill. Ct*DNA has units of cylces * ng/µL.

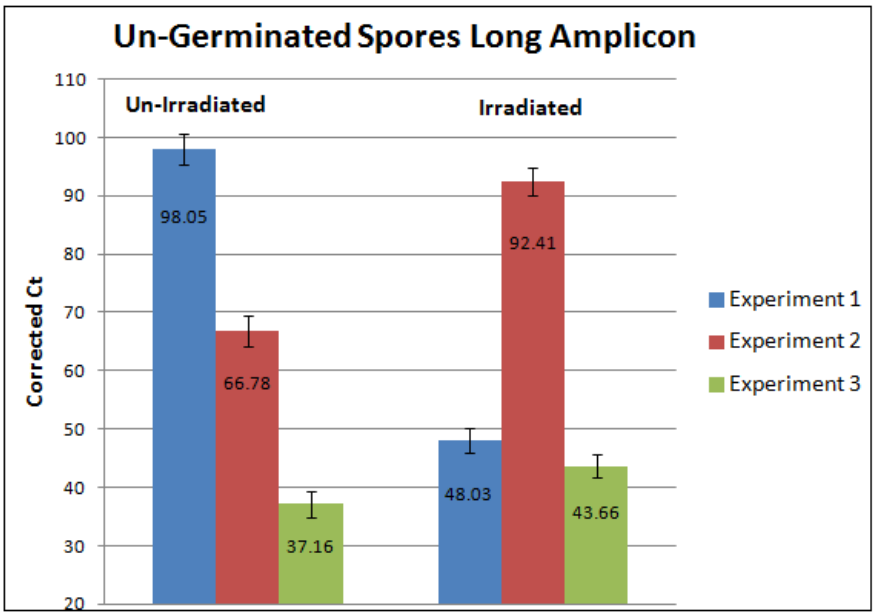

Figure 39. Un-germinated spores pre and post-irradiation. Samples for all 3 experiments are displayed. Error bars are included and individual Ct results displayed on the bars. These Ct results have been corrected by total DNA concentration. Data in this figure corresponds to the long amplicon, 547bps long. Irradiation of 1-log kill. Ct*DNA has units of cylces * ng/µL

Figures 40 and 41 below display the data from experiment 2, where germinated samples 0R and 1R were successfully amplified. Germinated samples were expected to have a lower Ct value. Because the cells are outgrowing and increasing in numbers, the number of plasmids (DNA template for PCR) should also be increasing. Because the opposite is observed, DNA isolation technique is most-likely to blame. Based on plating, the plasmid was never ejected from the Ba spore/cells. Therefore, the plasmid was subjected to the same DNA repair as the genomic DNA. In these figures, amplification is faster before irradiation then after, as expected.

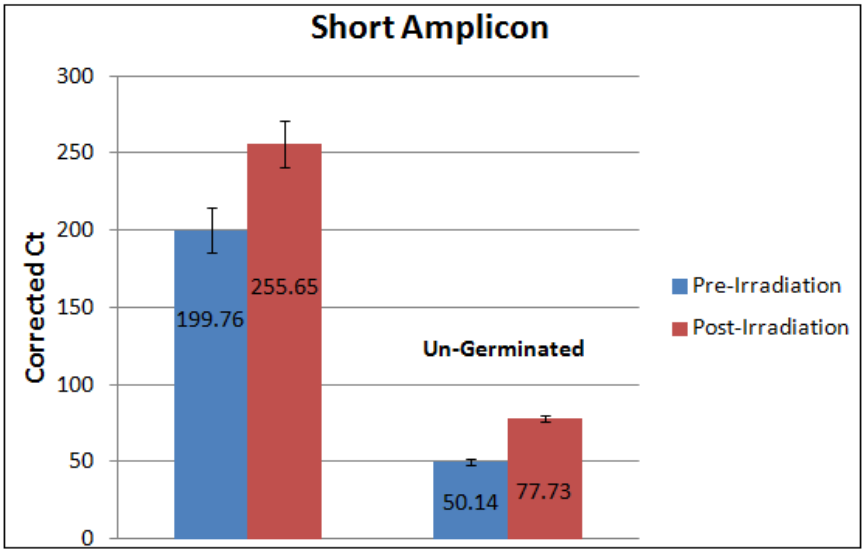

Figure 40. Experiment 2, Germinated vs Un-germinated spores. The bars in blue reflect un-irradiated spores and the bars in red reflect irradiated spores. Data in this figure corresponds to the short amplicon, 245bps long .Irradiation of 1-log kill. Ct*DNA has units of cylces * ng/µL

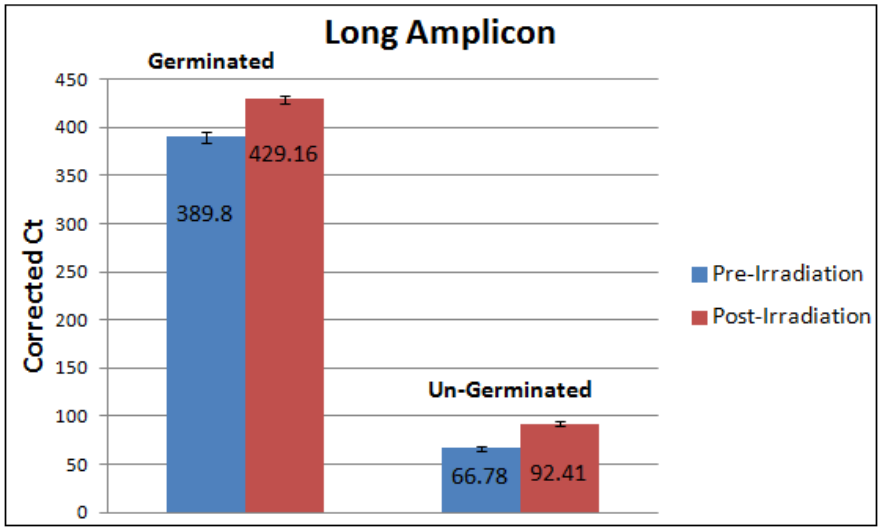

Figure 41. Experiment 2, Germinated vs Un-germinated spores. The bars in blue reflect un-irradiated spores and the bars in red reflect irradiated spores. Data in this figure corresponds to the long amplicon, 547bps long. Irradiation of 1-log kill. Ct*DNA has units of cylces * ng/µL

For un-germinated spores we have reason to believe that the DNA wasn't shredded and the data has validity. Since the isolation method for germinated spores seems to be improper, it is difficult to draw conclusions from this data. However, the isolation of un-germinated spores by bead beating was successful for all three experiments. Using only the un-germinated data, PCR is about 1.4 times less efficient for irradiated spores, then for un-irradiated.

Summary

Experimental data collected in this project included fluorescence measurements to monitor germination, AFM images to observe morphological changes in irradiated spores, survival curves to understand how Ba sterne is affected by UV radiation, and PCR measurements in an attempt to monitor DNA repair through germination and outgrowth.

Actinometry measurements were also collected to adjust the UV fluence dosage based on the efficiency of the LEDs. Overall, data collection and analysis was successful.

V. Conclusions and Recommendations

Chapter Overview

This chapter discusses conclusions drawn from the experimental data collected and also recommends future experiments that would support the currently presented data. The most crucial future recommendations are to investigate a better isolation method for germinated samples, and to solve the mystery of the taqman probe failure. Other future recommendations include redesign of the LED reactor and to conduct more survival curve experiments at different fluences. The end of the chapter also serves to conclude the entire thesis document.

Conclusions of Research

The primary objective of this research project was to develop *Bacillus anthracis* Sterne spore survival curves and to use PCR to measure DNA repair. These objectives were partially met. *Bacillus anthracis* survival curves were successfully developed. The survival curves, actinometry corrected, allowed for proper dosage of DNA repair experimentations. These survival curves are in agreement with other literature curves. PCR experiments were less than perfect. Some samples lacked any PCR amplification. PCR troubles have been attributed most likely to DNA isolation techniques and efficiency. To draw specific conclusions from the current PCR data is difficult. The data reveals an overall higher PCR efficiency from irradiated samples then from un-irradiated samples. This was not the expected outcome. Irradiated samples were expected to have greater DNA damage and therefore lower PCR amplification (corresponding to higher Ct values).

Future Recommendations

To further improve upon research collected in this project, a few important questions need to be answered, or solved. Developing a successful isolation technique for DNA must be achieved. The bead beating method used in this project is sufficient for spore DNA isolation, but is too harsh for cell DNA isolation. I recommend using a simple DNA plasmid isolation kit for Ba cells. In addition, plasmid isolation following spore DNA isolation may help isolate plasmid DNA from total genomic DNA in the initial samples. If the same experiments were to be repeated, collection times greater than 3 hours are unnecessary, as fluorescence measurements confirmed germination completion by this time. Collecting samples more frequently during the germination process would most likely allow for better modeling of repair.

Determining why the taqman probe failed would also be helpful. Occasionally, these probes just do not work. Since the primers operate efficiently, several probe sequences could be experimented with, until one working sequence is found. Investigation into a new sequencing company may also fix the issue.

Further investigation of AFM images following irradiation, during germination, and after outgrowth would be meaningful to the images already collected. It may also be beneficial to explore the adhesion properties of the spore surface before and after irradiation. AFM images displayed a clear morphological change in the spores following irradiation. More images would form statistically significant populations of different morphological changes in the irradiated spores.

Several additional experiments could be conducted in the future to support and improve the current presented data. The UV LED reactor works well, but is not a user friendly configuration. If care is not taken to properly turn on and off the LEDs, they can fail after even one operation[14]. I recommend constructing a reactor that operates in a more conducive manner to the frequency of sample collection that is necessary. Turning the LEDs on and off every 30 seconds (or less) is difficult, and not always accurate. If a port were designed that allowed for easier access sample collection, the LEDs would not need to be powered on and off as frequently.

The activity at the beginning of the survival curves is not well understood. Lack of enough data points between 0 and 50 J/m^2 could be overlooking an important shouldering feature. Other related research has reported shouldering effects at the beginning of Ba inactivation curves [48]. I recommend conducting more Ba survival curve experiments focusing on the smaller fluences to determine if the typical shouldering is indeed occurring. Tailing occurs at the end of the survival curves and is also a mystery to the researchers here at AFIT. In tandem with conducting more survival curve experiments at low fluences, I recommend sonication of the samples first, followed with close monitoring of the longer fluences. If the tailing is indeed from clusters of spores, sonication should eliminate this tailing.

Summary

This section provides a summary of the entire thesis project. Spores of *Bacillus anthracis* Ba Sterne were irradiated with 267nm UV LEDs. The pRB373 plasmid with a

[14] See Appendix for safe operation of LEDs

red fluorescent protein was transformed into Ba sterne cells prior. Following irradiation, germination media was added and the spores were incubated for various times, to allow for DNA repair. The pRB373 plasmid was isolated and analyzed using real-time PCR. Primers were designed across the RFP in the plasmid yielding two amplicons, 245bp and 547bp long. PCR amplification was not achieved for germinated samples. Spore samples isolated using bead beating methods were amplified. Results indicate a quicker amplification (lower Ct) for irradiated samples thsn for un-irradiated. Lack of PCR amplification in germinated samples is attributed to too rough an extraction method for Ba cells. This observation was not expected. Ba Survival Curves were also developed using the quadratic fit, $y = \alpha x + \beta x^2$. Averaging results form 3 experiments, α is reported as -0.0144 ± 0.008 and β as -0.00001 ± 0.0002. Fit parameters are reported to a 90% confidence interval. Actinometry experiments corrected for the efficiency of the LEDs in all experimentation. Fluorescence measurements monitored germination and outgrowth; they indicated a delay in germination of irradiated spores. AFM images showed morphological changes in irradiated spores. Spore coats and/or the exosporium appear detached from the spore following irradiation. Irradiated spores also show vegetative growth in much smaller clusters than un-irradiated spores.

Appendix

Microbial Technique & Preparation

Leighton-Doi Media Recipe

The following recipe prepares 1L of 10X sporulation media. Add the following ingredients and fill to 1L with dH_2O. Filter sterilization is recommended. Store at 4^oC. When ready to use, aseptically combine 9 parts 2X nutrient broth with 1 part 10X sporulation media.

10X Sporulation Media:

5grams $MgSO_4 \cdot 7H_2O$
20grams KCl
10grams glucose
2.4grams $Ca(NO_3)_2 \cdot 4H_2O$
0.2grams $MnCl_2 \cdot 7H_2O$
1mL 0.01M $FeSO_4 \cdot 7H_2O$ (0.28grams $FeSO_4 \cdot 7H_2O$ per 100mL H_2O)

Plasmid Fact sheet

The following information can be obtained on ATCC's website. This is a snapshot of the information provided by ATCC for the plasmid pRB373 used in this project [10].

ATCC

Product Sheet

pRB373 (ATCC® 77373™)

Please read this FIRST

Biosafety Level
1

Intended Use

This product is intended for research use only. It is not intended for any animal or human therapeutic or diagnostic use.

Citation of Strain

If use of this culture results in a scientific publication, it should be cited in that manuscript in the following manner: pRB373 (ATCC® 77373™)

Description

Designation: pRB373
Media:
ATCC® Medium 1227: LB Medium (ATCC medium 1065) with 50 mcg/ml ampicillin

Conditions

Temperature: 37.0°C

Vector Information

Size (kb): 5.8000001907348630
Vector: pRB373 (plasmid)
Construction: pUB110, pBR322
Marker(s):ampR,bleR,neoR
Construct size (kb): 5.800000190734863
Features: marker(s): ampR, neoR, bleR
replicon: pUB110, pMB1
terminator: rrnB, to phage lambd

References

References and other information relating to this product are available online at www.atcc.org.

Biosafety Level: 1

Appropriate safety procedures should always be used with this material. Laboratory safety is discussed in the current publication of the *Biosafety in Microbiological and Biomedical Laboratories* from the U.S. Department of Health and Human Services Centers for Disease Control and Prevention and National Institutes for Health.

Figure Appdx-1. ATCC pRB373 plasmid information. The pRB373 plasmid is best grown in LB medium with 50µg/mL of ampicillin at 37°C. The sheet also provides information about the size of the plasmid and its vector and construction.

Primer3Plus Primer Design

The primer3Plus images shown here were designed specifically for this project. The primers and probe operate across the RFP sequence shown below. The RFP was inserted into the pRB373 plasmid. When using the Primer3Plus software, one should pick a left forward primer and fix it. To view more options for reverse primer, select different reaction conditions. Pay special attention to the "self" number and "Tm". The "Tm" for all of the designed primers should be close to each other and the "self" number should be

as low as possible. The “self” number indicates the likelihood of the primer to anneal and stick to itself.

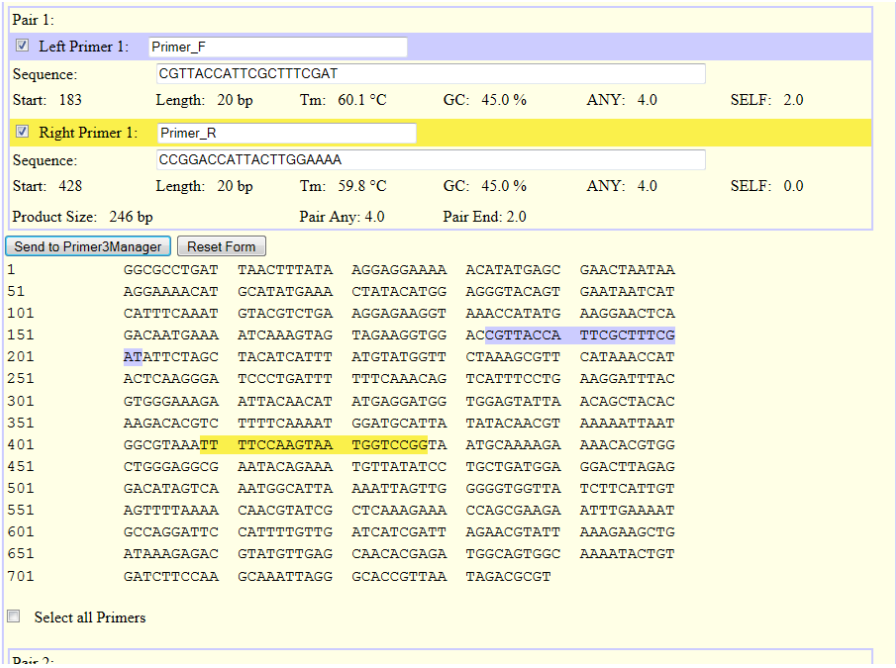

Figure Appdx-2 Primer3Plus software design of primers.

In Figure Appdx-2, the left primer begins at position 183. The first reverse primer begins at position 428. The product size (246) is the amplicon length including the primers’ sequence.

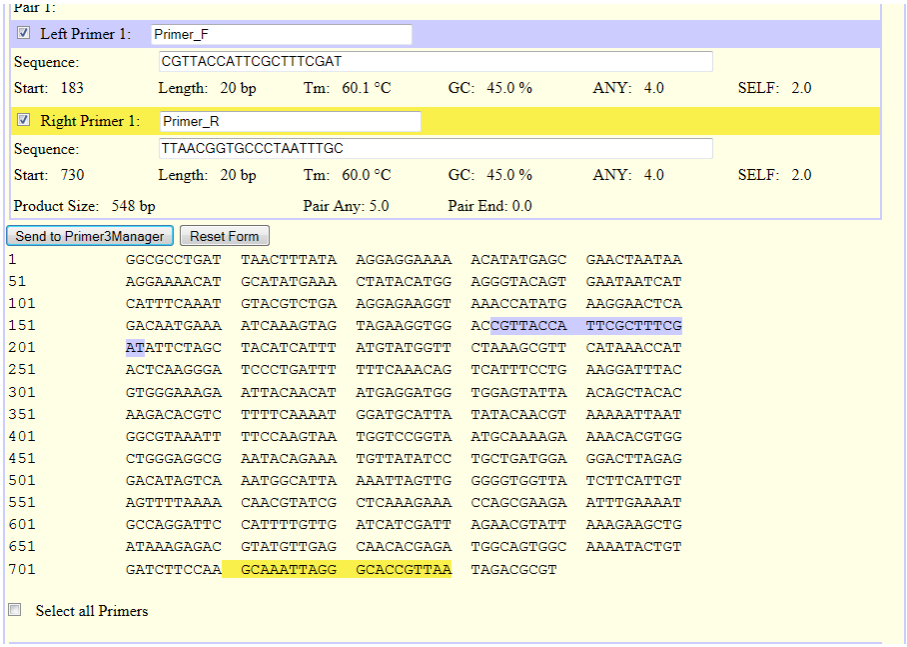

Pair 1:

Left Primer 1: Primer_F

Sequence: CGTTACCATTCGCTTTCGAT

Start: 183 Length: 20 bp Tm: 60.1 °C GC: 45.0 % ANY: 4.0 SELF: 2.0

Right Primer 1: Primer_R

Sequence: TTAACGGTGCCCTAATTTGC

Start: 730 Length: 20 bp Tm: 60.0 °C GC: 45.0 % ANY: 4.0 SELF: 2.0

Product Size: 548 bp Pair Any: 5.0 Pair End: 0.0

Send to Primer3Manager Reset Form

```
1    GGCGCCTGAT  TAACTTTATA  AGGAGGAAAA  ACATATGAGC  GAACTAATAA
51   AGGAAAACAT  GCATATGAAA  CTATACATGG  AGGGTACAGT  GAATAATCAT
101  CATTTCAAAT  GTACGTCTGA  AGGAGAAGGT  AAACCATATG  AAGGAACTCA
151  GACAATGAAA  ATCAAAGTAG  TAGAAGGTGG  ACCGTTACCA  TTCGCTTTCG
201  ATATTCTAGC  TACATCATTT  ATGTATGGTT  CTAAAGCGTT  CATAAACCAT
251  ACTCAAGGGA  TCCCTGATTT  TTTCAAACAG  TCATTTCCTG  AAGGATTTAC
301  GTGGGAAAGA  ATTACAACAT  ATGAGGATGG  TGGAGTATTA  ACAGCTACAC
351  AAGACACGTC  TTTTCAAAAT  GGATGCATTA  TATACAACGT  AAAAATTAAT
401  GGCGTAAATT  TTCCAAGTAA  TGGTCCGGTA  ATGCAAAAGA  AAACACGTGG
451  CTGGGAGGCG  AATACAGAAA  TGTTATATCC  TGCTGATGGA  GGACTTAGAG
501  GACATAGTCA  AATGGCATTA  AAATTAGTTG  GGGGTGGTTA  TCTTCATTGT
551  AGTTTTAAAA  CAACGTATCG  CTCAAAGAAA  CCAGCGAAGA  ATTTGAAAAT
601  GCCAGGATTC  CATTTTGTTG  ATCATCGATT  AGAACGTATT  AAAGAAGCTG
651  ATAAAGAGAC  GTATGTTGAG  CAACACGAGA  TGGCAGTGGC  AAAATACTGT
701  GATCTTCCAA  GCAAATTAGG  GCACCGTTAA  TAGACGCGT
```

Select all Primers

Figure Appdx-3. Primer3Plus Software design of the forward primer and second reverse primer.

The resulting amplicon length is 548 base pairs. Notice the Tm for the first reverse primer, the second reverse primer and the forward primer are all around 60.0°C. Keeping the temperatures close increases efficiency of the PCR.

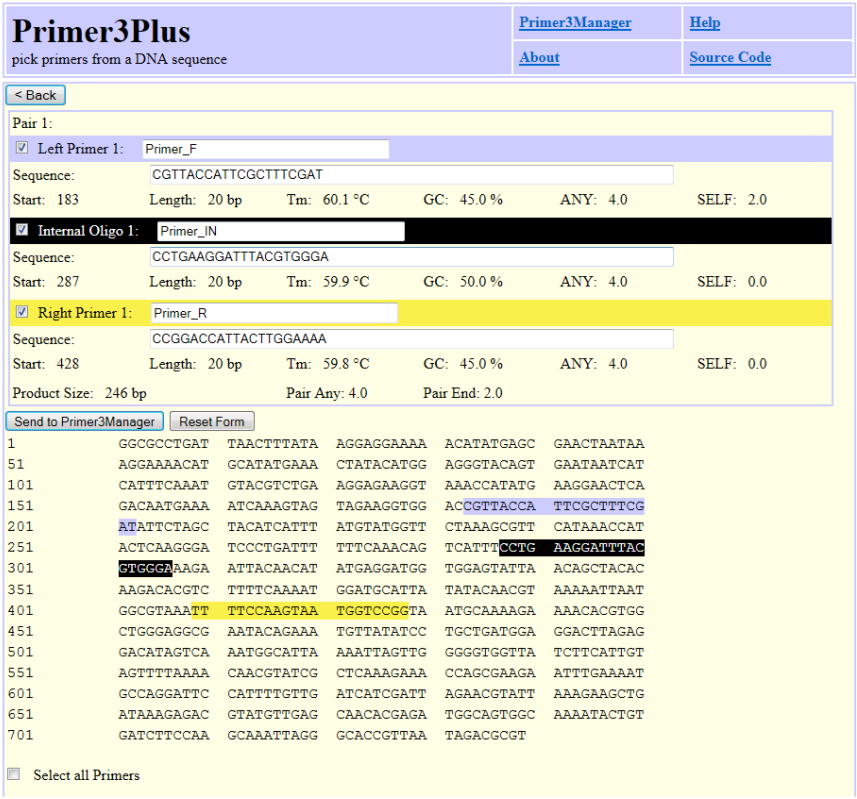

Primer3Plus
pick primers from a DNA sequence

Primer3Manager | Help | About | Source Code

< Back

Pair 1:

Left Primer 1: Primer_F
Sequence: CGTTACCATTCGCTTTCGAT
Start: 183 Length: 20 bp Tm: 60.1 °C GC: 45.0 % ANY: 4.0 SELF: 2.0

Internal Oligo 1: Primer_IN
Sequence: CCTGAAGGATTTACGTGGGA
Start: 287 Length: 20 bp Tm: 59.9 °C GC: 50.0 % ANY: 4.0 SELF: 0.0

Right Primer 1: Primer_R
Sequence: CCGGACCATTACTTGGAAAA
Start: 428 Length: 20 bp Tm: 59.8 °C GC: 45.0 % ANY: 4.0 SELF: 0.0

Product Size: 246 bp Pair Any: 4.0 Pair End: 2.0

Send to Primer3Manager | Reset Form

```
1    GGCGCCTGAT  TAACTTTATA  AGGAGGAAAA  ACATATGAGC  GAACTAATAA
51   AGGAAAACAT  GCATATGAAA  CTATACATGG  AGGGTACAGT  GAATAATCAT
101  CATTTCAAAT  GTACGTCTGA  AGGAGAAGGT  AAACCATATG  AAGGAACTCA
151  GACAATGAAA  ATCAAAGTAG  TAGAAGGTGG  ACCGTTACCA  TTCGCTTTCG
201  ATATTCTAGC  TACATCATTT  ATGTATGGTT  CTAAAGCGTT  CATAAACCAT
251  ACTCAAGGGA  TCCCTGATTT  TTTCAAACAG  TCATTTCCTG  AAGGATTTAC
301  GTGGGAAAGA  ATTACAACAT  ATGAGGATGG  TGGAGTATTA  ACAGCTACAC
351  AAGACACGTC  TTTTCAAAAT  GGATGCATTA  TATACAACGT  AAAAATTAAT
401  GGCGTAAATT  TTCCAAGTAA  TGGTCCGGTA  ATGCAAAAGA  AAACACGTGG
451  CTGGGAGGCG  AATACAGAAA  TGTTATATCC  TGCTGATGGA  GGACTTAGAG
501  GACATAGTCA  AATGGCATTA  AAATTAGTTG  GGGGTGGTTA  TCTTCATTGT
551  AGTTTTAAAA  CAACGTATCG  CTCAAAGAAA  CCAGCGAAGA  ATTTGAAAAT
601  GCCAGGATTC  CATTTTGTTG  ATCATCGATT  AGAACGTATT  AAAGAAGCTG
651  ATAAAGAGAC  GTATGTTGAG  CAACACGAGA  TGGCAGTGGC  AAAATACTGT
701  GATCTTCCAA  GCAAATTAGG  GCACCGTTAA  TAGACGCGT
```

Select all Primers

Figure Appdx-4. Primer3Plus software design of the internal oligo (or probe).

Once the probe was designed in Primer3Plus, the sequence was ordered through Life Technologies with a FAM fluorescence probe on one end and an MGB quencher on the other end. Again, note that the T_m of the probe is around 60.0°C.

RFP Sequence

The following information is provided about the turbo-RFP sequence. The primers and probe were designed across the sequence of the RFP.

Gene name: BaTurboRFP, Length: 739 bp, Vector name: pUC57,
Cloning strategy: pUC57,
Plasmid preparation: Custom plasmid preparation: 100 ug, Quality grade: Research Grade (Predominantly supercoiled),
Sequence:
GGCGCCTGATTAACTTTATAAGGAGGAAAAACATATGAGCGAACTAATAAAGGAAA
ACATGCATATGAAACTATACATGG
AGGGTACAGTGAATAATCATCATTTCAAATGTACGTCTGAAGGAGAAGGTAAACCAT
ATGAAGGAACTCAGACAATGAAA
ATCAAAGTAGTAGAAGGTGGACCGTTACCATTCGCTTTCGATATTCTAGCTACATCAT
TTATGTATGGTTCTAAAGCGTT
CATAAACCATACTCAAGGGATCCCTGATTTTTTCAAACAGTCATTTCCTGAAGGATTT
ACGTGGGAAAGAATTACAACAT
ATGAGGATGGTGGAGTATTAACAGCTACACAAGACACGTCTTTTCAAAATGGATGCA
TTATATACAACGTAAAAATTAAT
GGCGTAAATTTTCCAAGTAATGGTCCGGTAATGCAAAAGAAAACACGTGGCTGGGA
GGCGAATACAGAAATGTTATATCC
TGCTGATGGAGGACTTAGAGGACATAGTCAAATGGCATTAAAATTAGTTGGGGGTGG
TTATCTTCATTGTAGTTTTAAAA
CAACGTATCGCTCAAAGAAACCAGCGAAGAATTTGAAAATGCCAGGATTCCATTTTG
TTGATCATCGATTAGAACGTATT
AAAGAAGCTGATAAAGAGACGTATGTTGAGCAACACGAGATGGCAGTGGCAAAATA
CTGTGATCTTCCAAGCAAATTAGG
GCACCGTTAATAGACGCGT

Serial Dilution Procedure

Performing serial dilutions consistently and accurately is crucial for success in biological research. The following procedure was used for this experimentation.

1) Prepare 10 micro centrifuge tubes with 900µL of water each. Label them 10^{-1} through 10^{-10}.

2) Take 100µL of sample and place into the first tube (labeled 10^{-1}). This tube will be $1/10^{th}$ the concentration of your starting sample. Mix well.
3) Pipette 100µL of that tube into the next tube (10^{-2}). Do this until all tubes have been diluted. Now, the dilution series decreases in spore concentration by $1/10^{th}$ each sequential tube.
4) Plate 100µL of each tube in triplicate. The plates will be $1/10^{th}$ the concentration of the tube, and $1/100^{th}$ the concentration of the starting stock solution.

SYBR Green PCR Master Mix

For 1mL
500µL SYBR Green
500µL DNAse Free Water
1µL Forward Primer
1µL Reverse Primer 1
A second solution should be made with the Reverse Primer 2 (omitting Reverse Primer 1)
Note: SYBR Green does not require a hot start

Experimental Information

Proper LED Operation

To prevent the LEDs from failing, a certain order of operations has been developed. The LEDs should not be plugged in to the circuit board until the DASY Lab software has been turned on and the voltage turned up to approximately 1.0V on the voltage slider. Because the circuit board has an amplifier, a voltage of 1.0V in DASY Lab will cause the voltage in the board to be around 2.5V. Any fluctuations in voltage that will occur will

not lead to a negative voltage, as the play in the voltage will instead be around 2 volts. Since the start-up voltage for the LEDs is around 5 volts, the LEDs will still not be turned on. The following order of operations will protect the LEDs:

Turn-on

1) Turn on the computer and open up DASY Lab software.
2) Plug in the circuit board and turn on voltmeter to monitor voltage.
3) Slide voltage slider to 1.0V and hit play.
4) Rather than hitting stop and start each time you power off the LEDs, just change the slider and hit enter. Only hit stop when you are finished with the board. This prevents play in the voltage.
5) Plug in the LEDs (ground first).
6) Now set the slider to 10.0V to power on the LEDs. Because of the resistors, the Voltage will not go above the start-up voltage of the LEDs (5.3V), even if the slider is set to 10V.

Turn-off

1) The LEDs should be the first portion of the system to be shut off. First take the voltage slider back down to 1.0V. Ensure the LEDs are off by first checking the voltmeter and then checking the LEDs.
2) Unplug the LEDs, ground last.
3) Once the LEDs are unplugged, everything else can be shut-off in any order.

LED characterization and Manufacturer Specifications

The following three sheets were provided from the company SETi [46]. They provide manufacturer specifications for the LEDs purchased including voltage, current, and peak wavelength. These specifications were not explicitly used in data analysis, as an integrating sphere was used to more accurately peak wavelength and power output of the LEDs.

SETi SENSOR ELECTRONIC TECHNOLOGY, INC.

QC Inspection Report

SYSTEM 1	Customer	AFIT WP AFB			Date	3/31/2014	PO #	033114PM
	Part #	UVTOP	260	TO39	FW		Box #	0
SN: 03102007	Tested	JM3					Item #	0
#	Voltage*, V	Current, mA	Power*, W	Peak Wave*, nm	HB, nm	PSV*, W / nm		Date / Time
I6	5.354887	19.99	8.50E-04	268.4	10.9	6.24E-05		3/31/14 13:00
I7	5.372759	19.99	8.61E-04	268.4	10.9	6.30E-05		3/31/14 13:00
3								
4								
5								
6								
7								
8								
9								
10								
11								
12								
13								
14								
15								
16								
17								
18								
19								
20								
21								
22								
23								
24								
25								
26								
27								
28								
29								
30								
MIN	5.354887	19.99	8.50E-04	268.4	10.9	6.24E-05		
MAX	5.372759	19.99	8.61E-04	268.4	10.9	6.30E-05		
AVG	5.363823	19.99	8.56E-04	268.4	10.9	6.27E-05		
TESTED BY			JM3	*Peak wavelength measurement tolerance is +/- 2 nm				
QC INSPECTOR			FJ	*Optical power output measurement tolerance is +/- 10%				
				*Forward voltage measurement tolerance is +/- 2%				

Figure Appdx-5. SETi manufacturer specifications for purchased LEDs

SETi SENSOR ELECTRONIC TECHNOLOGY, INC.

QC Inspection Report

SYSTEM 2	Customer	AFIT WP AFB			Date	4/24/2014	PO #	042114PB
	Part #	UVTOP	260	TO39	FW		Box #	0
SN: 06206032	Tested	CWG					Item #	0
#	Voltage*, V	Current, mA	Power*, W	Peak Wave*, nm	HB, nm	PSV*, W / nm		Date / Time
X9	5.344748	20.00	1.10E-03	268.8	10.5	8.26E-05		4/24/14 8:26
Y2	5.332419	20.00	1.11E-03	268.8	10.5	8.32E-05		4/24/14 8:26
Y3	5.337442	20.00	1.10E-03	268.8	10.5	8.22E-05		4/24/14 8:27
Y4	5.340143	20.00	1.11E-03	268.8	10.5	8.30E-05		4/24/14 8:27
Y6	5.357629	20.00	1.12E-03	268.8	10.5	8.44E-05		4/24/14 8:28
6								
7								
8								
9								
10								
11								
12								
13								
14								
15								
16								
17								
18								
19								
20								
21								
22								
23								
24								
25								
26								
27								
28								
29								
30								
MIN	5.332419	20.00	1.10E-03	268.8	10.5	8.22E-05		
MAX	5.357629	20.00	1.12E-03	268.8	10.5	8.44E-05		
AVG	5.3424762	20.00	1.11E-03	268.8	10.5	8.31E-05		
TESTED BY			CWG	*Peak wavelength measurement tolerance is +/- 2 nm				
QC INSPECTOR			FJ	*Optical power output measurement tolerance is +/- 10%				
				*Forward voltage measurement tolerance is +/- 2%				

Figure Appdx-6. SETi manufacturer specifications for purchased LEDs.

SETi Sensor Electronic Technology, Inc.	QC Inspection Report							
	Customer	AFIT WP AFB			Date	6/2/2014	PO #	053014PB
	Part #	UVTOP	260	TO39	FW		Box #	0
	Tested	CWG					Item #	0
#	Voltage*, V	Current, mA	Power*, W	Peak Wave*, nm	HB, nm	PSV*, W / nm		Date / Time
X10	5.349346	20.00	1.08E-03	268.8	10.5	8.10E-05		6/2/14 8:49
Y1	5.368031	20.00	1.02E-03	268.8	10.5	7.65E-05		6/2/14 8:50
Y5	5.356182	20.00	1.04E-03	268.8	10.5	7.82E-05		6/2/14 8:50
4								
5								
6								
7								
8								
9								
10								
11								
12								
13								
14								
15								
16								
17								
18								
19								
20								
21								
22								
23								
24								
25								
26								
27								
28								
29								
30								
MIN	5.349346	20.00	1.02E-03	268.8	10.5	7.65E-05		
MAX	5.368031	20.00	1.08E-03	268.8	10.5	8.10E-05		
AVG	5.357853	20.00	1.05E-03	268.8	10.5	7.85E-05		
TESTED BY			CWG	*Peak wavelength measurement tolerance is +/- 2 nm				
QC INSPECTOR			FJ	*Optical power output measurement tolerance is +/- 10%				
				*Forward voltage measurement tolerance is +/- 2%				

Figure Appdx-7. SETi manufacturer specifications for purchased LEDs.

The following measurements were taken at AFIT using an integrating sphere. These measurements were used for the duration of the project. Total power measurements for each LED were taken in duplicate and then averaged. The peak wavelength chosen for this research was an average of all LEDs, 267nm.

Table Appdx-1. LED measurements collected using the integrating sphere. Two Power measurements were taken for each LED and averaged. Peak wavelength used for calculations throughout the project was 267nm, and average wavelength of all the LEDs.

LED	Total Power (W)	Average Total Power (W)	Peak Wavelength (nm)
Y1	0.00133	0.00130	267
Y1	0.00133		267
X10	0.00140	0.00140	267
X10	0.00141		267
Y5	0.00137	0.00136	267
Y5	0.00135		267
I7	0.00416	0.00416	268
I7	0.00416		268
I6	0.00139	0.00139	266
I6	0.00139		266
X9	0.00157	0.00157	267
X9	0.00157		267
Y2	0.00164	0.00164	266
Y2	0.00164		266
Y3	0.00157	0.00158	267
Y3	0.00159		267
Y4	0.00157	0.00157	267
Y4	0.00157		267
Y6	0.00163	0.00163	267
Y6	0.00163		267

Raw Data

Actinometry

Figure Appdx-8 below displays the raw data collected for both actinometry experiments. This data has not been corrected in quantum yield or fluence. However, the functionality is similar to the functionality of the apparent quantum yield vs. correct fluence.

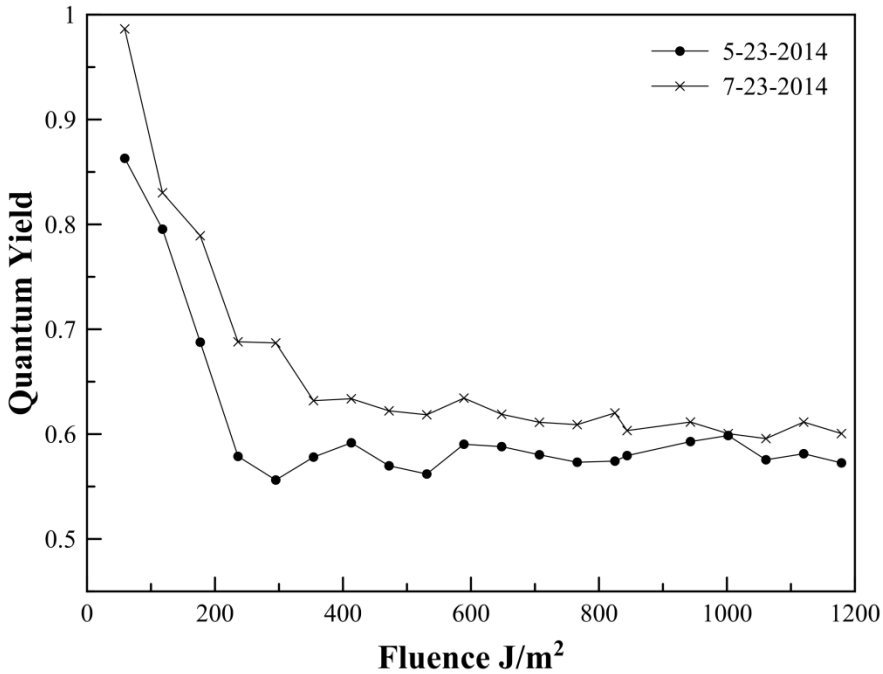

Figure Appdx-8. Quantum yield vs. Fluence for raw actinometry data. The fluence values have not been corrected and the quantum yield has not been temperature adjusted.

Tables Appdx-2 and Appdx-3 tabulate the data displayed in Figure Appdx-8 above. All the values necessary to calculate quantum yield are listed in these tables. Quantum yield in the far right columns has not been adjusted. Fluence values in column two are also not corrected. Note the temperature on collection days.

Table Appdx-2. Actinometry data collected on 5/23/2014, prior to experimentation. The temperature on this collection day was 21°C.

Collection Date: 5/23/2014 Temp: 21°C								
Irradiation Time, Seconds	**Fluence (J/m²)**	**Abs @ 352nm**	**Abs Blank**	**[I3⁻]**	**Moles [I3⁻]**	**Einsteins of UV absorbed at 267nm**	**Abs @ 267nm**	**Quantum Yield**
30	59	0.130	0.053	0.003	0.003	0.00000831	3.82	0.863
60	118	0.119	0.053	0.002	0.002	0.00000715	**Power (mWatts)**	0.795
90	177	0.185	0.053	0.005	0.005	0.00001428	1.44	0.688
120	236	0.235	0.053	0.007	0.007	0.00001971	**U(λ)**	0.579
150	295	0.300	0.053	0.009	0.009	0.00002678	447938.13	0.556
180	354	0.361	0.053	0.011	0.011	0.00003340	**Reflection Coeff.**	0.578
210	413	0.421	0.053	0.013	0.013	0.00003989	0.9	0.592
240	472	0.458	0.053	0.015	0.015	0.00004390		0.570
270	531	0.502	0.054	0.016	0.016	0.00004871		0.562
300	589	0.578	0.054	0.019	0.019	0.00005685		0.590
330	648	0.627	0.053	0.021	0.021	0.00006230		0.588
360	707	0.672	0.054	0.022	0.022	0.00006706		0.580
390	766	0.715	0.054	0.024	0.024	0.00007176		0.573
420	825	0.767	0.054	0.026	0.026	0.00007743		0.574
450	844	0.825	0.054	0.028	0.028	0.00008371		0.579
480	943	0.895	0.054	0.030	0.030	0.00009136		0.593
510	1002	0.957	0.054	0.033	0.033	0.00009801		0.599
540	1061	0.973	0.054	0.033	0.033	0.00009977		0.576
570	1120	1.034	0.054	0.035	0.035	0.00010636		0.581
600	1179	1.070	0.054	0.037	0.037	0.00011028		0.573

Table Appdx-3. Actinometry data collected on 7/21/2014, following all experimentation. The temperature on this collection day was 22°C.

Collection Date: 7/21/2014 Temp: 22°C								
Irradiation Time, Seconds	**Fluence (J/m²)**	**Abs @ 352nm**	**Abs Blank**	**[I3⁻]**	**Moles [I3⁻]**	**Einsteins of UV absorbed at 267nm**	**Abs @ 267nm**	**Quantum Yield**
30	59	0.189	0.059	0.005	0.00001410	0.00000963	3.82	0.986
60	118	0.206	0.059	0.005	0.00001599	0.00001926	**Power (mWatts)**	0.830
90	177	0.270	0.060	0.008	0.00002280	0.00002889	1.44	0.789
120	236	0.306	0.062	0.009	0.00002650	0.00003852	**U(λ)**	0.688
150	295	0.368	0.063	0.011	0.00003308	0.00004815	447938.13	0.687
180	354	0.400	0.063	0.012	0.00003651	0.00005778	**Reflection Coeff.**	0.632
210	413	0.456	0.063	0.014	0.00004272	0.00006741	0.9	0.634
240	472	0.504	0.062	0.016	0.00004794	0.00007705		0.622
270	531	0.557	0.063	0.018	0.00005360	0.00008668		0.618
300	589	0.626	0.063	0.020	0.00006109	0.00009631		0.634
330	648	0.666	0.062	0.022	0.00006557	0.00010594		0.619
360	707	0.712	0.061	0.024	0.00007064	0.00011557		0.611
390	766	0.765	0.063	0.025	0.00007625	0.00012520		0.609
420	825	0.832	0.062	0.028	0.00008362	0.00013483		0.620
450	844	0.864	0.061	0.029	0.00008716	0.00014446		0.603
480	943	0.929	0.061	0.031	0.00009423	0.00015409		0.612
510	1002	0.968	0.062	0.033	0.00009830	0.00016372		0.600
540	1061	1.013	0.062	0.034	0.00010327	0.00017335		0.596
570	1120	1.092	0.061	0.037	0.00011189	0.00018298		0.611
600	1179	1.127	0.061	0.039	0.00011566	0.00019261		0.600

Survival Curve Data

This sections presents then raw data collected for Survival Curves 1 through 3. N and N_o are representative of physical plate counts, an average of three plates counted in triplicate.

Table Appdx-4. Survival Curve 1 data. The fluence values used are the corrected fluence values, determined from the actinometry experiments. N/N_o is termed the surviving fraction. Survival Curve 1 data was collected on 6/13/2014.

Experiment #1 6/13/2014					
Time (Sec)	Corrected Fluence	No	N	N/No	Counting Error
0	0	2000000	2000000	1	0
26	44.82	2000000	430000	0.215	0.00168095
26	44.82	2000000	380000	0.19	0.00176963
26	44.82	2000000	320000	0.16	0.00190394
51	87.88	2000000	90000	0.045	0.00340751
51	87.88	2000000	120000	0.06	0.00297209
51	87.88	2000000	60000	0.03	0.00414327
77	132.70	2000000	52000	0.026	0.00444193
77	132.70	2000000	48000	0.024	0.0046188
77	132.70	2000000	36000	0.018	0.00531769
102	175.76	2000000	22000	0.011	0.00677898
102	175.76	2000000	17000	0.0085	0.00770218
102	175.76	2000000	9000	0.0045	0.01056462
127	219.70	2000000	3600	0.0018	0.01668166
127	219.70	2000000	4200	0.0021	0.01544653
127	219.70	2000000	2200	0.0011	0.02133179
178	307.58	2000000	200	0.0001	0.07071421
178	307.58	2000000	100	0.00005	0.1000025
178	307.58	2000000	100	0.00005	0.1000025
229	395.46	2000000	1	0.0000005	1.00000025
229	395.46	2000000	2	0.000001	0.70710713
229	395.46	2000000	2	0.000001	0.70710713
331	571.22	2000000	1	0.0000005	1.00000025
331	571.22	2000000	2	0.000001	0.70710713
331	571.22	2000000	1	0.0000005	1.00000025
433	747.86	2000000	3	0.0000015	0.5773507
433	747.86	2000000	1	0.0000005	1.00000025
433	747.86	2000000	1	0.0000005	1.00000025
560	966.68	2000000	0	0	1
560	966.68	2000000	0	0	1
560	966.68	2000000	0	0	1

Table Appdx-5. Survival Curve 2 data. The fluence values used are the corrected fluence values, determined from the actinometry experiments. N/N_o is termed the surviving fraction. Survival Curve 1 data was collected on 6/14/2014.

Experiment #2 6/14/2014					
Time (Sec)	Corrected Fluence	No	N	N/No	Counting Error
0	0	1000000	1000000	1	0
26	44.82	1000000	440000	0.44	0.00180907
26	44.82	1000000	270000	0.27	0.0021688
26	44.82	1000000	350000	0.35	0.00196396
51	87.88	1000000	100000	0.1	0.00331662
51	87.88	1000000	130000	0.13	0.00294827
51	87.88	1000000	140000	0.14	0.00285357
77	132.70	1000000	7000	0.007	0.01199405
77	132.70	1000000	13000	0.013	0.0088274
77	132.70	1000000	11000	0.011	0.00958692
90	155.55	1000000	4300	0.0043	0.01528261
90	155.55	1000000	3600	0.0036	0.01669664
90	155.55	1000000	4700	0.0047	0.01462074
102	175.76	1000000	1000	0.001	0.03163858
102	175.76	1000000	1500	0.0015	0.02583925
102	175.76	1000000	800	0.0008	0.03536948
115	198.61	1000000	570	0.00057	0.04189733
115	198.61	1000000	340	0.00034	0.05424183
115	198.61	1000000	510	0.00051	0.04429203
127	219.70	1000000	490	0.00049	0.04518646
127	219.70	1000000	370	0.00037	0.05199714
127	219.70	1000000	420	0.00042	0.04880525
150	259.25	1000000	28	0.000028	0.18898488
150	259.25	1000000	21	0.000021	0.21822018
150	259.25	1000000	14	0.000014	0.26726311
178	307.58	1000000	13	0.000013	0.2773519
178	307.58	1000000	14	0.000014	0.26726311
178	307.58	1000000	6	0.000006	0.40824952
229	395.46	1000000	7	0.000007	0.3779658
229	395.46	1000000	10	0.00001	0.31622935
229	395.46	1000000	5	0.000005	0.44721471
331	571.22	1000000	1	0.000001	1.0000005
331	571.22	1000000	3	0.000003	0.57735114
331	571.22	1000000	2	0.000002	0.70710749
433	747.86	1000000	1	0.000001	1.0000005
433	747.86	1000000	1	0.000001	1.0000005
433	747.86	1000000	1	0.000001	1.0000005
560	966.68	1000000	0	0	1
560	966.68	1000000	0	0	1
560	966.68	1000000	0	0	1

Table Appdx-6. Survival Curve 3 data. The fluence values used are the corrected fluence values, determined from the actinometry experiments. N/N_o is termed the surviving fraction. Survival Curve 3 data was collected on 6/18/2014.

Experiment #3 6/18/2014					
Time (Sec)	Corrected Fluence	No	N	N/No	Counting Error
0	0	2500000	2500000	1	0
26	44.82	2500000	280000	0.112	0.001992844
26	44.82	2500000	340000	0.136	0.001827889
26	44.82	2500000	200000	0.08	0.00232379
51	87.88	2500000	120000	0.048	0.002955221
51	87.88	2500000	90000	0.036	0.003392803
51	87.88	2500000	70000	0.028	0.003832194
77	132.70	2500000	9000	0.0036	0.010559882
77	132.70	2500000	7000	0.0028	0.011969008
77	132.70	2500000	10000	0.004	0.01001998
90	155.55	2500000	3600	0.00144	0.016678662
90	155.55	2500000	4800	0.00192	0.014447606
90	155.55	2500000	4200	0.00168	0.015443291
102	175.76	2500000	800	0.00032	0.035360995
102	175.76	2500000	700	0.00028	0.037801738
102	175.76	2500000	600	0.00024	0.040829728
115	198.61	2500000	200	0.00008	0.070713506
115	198.61	2500000	300	0.00012	0.057738491
115	198.61	2500000	400	0.00016	0.050004
127	219.70	2500000	160	0.000064	0.079059471
127	219.70	2500000	150	0.00006	0.081652108
127	219.70	2500000	130	0.000052	0.087708082
150	259.25	2500000	25	0.00001	0.200001
150	259.25	2500000	29	0.0000116	0.185696415
150	259.25	2500000	19	0.0000076	0.229416606
178	307.58	2500000	11	0.0000044	0.301512008
178	307.58	2500000	10	0.000004	0.316228398
178	307.58	2500000	10	0.000004	0.316228398
229	395.46	2500000	4	0.0000016	0.5000004
229	395.46	2500000	4	0.0000016	0.5000004
229	395.46	2500000	4	0.0000016	0.5000004
331	571.22	2500000	3	0.0000012	0.577350616
331	571.22	2500000	1	0.0000004	1.0000002
331	571.22	2500000	1	0.0000004	1.0000002
433	747.86	2500000	1	0.0000004	1.0000002
433	747.86	2500000	1	0.0000004	1.0000002
433	747.86	2500000	1	0.0000004	1.0000002
560	966.68	2500000	0	0	1
560	966.68	2500000	0	0	1
560	966.68	2500000	0	0	1

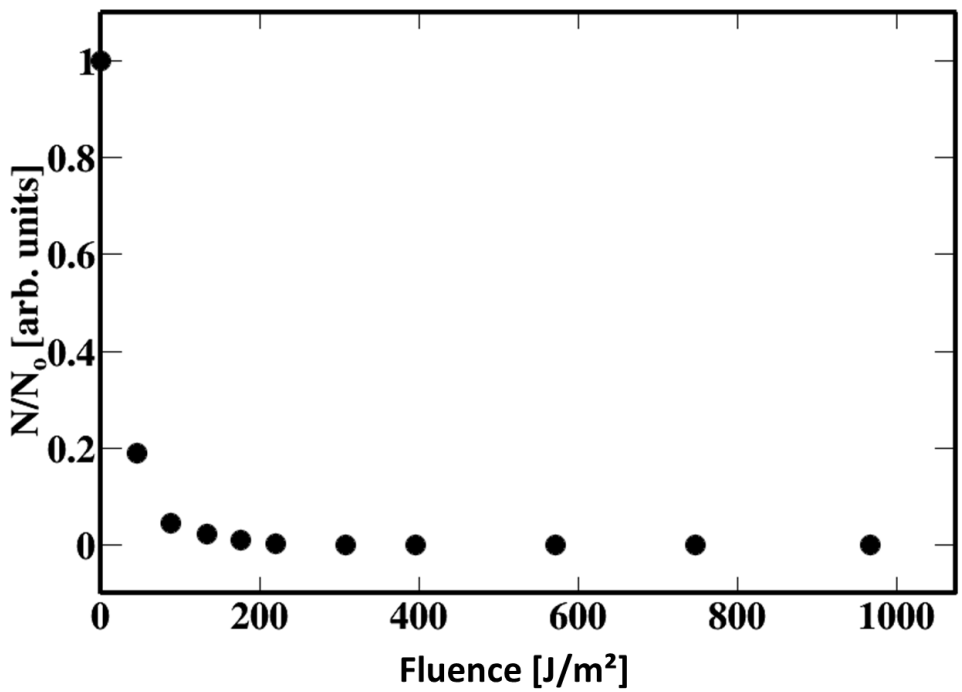

Figure Appdx-9. Survival Curve 1 surviving fraction. Ideally, more points would be placed in the 0 to 200J/m^2 range, to determine if shouldering is occurring.
The next table and figure display the fitting and fitting parameters for Survival Curve 1.

Of all three survival curves, R^2 was the worst for Survival Curve 1.

Table Appdx-7. Survival Curve 1 fitting statistics. Note that for survival curve 1, β is positive. B is negative for the other two survival curves.

Survival Curve #1	
α	-0.015
β	0.000012
Reduced X^2	0.3858
R^2	0.986

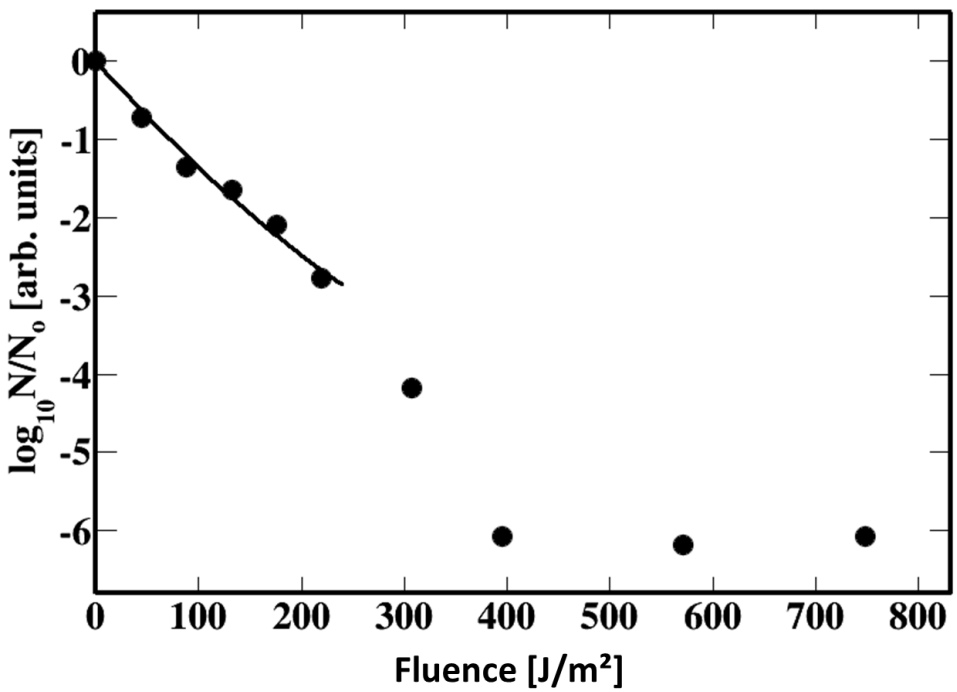

Figure Appdx-10. Survival Curve 1, fitting to 240J/m^2. Note that this particular fit seems to have a slight curve, due to the fact that β is positive.

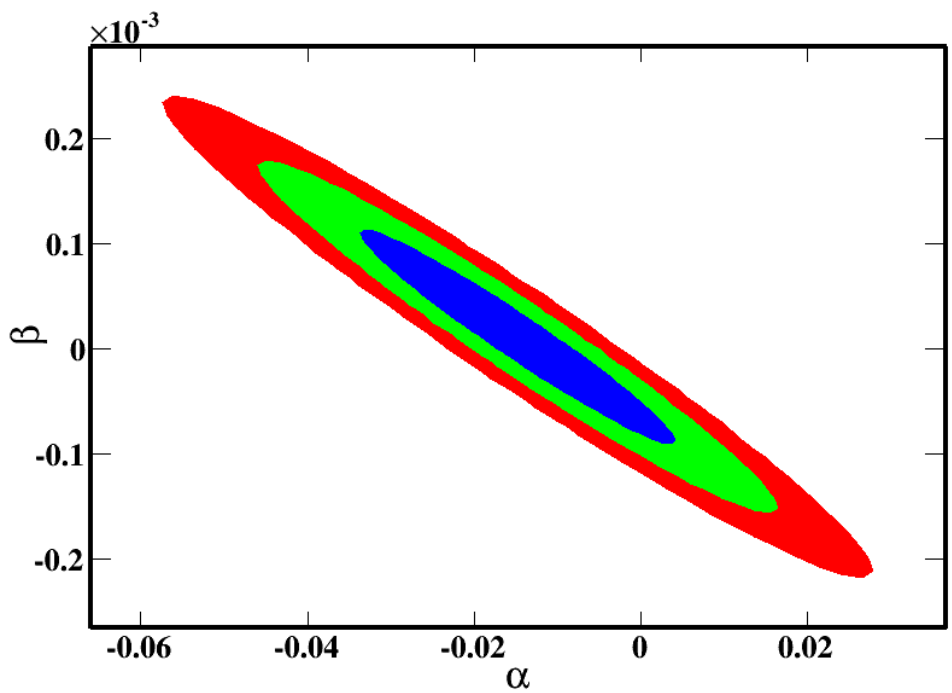

Figure Appdx-11. Pearson product-moment correlation plot for Survival Curve 1. The two fit parameters α and β are negatively correlated. The blue area indicates 1 standard

deviation from the mean, where 68% of the data lies. The green area indicates 2 standard deviations from the mean, where 95% of the data lies. The red area indicates 3 standard deviations from the mean, where 99.7% of the data lies.

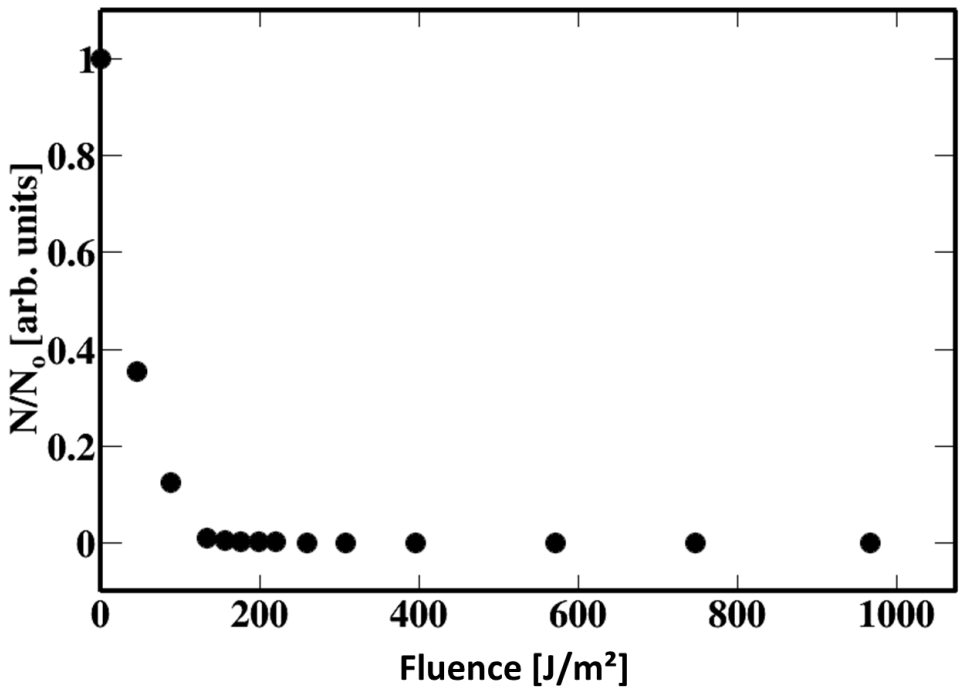

Figure Appdx-12. Survival Curve 2 surviving fraction.

Table Appdx-8. Fitting parameters and statistics for Survival Curve 2.

Survival Curve #2	
α	-0.01
β	-0.000025
Reduced X^2	0.3858
R^2	0.980

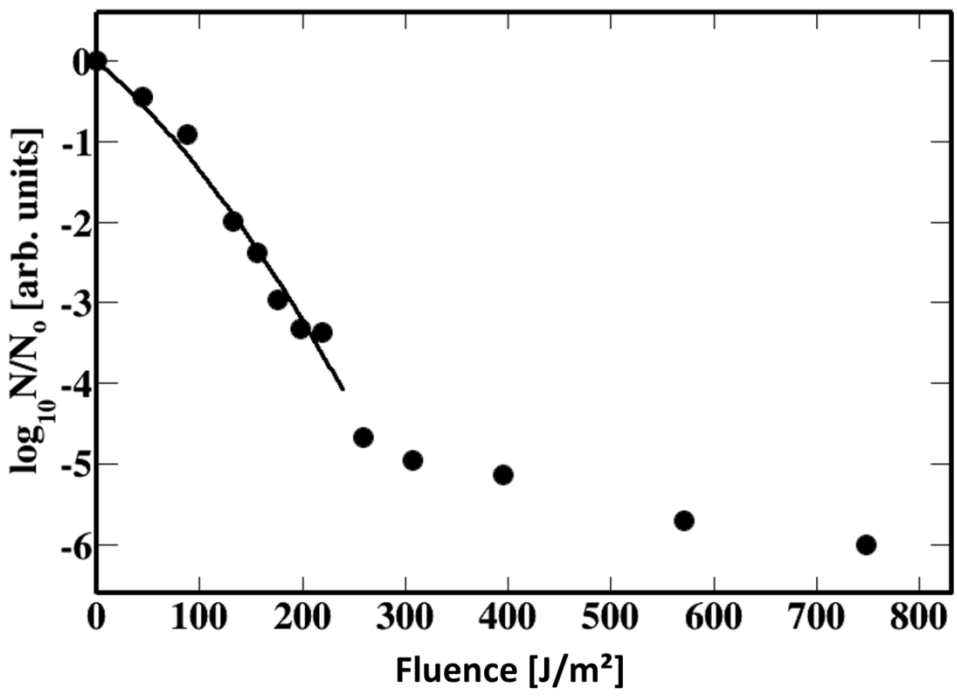

Figure Appdx-13. Survival Curve 2 log-linear fit of data up to 240 J/m^2. Fit parameters and statistics are displayed in Table Appdx-8 above.

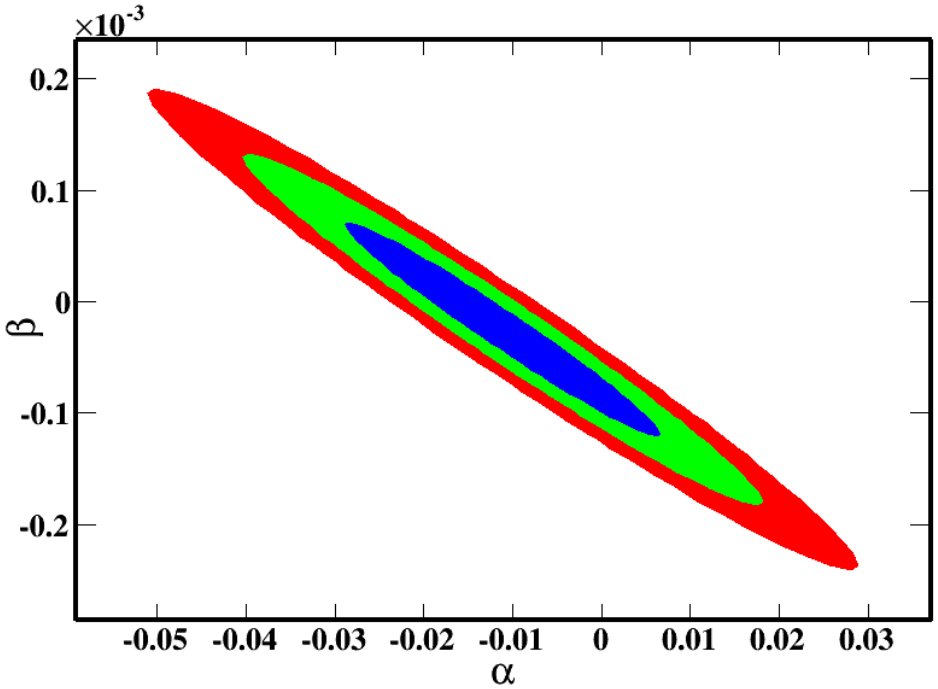

Figure Appdx-14. Pearson product-moment correlation plot for Survival Curve 2. The two fit parameters α and β are negatively correlated. The blue area indicates 1 standard deviation from the mean, where 68% of the data lies. The green area indicates 2 standard deviations from the mean, where 95% of the data lies. The red area indicates 3 standard deviations from the mean, where 99.7% of the data lies.

DNA Damage & Repair Experimentation

Table Appdx-9. Plate counts for DNA damage and repair experimentation control experiment. For the control experiment, no irradiation was incurred. The spores were simply placed in the germination media and allowed to sporulate. The final column displays the surviving fraction. The control experiment was conducted on 7/14/2014.

Control 7/14/2014					
Incubation Time, Minutes	Colony Count 1	Colony Count 2	Colony Count 3	Average Colony Count, S	S/So
Control (So)	140000	138000	154000	144000.00	
0	145000	173000	124000	147333.33	1.02
30	133000	154000	156000	147666.67	1.03
60	156000	148000	162000	155333.33	1.08
90	145000	182000	164000	163666.67	1.14
120	182000	165000	142000	163000.00	1.13
150	178000	162000	138000	159333.33	1.11
180	156000	147000	183000	162000.00	1.13
210	145000	153000	168000	155333.33	1.08
270	183000	174000	127000	161333.33	1.12
330	161000	157000	153000	157000.00	1.09
390	175000	147000	157000	159666.67	1.11
450	187000	158000	163000	169333.33	1.18

Table Appdx-10. Plate counts for DNA damage and repair Experiment #1. The experiment was conducted on 7/9/2014.

Experiment #1 7/9/2014					
Incubation Time, Minutes	Colony Count 1	Colony Count 2	Colony Count 3	Average Colony Count, S	S/So
Control (So)	231000	352000	283000	288666.67	
0	142000	114000	202000	152666.67	0.53
30	40000	55000	80000	58333.33	0.20
60	31000	30000	24000	28333.33	0.10
90	19000	26000	24000	23000.00	0.08
120	40000	19000	22000	27000.00	0.09
150	15000	11000	20000	15333.33	0.05
180	26000	35000	20000	27000.00	0.09
210	11000	20000	27000	19333.33	0.07
270	55000	23000	18000	32000.00	0.11
330	28000	39000	33000	33333.33	0.12
390	4000	0	4000	2666.67	0.01
450	0	0	0	0.00	0.00

Table Appdx-11. Plate counts for DNA damage and repair Experiment #2. The experiment was conducted on 7/14/2014.

Experiment #2 7/14/2014					
Incubation Time, Minutes	**Colony Count 1**	**Colony Count 2**	**Colony Count 3**	**Average Colony Count, S**	**S/So**
Control (So)	314000	329000	359000	334000.00	
0	156000	153000	154000	154333.33	0.46
30	38000	41000	47000	42000.00	0.13
60	54000	45000	43000	47333.33	0.14
90	39000	9000	19000	22333.33	0.07
120	28000	27000	28000	27666.67	0.08
150	29000	44000	24000	32333.33	0.10
180	14000	12000	17000	14333.33	0.04
210	24000	25000	25000	24666.67	0.07
270	63000	39000	50000	50666.67	0.15
330	31000	21000	23000	25000.00	0.07
390	14000	12000	15000	13666.67	0.04
450	0	0	0	0.00	0.00

Table Appdx-12. Plate counts for DNA damage and repair Experiment #3. The experiment was conducted on 7/17/2014.

Experiment #3 7/17/2014					
Incubation Time, Minutes	**Colony Count 1**	**Colony Count 2**	**Colony Count 3**	**Average Colony Count, S**	**S/So**
Control (So)	302000	333000	383000	339333.33	
0	148000	169000	104000	140333.33	0.41
30	38000	33000	34000	35000.00	0.10
60	36000	34000	52000	40666.67	0.12
90	22000	23000	24000	23000.00	0.07
120	40000	47000	26000	37666.67	0.11
150	24000	15000	8000	15666.67	0.05
180	65000	62000	71000	66000.00	0.19
210	40000	39000	53000	44000.00	0.13
270	88000	53000	50000	63666.67	0.19
330	76000	62000	65000	67666.67	0.20
390	54000	58000	41000	51000.00	0.15
450	0	0	0	0.00	0.00

Table Appdx-13. PCR results for Experiment 1. Duplicate samples were analyzed for the control dilution of RFP DNA. Experimental samples were all analyzed in triplicate. A second serial dilution of control values is seen half way down the table because experiments were analyzed in two separate PCR runs. Cq is determined by a threshold fluorescence value that is just above background fluorescence. The number of cycles required to reach this threshold fluorescence is termed Cq.

Experiment 1												
Sample	**10^{-1} PR1**	**10^{-2} PR1**	**10^{-3} PR1**	**10^{-4} PR1**	**10^{-5} PR1**	**10^{-6} PR1**	**10^{-7} PR1**	**10^{-8} PR1**	**10^{-9} PR1**	**10^{-10} PR1**		
Cq	5.01	2.17	9.13	14.14	19.01	22.35	25.41	27.63	25.91	26.82		
Cq	6.1	2.11	9.2	14.14	17.97	22.02	26.4	27.06	26.62	26.71		
Sample	**10^{-1} PR2**	**10^{-2} PR2**	**10^{-3} PR2**	**10^{-4} PR2**	**10^{-5} PR2**	**10^{-6} PR2**	**10^{-7} PR2**	**10^{-8} PR2**	**10^{-9} PR2**	**10^{-10} PR2**		
Cq	N/R	4.01	10.24	16.74	21.03	26.45	31.13	31.42	31.16	31.17		
Cq	8.95	3.79	10.21	16.72	21.31	26.23	31.91	31.6	31.43	31.23		
Sample	**0R PR1**	**0R PR1**	**0R PR1**	**0NR PR1**	**0NR PR1**	**0NR PR1**	**1R PR1**	**1R PR1**	**1R PR1**	**1NR PR1**	**1NR PR1**	**1NR PR1**
Cq	N/R	N/R	N/R	18.62	18.67	18.55	N/R	N/R	N/R	19.59	19.62	19.42
Sample	**0R PR2**	**0R PR2**	**0R PR2**	**0NR PR2**	**0NR PR2**	**0NR PR2**	**1R PR2**	**1R PR2**	**1R PR2**	**1NR PR2**	**1NR PR2**	**1NR PR2**
Cq	N/R	N/R	N/R	23.18	22.63	22.6	N/R	N/R	N/R	22.01	21.8	21.69
Sample	**2 PR1**	**2 PR1**	**2 PR1**	**3 PR1**	**3 PR1**	**3 PR1**	**4 PR1**	**4 PR1**	**4 PR1**	**5 PR1**	**5 PR1**	**5 PR1**
Cq	N/R	N/R	N/R	N/R	N/R	N/R	N/R	N/R	N/R	N/R	N/R	N/R
Sample	**2 PR2**	**2 PR2**	**2 PR2**	**3 PR2**	**3 PR2**	**3 PR2**	**4 PR2**	**4 PR2**	**4 PR2**	**5 PR2**	**5 PR2**	**5 PR2**
	N/R	N/R	N/R	N/R	N/R	N/R	N/R	N/R	N/R	N/R	N/R	N/R
Sample	**10^{-1} PR1**	**10^{-2} PR1**	**10^{-3} PR1**	**10^{-4} PR1**	**10^{-5} PR1**	**10^{-6} PR1**	**10^{-7} PR1**	**10^{-8} PR1**	**10^{-9} PR1**	**10^{-10} PR1**		
Cq	5.61	2.16	9.25	14.02	17.46	19.39	18.91	19.7	19.27	19.58		
Cq	6.49	2.26	9.07	13.76	17.85	19.15	19.58	19.51	19.44	19.35		
Sample	**10^{-1} PR2**	**10^{-2} PR2**	**10^{-3} PR2**	**10^{-4} PR2**	**10^{-5} PR2**	**10^{-6} PR2**	**10^{-7} PR2**	**10^{-8} PR2**	**10^{-9} PR2**	**10^{-10} PR2**		
Cq	10.79	4.06	10.4	16.66	22.21	25.52	26.21	26.28	22.34	30.73		
Cq	N/A	4.03	10.71	16.89	21.73	25.09	26.04	27.16	26.78	30.26		
Sample	**6 PR1**	**6 PR1**	**6 PR1**	**7 PR1**	**7 PR1**	**7 PR1**	**8 PR1**	**8 PR1**	**8 PR1**	**9 PR1**	**9 PR1**	**9 PR1**
Cq	N/R	N/R	N/R	N/R	N/R	N/R	N/R	N/R	N/R	N/R	N/R	N/R
Sample	**6 PR2**	**6 PR2**	**6 PR2**	**7 PR2**	**7 PR2**	**7 PR2**	**8 PR2**	**8 PR2**	**8 PR2**	**9 PR2**	**9 PR2**	**9 PR2**
Cq	N/R	N/R	N/R	N/R	N/R	N/R	N/R	N/R	N/R	N/R	N/R	N/R
Sample	**10 PR1**	**10 PR1**	**10 PR1**	**11 PR1**	**11 PR1**	**11 PR1**	**12 PR1**	**12 PR1**	**12 PR1**			
Cq	N/R	N/R	N/R	N/R	N/R	N/R	N/R	N/R	N/R			
Sample	**10 PR2**	**10 PR2**	**10 PR2**	**11 PR2**	**11 PR2**	**11 PR2**	**12 PR2**	**12 PR2**	**12 PR2**			
Cq	N/R	N/R	N/R	N/R	N/R	N/R	N/R	N/R	N/R			

Table Appdx-14. PCR results for Experiment 2. Duplicate samples were analyzed for the control dilution of RFP DNA. Experimental samples were all analyzed in triplicate. A second serial dilution of control values is seen half way down the table because experiments were analyzed in two separate PCR runs. Cq is determined by a threshold fluorescence value that is just above background fluorescence. The number of cycles required to reach this threshold fluorescence is termed Cq.

Experiment 2												
Sample	**10^{-1} PR1**	**10^{-2} PR1**	**10^{-3} PR1**	**10^{-4} PR1**	**10^{-5} PR1**	**10^{-6} PR1**	**10^{-7} PR1**	**10^{-8} PR1**	**10^{-9} PR1**	**10^{-10} PR1**		
Cq	5.68	3.19	9.57	14.16	17.22	18.76	19.27	18.44	18.73	19.04		
Cq	N/A	2.98	9.16	14.11	17.23	18.85	19.28	19.11	19.13	19.51		
Sample	**10^{-1} PR2**	**10^{-2} PR2**	**10^{-3} PR2**	**10^{-4} PR2**	**10^{-5} PR2**	**10^{-6} PR2**	**10^{-7} PR2**	**10^{-8} PR2**	**10^{-9} PR2**	**10^{-10} PR2**		
Cq	6.83	3.85	10.24	16.57	22.2	24.31	24.94	23.28	25.09	26.48		
Cq	7.71	3.79	10.28	17.02	21.37	24.42	26.8	23.06	25.14	26.27		
Sample	**0R PR1**	**0R PR1**	**0R PR1**	**0NR PR1**	**0NR PR1**	**0NR PR1**	**1R PR1**	**1R PR1**	**1R PR1**	**1NR PR1**	**1NR PR1**	**1NR PR1**
Cq	14.1	19.23	20.66	19.28	19.41	19.16	20.68	21.8	19.37	18.56	18.5	18.46
Sample	**0R PR2**	**0R PR2**	**0R PR2**	**0NR PR2**	**0NR PR2**	**0NR PR2**	**1R PR2**	**1R PR2**	**1R PR2**	**1NR PR2**	**1NR PR2**	**1NR PR2**
Cq	35.53	35.08	34.74	25.47	25.57	26.01	34.61	34.48	34.74	22.14	22.03	21.84
Sample	**2 PR1**	**2 PR1**	**2 PR1**	**3 PR1**	**3 PR1**	**3 PR1**	**4 PR1**	**4 PR1**	**4 PR1**	**5 PR1**	**5 PR1**	**5 PR1**
Cq	N/R	N/R	N/R	N/R	N/R	N/R	N/R	N/R	N/R	N/R	N/R	N/R
Sample	**2 PR2**	**2 PR2**	**2 PR2**	**3 PR2**	**3 PR2**	**3 PR2**	**4 PR2**	**4 PR2**	**4 PR2**	**5 PR2**	**5 PR2**	**5 PR2**
	N/R	N/R	N/R	N/R	N/R	N/R	N/R	N/R	N/R	N/R	N/R	N/R
Sample	**10^{-1} PR1**	**10^{-2} PR1**	**10^{-3} PR1**	**10^{-4} PR1**	**10^{-5} PR1**	**10^{-6} PR1**	**10^{-7} PR1**	**10^{-8} PR1**	**10^{-9} PR1**	**10^{-10} PR1**		
Cq	5.59	3.03	9.51	14.31	17.32	19.15	19.26	19.27	19.14	19.55		
Cq	5.83	3.25	9.82	14.22	17.49	19.28	19.32	19.28	19.27	19.43		
Sample	**10^{-1} PR2**	**10^{-2} PR2**	**10^{-3} PR2**	**10^{-4} PR2**	**10^{-5} PR2**	**10^{-6} PR2**	**10^{-7} PR2**	**10^{-8} PR2**	**10^{-9} PR2**	**10^{-10} PR2**		
Cq	9.88	4.4	11.65	16.93	21.68	24.58	24.75	23.23	25.22	26.42		
Cq	7.58	4.38	10.99	17.37	21.18	24.21	24.7	23.15	24.97	26.5		
Sample	**6 PR1**	**6 PR1**	**6 PR1**	**7 PR1**	**7 PR1**	**7 PR1**	**8 PR1**	**8 PR1**	**8 PR1**	**9 PR1**	**9 PR1**	**9 PR1**
Cq	N/R	N/R	N/R	N/R	N/R	N/R	N/R	N/R	N/R	N/R	N/R	N/R
Sample	**6 PR2**	**6 PR2**	**6 PR2**	**7 PR2**	**7 PR2**	**7 PR2**	**8 PR2**	**8 PR2**	**8 PR2**	**9 PR2**	**9 PR2**	**9 PR2**
Cq	N/R	N/R	N/R	N/R	N/R	N/R	N/R	N/R	N/R	N/R	N/R	N/R
Sample	**10 PR1**	**10 PR1**	**10 PR1**	**11 PR1**	**11 PR1**	**11 PR1**	**12 PR1**	**12 PR1**	**12 PR1**			
Cq	N/R	N/R	N/R	N/R	N/R	N/R	N/R	N/R	N/R			
Sample	**10 PR2**	**10 PR2**	**10 PR2**	**11 PR2**	**11 PR2**	**11 PR2**	**12 PR2**	**12 PR2**	**12 PR2**			
Cq	N/R	N/R	N/R	N/R	N/R	N/R	N/R	N/R	N/R			

Table Appdx-15. PCR results for Experiment 3. Duplicate samples were analyzed for the control dilution of RFP DNA. Experimental samples were all analyzed in triplicate. A second serial dilution of control values is seen half way down the table because experiments were analyzed in two separate PCR runs. Cq is determined by a threshold fluorescence value that is just above background fluorescence. The number of cycles required to reach this threshold fluorescence is termed Cq.

Experiment 3												
Sample	**10^{-1} PR1**	**10^{-2} PR1**	**10^{-3} PR1**	**10^{-4} PR1**	**10^{-5} PR1**	**10^{-6} PR1**	**10^{-7} PR1**	**10^{-8} PR1**	**10^{-9} PR1**	**10^{-10} PR1**		
Cq	4.35	2.86	9.37	14.25	17.27	19.00	19.39	19.21	19.28	19.36		
Cq	6.32	3.26	10.23	14.43	17.50	19.16	20.03	19.16	19.30	19.46		
Sample	**10^{-1} PR2**	**10^{-2} PR2**	**10^{-3} PR2**	**10^{-4} PR2**	**10^{-5} PR2**	**10^{-6} PR2**	**10^{-7} PR2**	**10^{-8} PR2**	**10^{-9} PR2**	**10^{-10} PR2**		
Cq	9.90	4.18	10.88	17.47	21.42	25.45	25.00	23.25	25.41	27.53		
Cq	7.70	4.39	11.16	17.20	21.79	26.18	24.95	23.46	25.23	26.43		
Sample	**0R PR1**	**0R PR1**	**0R PR1**	**0NR PR1**	**0NR PR1**	**0NR PR1**	**1R PR1**	**1R PR1**	**1R PR1**	**1NR PR1**	**1NR PR1**	**1NR PR1**
Cq	N/R	N/R	N/R	19.02	18.66	18.49	N/R	N/R	N/R	18.23	17.49	17.80
Sample	**0R PR2**	**0R PR2**	**0R PR2**	**0NR PR2**	**0NR PR2**	**0NR PR2**	**1R PR2**	**1R PR2**	**1R PR2**	**1NR PR2**	**1NR PR2**	**1NR PR2**
Cq	N/R	N/R	N/R	21.80	21.94	21.84	N/R	N/R	N/R	20.01	19.94	19.58
Sample	**2 PR1**	**2 PR1**	**2 PR1**	**3 PR1**	**3 PR1**	**3 PR1**	**4 PR1**	**4 PR1**	**4 PR1**	**5 PR1**	5 PR1	5 PR1
Cq	N/R	N/R	N/R	N/R	N/R	N/R	N/R	N/R	N/R	N/R	N/R	N/R
Sample	**2 PR2**	**2 PR2**	**2 PR2**	**3 PR2**	**3 PR2**	**3 PR2**	**4 PR2**	**4 PR2**	**4 PR2**	**5 PR2**	5 PR2	5 PR2
	N/R	N/R	N/R	N/R	N/R	N/R	N/R	N/R	N/R	N/R	N/R	N/R
Sample	**10^{-1} PR1**	**10^{-2} PR1**	**10^{-3} PR1**	**10^{-4} PR1**	**10^{-5} PR1**	**10^{-6} PR1**	**10^{-7} PR1**	**10^{-8} PR1**	**10^{-9} PR1**	**10^{-10} PR1**		
Cq	N/R	3.43	10.55	14.98	18.90	22.01	24.25	22.09	23.81	26.26		
Cq	N/R	3.31	10.18	14.67	18.46	21.65	24.29	21.97	23.81	26.44		
Sample	**10^{-1} PR2**	**10^{-2} PR2**	**10^{-3} PR2**	**10^{-4} PR2**	**10^{-5} PR2**	**10^{-6} PR2**	**10^{-7} PR2**	**10^{-8} PR2**	**10^{-9} PR2**	**10^{-10} PR2**		
Cq	**10.30**	**5.07**	**11.13**	**17.90**	**22.40**	**25.52**	**27.94**	**24.54**	**28.17**	**28.79**		
Cq	N/R	**4.91**	**11.30**	**17.80**	**22.83**	**25.70**	**27.68**	**24.41**	**28.32**	**29.65**		
Sample	**6 PR1**	**6 PR1**	**6 PR1**	**7 PR1**	**7 PR1**	**7 PR1**	**8 PR1**	**8 PR1**	**8 PR1**	**9 PR1**	**9 PR1**	**9 PR1**
Cq	N/R	N/R	N/R	N/R	N/R	N/R	N/R	N/R	N/R	N/R	N/R	N/R
Sample	**6 PR2**	**6 PR2**	**6 PR2**	**7 PR2**	**7 PR2**	**7 PR2**	**8 PR2**	**8 PR2**	**8 PR2**	**9 PR2**	**9 PR2**	**9 PR2**
Cq	N/R	N/R	N/R	N/R	N/R	N/R	N/R	N/R	N/R	N/R	N/R	N/R
Sample	**10 PR1**	**10 PR1**	**10 PR1**	**11 PR1**	**11 PR1**	**11 PR1**	**12 PR1**	**12 PR1**	**12 PR1**			
Cq	N/R	N/R	N/R	N/R	N/R	N/R	N/R	N/R	N/R			
Sample	**10 PR2**	**10 PR2**	**10 PR2**	**11 PR2**	**11 PR2**	**11 PR2**	**12 PR2**	**12 PR2**	**12 PR2**			
Cq	N/R	N/R	N/R	N/R	N/R	N/R	N/R	N/R	N/R			

Bibliography

[1] R. C. Spencer, "Bacillus anthracis," *Journal of Clinical Pathology*, vol. 56, pp. 182-187, 2003.

[2] D. F. Zygmunt, "Anthrax," in *Medical Aspects of Biological Warfare*, Washington D.C., Walter Reed Army Medical Center, 2007, pp. 69-90.

[3] J. Miller, W. J. Broad, W. Broad and S. Engelberg, Germs: Biological Weapons and America's Secret War, New York : Touchstone, 2002.

[4] A. X. Hurst, "Modeling of Bacillus Spores: Inactivation and Outgrowth," WPAFB, 2011.

[5] E. A. Knight, "Modeling Thermal Inactivation of Bacillus Sporea," WPAFB, 2009.

[6] L. W. Burggraf, "Mechanism of Ionizing Radiation Damage to Ba Spores," WPAFB, 2011.

[7] CDC, August 2009. [Online]. Available: http://www.cdc.gov/nczved/divisions/dfbmd/diseases/anthrax_sterne/.

[8] T. N. Tran, "Comparison of Continuous Versus Pulsed Ultraviolet Light Emitting Diode Use in Water Disinfection on Bacillus Globigii Spores," WPAFB, 2014.

[9] M. A. Wurtele, T. Kolbe, M. Lipsz, A. Kulberg, M. Weyers, M. Kneissl and M. Jekel, "Application of GaN-based Ultraviolet-C Light Emitting diodes-UV LEDs- For Water Disinfection," *Water Research*, vol. 45, pp. 1481-1489, 2011.

[10] American Type Culture Collection, February 2006. [Online]. Available: www.ATCC.com.

[11] MRSEC Education Group, "University of Wisconsin-Madison," funding from the National Science Foundation under award numbers DMR-1121288, DMR-0520527, DMR-0079983, and EEC-0908782, January 2014. [Online]. Available: http://www.education.mrsec.wisc.edu/132.htm.

[12] W. S. Klug and S. R. Cummings, Concepts of Genetics, 5 ed., Prentice-Hall Inc, 1997.

[13] L. Yang and L. Li, "The Enzyme-Mediated Direct Reversal of a Dithymine Photoproduct in Germinating Endospores," *International Journal of Molecular Sciences*, vol. 14, pp. 13137-13153, June 2013.

[14] J. G. Calvert and J. N. Pitts, Photochemistry, 2nd ed., John Wiley and Sons, 1967.

[15] IUPAC, "Compendium of Chemical Terminology, The Gold Book," Oxford, 1997. [Online]. Available: http://goldbook.iupac.org/Q04991.html.

[16] Wolrd Health Organization, 2014. [Online]. Available: http://www.who.int/uv/faq/whatisuv/en/index2.html.

[17] John Wiley & Sons Publishing, 2002. [Online]. Available: http://www.wiley.com/college/boyer/0470003790/cutting_edge/anthrax/anthrax.htm.

[18] R. Pandey, A. T. Beek, N. O. Vischer, J. P. Smelt and S. Brul, "Live Cell Imaging of Germination and Outgrowth of Individual Bacillus Subtilis Spores; The Effect of Heat Stress Quantitatively Analyzed with SporeTracker," *PLOS One*, vol. 8, no. 3, March 2013.

[19] L. J. Hoffman, "Thermogravimetric Analysis of Bacillus anthracis Spores of DNA by Spectroscopy and Chromatography of Pyrolysis Products," WPAFB, 2013.

[20] P. Setlow, "Spore Germination," *Current Opinion in Microbiology*, vol. 6, pp. 550-556, 2003.

[21] P. Setlow, "Spores of Bacillus subtilis: Their Resistance to and Killing by Radiation, Heat, and Chemicals," *Journal of Applied Microbiology*, vol. 101, pp. 514-525, 2006.

[22] A. Driks, "Bacillus Subtilis Spore Coat," *Journal of Microbiology and Molecular Biology,* vol. 63, no. 1, pp. 1-20, March 1999.

[23] B. Setlow and P. Setlow, "Role of DNA Repair in Bacillus subtilis Spore Resistance," *Journal of Bacteriology,* vol. 178, no. 12, pp. 3486-3495, 1996.

[24] J. M. Mason and P. Setlow, "Essential Rold of Small, Acid-soluble Spore Proteins in Resistance of Bacillus Subtilis Spores to UV Light," *Journal of Bacteriology,* vol. 167, no. 1, pp. 174-178, 1986.

[25] R. Moeller, P. Setlow, G. Horneck, T. Berger, G. Reitz, P. Rettberg, A. J. Doherty, R. Okayasu and W. L. Nicholson, "Roles of Major, Small, Acid-Soluble Spore Proteins and Spore-Specific and Universal DNA Repair Mechanisms in Resistance of Bacillus subtilis Spores to Ionizing Radiation from X Rays and High-Energy Charged-Particle Bombardment," *Journal of Bacteriology* , vol. 190, no. 3, pp. 1134-1140, February 2008.

[26] B. Setlow, S. Atluri, R. Kitchel, K. Koziol-Dube and P. Setlow, "Role of Dipicolinic Acid in Resistance and Stability of Spores of Bacillus Subtilis with or without DNA-Protective alpha/beta-Type Small Acid-Soluble Proteins," *Journal of Bacteriology,* vol. 188, no. 11, pp. 3740-3747, June 2006.

[27] S. Sarasanandarajah, J. Kunnil, B. V. Bronk and L. Reinisch, "Two-dimensional multiwavelength fluorescence spectra of dipicolinic acid and calcium dipicolinate," *Journal of Applied Optics,* vol. 44, no. 7, pp. 1182-1187, March 2005.

[28] T. Douki, B. Setlow and P. Setlow, "Photosensitization of DNA by Dipicolinic Acid, a Major Component of Spores of Bacillus Species," *Photochemistry and Photobiology Sciences,* vol. 4, pp. 591-597, June 2005.

[29] J.-L. Ravanat, T. Douki and J. Cadet, "Direct and Indirect effects of UV radiation on DNA and its components," *Journal of Photochemistry and Photobiology B: Biology,* vol. 63, pp. 88-102, August 2001.

[30] D. R. Koehler, J. Courcelle and P. C. Hanawalt, "Kinetics of Pyrimidine(6-4)Pyrimidone Photoproduct Repair in E. Coli.," *Journal of Bacteriology,* vol. 178, no. 5, pp. 1347-1350, March 1996.

[31] F. H. Ramirez-Guadiana, M. Barraza-Salas, N. Ramirez-Ramired, M. Ortiz-Cortes, P. Setlow and M. Pedraza-Reyes, "Alternative Excision Repair of Ultraviolet B and C-Induced DNA Damage in Dormant and Developing Spores of Bacillus subtilis," *Journal of Bacteriology,* vol. 194, no. 22, pp. 6096-6104, September 2012.

[32] Y. Xue and W. L. Nicholson, "The Two Major Spore DNA Repair Pathways, Nucleotide Excision Repair and Spore Photoproduct Lyase, Are Sufficient for the Resistance of Bacillus subtillis Spores to Artificial UV-C and UV-B but Not to Solar Radiation," *Applied and Environmental Microbiology ,* vol. 62, no. 7, pp. 2221-2227, July 1996.

[33] L. Yang, G. Lin, D. Liu, K. J. Dria, J. Tesler and L. Li, "Probing the Reaction Mechanism of Spore Photoproduct Lyase (SPL) via Diastereoselectivity Labeled Dinucleotide SP TpT substrates," *Journal of The American Chemical Society,* vol. 133, pp. 10434-10447, June 2011.

[34] C. Kisker, "Prokaryotic Nucleotide Excision Repair," *Cold Spring Harbor Perspectives in Biology,* vol. 5, no. 3, March 2013.

[35] J. R. Bolton, M. I. Stefan, P.-S. Shaw and K. R. Lykke, "Determination of the Quantum Yields of the Potassium Ferrioxalate and Potassium iodide-iodate Actinometers and a Method for the Calibration of Radiometer Detectors," *Journal of Photochemistry and Photobiology A: Chemistry,* vol. 222, pp. 166-169, 2011.

[36] R. O. Rahn, M. I. Stefan, J. R. Bolton, E. Goren, P.-S. Shaw and K. R. Lykke, "Quantum Yield of the Iodide-Iodate Chemical Actinometer: Dependence on Wavelength and Concentration," *Photochemistry and Photobiology,* vol. 78, no. 2, pp. 146-152, 2003.

[37] R. A. Serway and J. W. Jewett Jr., Physics for Scientists and Engineers, Seventh ed., Belmont, CA: Brooks/Cole, 2008.

[38] A. G. Li, Y. Xing and L. W. Burggraf, "Thermal Effects on Surface Structures and Properties of Bacillus," *Langmuir,* vol. 29, pp. 8343-8354, 2013.

[39] D. T. Lamkin and USAF-SAM, *Initial Samples of pRB373 Plasmid, Bacillus anthracis sterne, and Ba Turbo RFP,* 2014.

[40] New England Biolabs, 2012. [Online]. Available: www.neb.com/protocols/2012/11/20/transformation-protocol-c2925.

[41] Qiagen, 2005. [Online]. Available: http://www.qiagen.com/resources/resourcedetail?id=f8ed5bab-15c3-4211-bfa8-4fbe207aad74&lang=en.

[42] T. M. Koehler, Z. Dai and M. Kaufman-Yarbray, "Regulation of the Bacillus anthracis Protective Antigen Gene: CO2 and a trans-Acting Element Activate Transcription from One of Two Promoters," *Journal of Bacteriology,* vol. 176, no. 3, pp. 586-595, February 1994.

[43] Bio-Rad Laboratories, [Online]. Available: http://www.bio-rad.com/en-us/sku/165-2088-gene-pulser-micropulser-cuvettes.

[44] T. Leighton and R. Doi, "The Stability of Messenger Ribonucleic Acid during Sporulation in Bacillus subtilis," *The Journal of Biological Chemistry,* vol. 246, no. 10, pp. 3189-95, May 1971.

[45] United States Environmental Protection Agency, "Biological Sample Preparation Project: Detection of Bacillus anthracis Spores in Soil," January 2011.

[46] SETi, 2011. [Online]. Available: http://www.s-et.com/spec-sheets/TO39.pdf.

[47] M. Spencer, "Design Considerations for a Water Treatment System Utilizing Ultra-Violet Light Emitting Diodes," Wright-Patterson Air Force Base, 2014.

[48] W. L. Nicholson and B. Galeano, "UV Resistance of Bacillus anthracis Spores Revisted: Validation of Bacillus subtilis Spores as UV surrogates for Spores of B anthracis Sterne," *Applied and Environmental Microbiology,* vol. 69, no. 2, pp. 1327-1330, 2003.

[49] Thermo Scientific, [Online]. Available: http://www.thermoscientific.com/content/dam/tfs/LPG/LED/LED%20Documents/Catalogs%20%26%20Brochures/Temperature%20Control/Bath%20Circulator%20and%20Chiller%20Accessories/Miscellaneous%20Bath%20Accessories/D11049~.pdf.

[50] Norton, Maine 2012. [Online]. Available: http://www.mccdaq.com/products/dasylab.htm.

[51] Qiagen, "IT 1-2-3 QGlow dna Sample Purification Kit," 2011. [Online]. Available: www.QIAGEN.com. [Accessed 2014].

[52] Wageningen UR, "Wageningen Bioinformatics Webportal," July 2014. [Online]. Available: http://www.bioinformatics.nl/cgi-bin/primer3plus/primer3plus.cgi.

[53] Bio-Rad, "CFX96 Touch, CFX96 Touch Deep Well, CFX Connect, and CFX384 Touch Real-Time PCR Detection Systems," 2013. [Online]. Available: http://www.bio-rad.com/webroot/web/pdf/lsr/literature/10021337.pdf. [Accessed 1 August 2014].

[54] University of Alabama in Huntsville, 2014. [Online]. Available: http://www.math.uah.edu/stat/sample/CLT.html.

[55] Laerd Statistics, 2013. [Online]. Available: https://statistics.laerd.com/statistical-guides/pearson-correlation-coefficient-statistical-guide.php.

[56] L. Kong, P. Zhang, J. Yu, P. Setlow and Y.-q. Li, "Monitoring the Kinetics of Uptake of a Nucleic Acid Dye during the Germination of Single Spores of Bacillus Specie," *Journal of Analytical Chemistry*, vol. 82, pp. 8717-8724, 2010.

[57] Y. Xing, *AFM Images of Bacillus anthracis spores: UV irradiated and un-irradiated*, WPAFB, 2014.

[58] K. Rudi, B. C. Johnsrud, G. Skjefstad, I. Tryland and I. Hagen, "Different Length (DL) qPCR for Quantification of Cell Killing by UV-induced DNA Damage," *international Journal of Environmental Research and Public Health*, vol. 7, pp. 3376-3381, 2010.

[59] R. O. Rahn, "Potassium Iodide as a Chemical Actinometer for 254nm Radiation: Use of Iodate as an Electron Scavenger," *Photochemistry and Photobiology*, vol. 66, no. 4, pp. 450-455, June 1197.

[60] A. C. Eischeid, J. N. Meyer and K. G. Linden, "UV Disinfection of Adenoviruses: Molecular Indications of DNA Damage Efficiency," *Applied and Environmental Microbiology,* vol. 75, no. 1, pp. 23-28, Januaey 2009.

[61] M. T. Iannotti and R. Pisani Jr., "Inactivation of Bacillus atrophaeus Spores in Healthcare Waste by UV Light Coupled with H2O2," *Brazilian Journal of Chemical Engineering,* vol. 30, no. 03, pp. 507-519, July-September 2013.

[62] S. Leuko, B. A. Neilan, B. P. Burns, M. R. Walter and L. J. Rothschild, "Molecular Assessment of UVC Radiation-Induced DNA Damage Repair in the Stromatolitic Halophilic Archaeon, Halococcus Hamelinensis," *Journal of Photochemistry and Photobiology B: Biology,* vol. 102, pp. 140-145, October 2011.

[63] R. Moeller, T. Douki, J. Cadet, E. Stackebrandt, W. L. Nicholson, P. Rettberg, G. Reitz and G. Horneck, "UV Radiation Induced Formation of DNA Bipurimidine Photoproducts in Bacillus subtillis Endospores and Their Repair During Germination," *International Microbiology,* vol. 10, pp. 39-46, January 2007.

[64] L. d. C. H. Espita, C. Caley, I. Bagyan and P. Setlow, "Base-change Mutations Induced by Various Treatments of Bacillus subtillis Spores with and without DNA Protective Small, Acid-soluble Proteins," *Mutation Research,* vol. 503, pp. 77-84, April 2002.

[65] V. A. Luna, D. King, C. Davis, T. Rycerz, M. Ewert, A. Cannons, P. Amuso and J. Cattani, "Novel Sample Preparation Method for Safe and Rapid Detection of Bacillus anthracis Spores in Environmental Powders and Nasal Swabs," *Journal of Clinical Microbiology,* vol. 41, no. 3, pp. 1252-1255, November 2003.

[66] J. Sub, S. Volz, U. Obst and T. Schwartz, "Application of a Molecular Biology Concept for the Detection of DNA Damage and Repair During UV Disinfection," *Water Research,* vol. 43, pp. 3705-3716, June 2009.

[67] P. J. Riesenman and W. L. Nicholson, "Role of the Spore Coat Layers in Bacillus subtilis Spore Resistance to Hydrogen Peroxide, Artificial UV-C, UV-B, and Solar Radiation," *Applied and Environmental Microbiology,* vol. 66, no. 2, pp. 620-626, November 2000.

[68] J. A. Sikorsky, D. A. Primerano, T. W. Fenger and J. Denvir, "Effect of DNA Damage on PCR Amplication Efficiency with the Relative Threshold Cycle Method," *Biochemical and Biophysical Research Communications,* vol. 323, pp. 823-830, 2004.

[69] U.S. Environmental Protection Agency, "Ultraviolet (UV) Light Emitting Diode (LED) Use in Advanced Oxidation Process (AOP)," WPAFN, 2012.

[70] T. Douki, B. Setlow and P. Setlow, "Effects of the Binding of alpha/Beta-type Small, Acid-soluble Spore Proteins on the Photochemistry of DNA in Spores of Bacillus subtilis and In Vitro," *Photochemistry and Photobiology,* vol. 81, pp. 163-169, 2005.

[71] S. A. Bustin, V. Benes, J. A. Garson, J. Hellemans, J. Huggett, M. Kubista, R. Mueller, T. Nolan, T. Nolan, M. W. Pfaffl, G. L. Shipley, J. Vandesompele and C. T. Wittwer, "The MIQE Guidelines: Minimum Information for Publication of Quantitative Real-Time PCR Experiments," *Clinical Chemistry,* vol. 55, no. 4, pp. 611-622, 2009.

[72] G. B. Knudson, "Photoreactivation of Ultraviolet-Irradiated, Plasmid-Bearing, and Plasmid-Free Strains of Bacillus anthracis," *Applied and Environmental Microbiology,* vol. 52, no. 3, pp. 444-449, September 1986.

[73] M. Dizdaroglu, P. Jaruga, M. Birincolglu and H. Rodriguez, "Free Radical-Induced Danade to DNA: Mechanisms and Measurement," *Free Radical Biology and Medicine,* vol. 32, no. 11, pp. 1102-1115, March 2002.

[74] S. Goldstein and J. Rabani, "The Ferrioxalate and iodide-iodate Actinometers in the UV Region," *Journal of Photochemistry and Photobiology A: Chemistry,* vol. 193, pp. 50-55, 2008.

[75] S. Goldstein and J. Rabani, "Supplementary Material," *Journal of Photochemistry and Photobiology A: Chemistry,* p. Private Communication, 2009.

[76] R. O. Rahn, J. Bolton and M. I. Stepan, "the Iodide/Iodate Actinometer in UV Disinfection: Determination of the Fluence Rate Distribution in UV Reactors," *Photochemistry and Photobiology,* vol. 82, pp. 611-615, 2006.

[77] L. J. Rose and H. O'Connell, "UV Light Inactivation of Bacterial Biothreat Agents," *Applied and Environmental Microbiology* , vol. 75, no. 9, pp. 2987-2990, 2009.

[78] H. Mamane-Gravetz and K. G. Linden, "Relationship Between Physiochemical Properties, Aggregation and UV Inactivation of Isolated Indigenous Spores in Water," *Journal of Applied Microbiology,* vol. 98, pp. 351-363, 2005.

[79] R. Goodacre, B. Shann, R. J. Gilbert, E. M. Timmins, A. C. McGovern, B. K. Alsberg, D. B. Kell and N. A. Logan, "Detection of the Dipicolonic Acid Biomarker in Bacillus Spores using Curie-Point Pyrolysis Mass Spectrometry and Fourier Transform Infrared Spectroscopy," *Journal of Analytical Chemistry,* vol. 72, no. 1, pp. 119-127, January 2000.

REPORT DOCUMENTATION PAGE		Form Approved OMB No. 0704–0188

The public reporting burden for this collection of information is estimated to average 1 hour per response, including the time for reviewing instructions, searching existing data sources, gathering and maintaining the data needed, and completing and reviewing the collection of information. Send comments regarding this burden estimate or any other aspect of this collection of information, including suggestions for reducing this burden to Department of Defense, Washington Headquarters Services, Directorate for Information Operations and Reports (0704–0188), 1215 Jefferson Davis Highway, Suite 1204, Arlington, VA 22202–4302. Respondents should be aware that notwithstanding any other provision of law, no person shall be subject to any penalty for failing to comply with a collection of information if it does not display a currently valid OMB control number. PLEASE DO NOT RETURN YOUR FORM TO THE ABOVE ADDRESS.

1. REPORT DATE (DD–MM–YYYY)	2. REPORT TYPE	3. DATES COVERED (*From — To*)
18-09-2014	Master's Thesis	June 2012-September 2014

4. TITLE AND SUBTITLE	5a. CONTRACT NUMBER
Measurements of DNA Damage and Repair in *Bacillus anthracis* Sterne Spores by UV Radiation	5b. GRANT NUMBER
	5c. PROGRAM ELEMENT NUMBER
6. AUTHOR(S) Chelsea C Marcum	5d. PROJECT NUMBER
	5e. TASK NUMBER
	5f. WORK UNIT NUMBER
7. PERFORMING ORGANIZATION NAME(S) AND ADDRESS(ES) Air Force Institute of Technology Graduate School of 2950 Hobson Way WPAFB OH 45433-7765	8. PERFORMING ORGANIZATION REPORT NUMBER
9. SPONSORING / MONITORING AGENCY NAME(S) AND ADDRESS(ES) Environmental Protection Agency National Homeland Security Research Center 26 West Martin Luther King DR Cincinnati Ohio 45268 http://www.epa.gov/nhsrc/ Air Force Nuclear Weapons Center 1900 Wyoming Blvd SE Kirtland Air Force Base New Mexico 87117 Mark.Suriano@us.af.mil	10. SPONSOR/MONITOR'S ACRONYM(S) EPA NHSRC & AF NWC 11. SPONSOR/MONITOR'S REPORT NUMBER(S)

12. DISTRIBUTION / AVAILABILITY STATEMENT

Distribution Statement A. Approved for Public Release; Distribution Unlimited

13. SUPPLEMENTARY NOTES

This work is declared a work of the U.S. Government and is not subject to copyright protection in the United States.

14. ABSTRACT

Spores of *Bacillus anthracis* (Ba) sterne were irradiated with 267nm UV light using small light emitting diodes. The pRB373 plasmid with a red fluorescent protein was transformed into Ba sterne cells prior to irradiation. Following irradiation, germination media was added and the spores were incubated for various times, to allow for DNA repair. The pRB373 plasmid was isolated and analyzed using real-time PCR. Primers were designed across the RFP in the plasmid yielding two amplicons, 245bp and 547bp long. PCR amplification was not achieved for germinated samples. Spore samples isolated using bead beating methods were amplified. Results indicate a quicker amplification (lower Ct) for irradiated samples then for un-irradiated. Lack of PCR amplification in germinated samples is attributed to too damaging an extraction method for Ba cells. This observation was not expected. Ba Survival Curves were also developed using the quadratic fit, $y = \alpha x + \beta x^2$. Averaging results form 3 experiments, α is reported as -0.0144 ± 0.008 and β as -0.00001 ± 0.0002. Actinometry experiments corrected for the efficiency of the LEDs in all experimentation. Fluorescence measurements monitored germination and outgrowth; they indicated a delay in germination of irradiated spores. AFM images showed morphological changes in irradiated spores.

15. SUBJECT TERMS

DNA Damage and Repair; *Bacillus anthracis* spores

16. SECURITY CLASSIFICATION OF:			17. LIMITATION OF ABSTRACT	18. NUMBER OF PAGES	19a. NAME OF RESPONSIBLE PERSON
a. REPORT	b. ABSTRACT	c. THIS PAGE	UU	141	Dr. Larry W. Burggraf, AFIT/ENP 19b. TELEPHONE NUMBER (Include Area Code) (937)255-6565 x4507 Larry.Burggraf@afit.edu